ISTC Reports

Illinois Sustainable Technology Center

Feasibility of Groundwater Source Heat Pumps for Space Heating and Cooling in Mason County and the American Bottoms Area, Illinois

Thomas R. Holm
Illinois State Water Survey

Xinli Lu
Illinois Sustainable Technology Center

David R. Larson
Illinois State Geological Survey

ILLINOIS SUSTAINABLE TECHNOLOGY CENTER
PRAIRIE RESEARCH INSTITUTE

RR-127
March 2015
www.istc.illinois.edu

RR-127

Feasibility of Groundwater Source Heat Pumps for Space Heating and Cooling in Mason County and the American Bottoms Area, Illinois

Thomas R. Holm
Illinois State Water Survey

Xinli Lu
Illinois Sustainable Technology Center

David R. Larson
Illinois State Geological Survey

March 2015

Submitted to the
Illinois Sustainable Technology Center
Prairie Research Institute
University of Illinois at Urbana-Champaign
www.istc.illinois.edu

The report is available on-line at:
http://www.istc.illinois.edu/info/library_docs/RR/RR-127.pdf

Printed by the Authority of the State of Illinois
Bruce Rauner, Governor

ACKNOWLEDGEMENTS

The authors thank the following people:

- Todd Rusk for his efforts in the early stages of the project.
- Wanki Yuen for assistance with updating the water-quality database, map preparation, and thermal modeling.
- Tim Bryant for map preparation.
- Douglas Hermann for his guidance in developing the proposal and in the early stages of the project.
- Daniel Abrams and Walt Kelly for their helpful comments on the draft report.

This project was supported by the Illinois Sustainable Technology Center, a division of the Prairie Research Institute at the University of Illinois at Urbana-Champaign (Grant No. HWR12225).

Table of Contents

List of Tables

List of Figures

List of Abbreviations and Symbols

A	Dimensionless coefficient used in estimating heating load
(aq)	Aqueous phase, in chemical Equation
b	Saturated thickness
BTU	British thermal unit
°C	Degrees Celsius
CBE	Charge balance error
CDD	Cooling degree days
COP	Coefficient of performance for heat pump in heating mode
COP_c	Coefficient of performance for heat pump in cooling mode
C_p	Specific heat of water
ft	Feet or foot
gpd	Gallons per day
gpd/ft	Gallons per day per foot
gpm	Gallons per minute
gpm/ft	Gallons per minute per foot
GSHP	Groundwater source heat pump
HDD	Heating degree days (monthly)
HL	Heating load required for a building per month
HL_c	Cooling load required for a building per month
hr	Hour
IDOT	Illinois Department of Transportation
IEPA	Illinois Environmental Protection Agency
ISWS	Illinois State Water Survey
k_{house}	House overall heat transfer coefficient
K_{so}	Solubility product
LBL	Lawrence Berkeley Laboratory
Log_{10}	Logarithm, base 10
m^2	Square meters
meq/L	Milliequivalents per liter
mgd	Million gallons per day
mg/L	Milligrams per liter
µg/L	Micrograms per liter
m_{gw}	Mass flowrate of groundwater into the Heat Exchanger in heating mode
$m_{gw,c}$	Mass flowrate of groundwater into the Heat Exchanger in cooling mode
$\bar{m}_{gw}$	Monthly averaged mass flowrate of the groundwater necessary to supply the heating requirements
$\bar{m}_{gw,c}$	Monthly averaged mass flowrate of the groundwater necessary to supply the cooling requirement
MRCC	Midwestern Regional Climate Center
MW	Megawatts
NIST	National Institute of Standards and Technology, formerly National Bureau of Standards
PSL	Public Service Laboratory, ISWS
Q	Pumping rate

Q_{gw} Heat exchanged between GSHP and groundwater in heating mode, considered as groundwater heating potential in this study

$Q_{gw,c}$ Heat exchanged between GSHP and groundwater in cooling mode (Figure 1); considered as groundwater cooling potential in this study

Q_{hp} Heating load supplied by the heat pump to the buildings or users

$Q_{hp,c}$ Cooling load supplied by the heat pump to the buildings or users

R Resistance to heat transfer

R_{LS} Larson-Skold ratio

s Drawdown

(s) Solid phase, in chemical Equation

SC Specific capacity

SI Saturation index

sq ft Square foot

T Transmissivity (groundwater availability) or Temperature (heat pump performance, water quality)

ΔT Groundwater temperature difference while passing through the Heat Exchanger in heating mode, i.e., the difference between T_{gw} and T_{out}

ΔT_c Groundwater temperature difference while passing through the Heat Exchanger in cooling mode, i.e., the difference between $T_{gw,c}$ and $T_{out,c}$

T_{gw} Groundwater temperature, supplied to the Heat Exchanger in heating mode

$T_{gw,c}$ Groundwater temperature supplied to the Heat Exchanger in cooling mode

t_{month} Total hours per month

T_{out} Outlet groundwater temperature at the Heat Exchanger in heating mode

$T_{out,c}$ Outlet groundwater temperature at the Heat Exchanger in cooling mode

TotAnion Sum of anionic charges

TotCation Sum of cationic charges

W_p Power (electricity) necessary to operate the heat pump in heating mode

$W_{p,c}$ Power (electricity) necessary to operate the heat pump in cooling mode

ABSTRACT

While air temperatures in Illinois vary greatly, shallow groundwater temperatures are nearly constant. Groundwater source geothermal heat pump systems can exploit this temperature difference for energy-efficient space heating, space cooling, and refrigeration. Such systems may contribute to energy efficiency gains and sustainable economic development. This project characterized two areas for geothermal heating and cooling potential. Mason County in central Illinois is mostly rural. The American Bottoms area of Madison and St. Clair Counties in southwestern Illinois is largely urban. Both areas are underlain by a thick sand and gravel aquifer. Although there are numerous water supply wells in both areas, groundwater is readily available for groundwater source heat pump systems.

The heating and cooling requirements for a single-family house were estimated using two independent models that use weather data as input. Weather data, including monthly high and low temperatures and heating and cooling degree days, were compiled for both study areas. The groundwater pumping rates for these heating and cooling requirements were then calculated. The performance of a heat pump is expressed as the coefficient of performance (COP), the ratio of heating or cooling rate to the electrical energy input. For groundwater heat pumps, the heating COP value is 3.0 to 4.0. For cooling, COP ranges from 3.5 to 6.7. Calculations were performed using these ranges of COP.

The groundwater in both study areas has fairly high hardness and iron concentrations and is close to saturation with calcium and iron carbonates. Using the groundwater for cooling will probably induce the precipitation of moderate amounts of one or both of these minerals. Periodic cleaning of heat exchanger surfaces, other system piping, and possibly well screens will be needed to remove these deposits.

INTRODUCTION

Ground source heat pump (GSHP) systems exploit the temperature difference between the air and the shallow subsurface. Because of insulation from the ground and the high heat capacities of soil and water, the groundwater temperature stays relatively constant. For example, the range of ground temperatures at 5 m depth is only about 2°C (3.6°F) in central England (Staffell et al. 2012) and Ontario, Canada (Self et al., 2013). On the other hand, air temperatures vary widely over a year. For example, the average air temperature in Champaign, IL was 31.5°F (-0.3°C) in January 2012 and 81.6 °F (27.6°C) in July 2012 (Anonymous, 2013). The average temperature of groundwater within 300 feet of ground surface in central Illinois is about 54°F (12°C) (USEPA 2012). Because of these temperature differences, GSHPs can withdraw heat from the groundwater during the heating season and discard heat to the ground in the cooling season.

The heat output of a GSHP heating system exceeds the electrical energy used by the heat pump and, for groundwater systems, the well pump. The heat output of a conventional heating system is limited by the energy content of the fuel. Therefore, GSHP heating systems are more efficient than conventional heating systems on an energy input-output basis. Similarly, GSHP cooling systems are more efficient than conventional air conditioners (Liu, 2010) because the heat is discharged to groundwater at a lower temperature than that of hot air and also because of the much higher heat capacity of water than that of air. GSHP equipment tends to be more expensive than conventional furnaces and air conditioners. The pay-back time (the time at which the total cost of equipment, installation, and electricity equals the cost of equipment, installation, electricity, and fuel of a conventional heating system) depends on the price of electricity and fuel, which varies greatly around the world, and any economic incentives for alternative heating or cooling (Self et al., 2013). Also, the initial cost of a GSHP system would clearly be higher if a well had to be drilled than if an existing well could be used as a source of groundwater. Another advantage of GSHP systems is that they produce smaller quantities of greenhouse gases than conventional systems per unit of heating or cooling (Berntsson, 2002; Liu 2010; Bayer et al., 2012; Self et al., 2013).

Existing high-capacity dewatering wells may be a potential source of groundwater for heating or cooling. This option would use existing infrastructure (e.g., wells, drainage), which may favorably affect the economics of such a system. For example, Kuo and Liao (2012) studied a system of dewatering wells that will be used to reduce uplift pressure on a subway system in Taipei, Taiwan. They concluded that it would be feasible to use some of the extracted groundwater for cooling. As another example, the Illinois Department of Transportation operates over 60 high-capacity dewatering wells in the East St. Louis area that withdraw approximately 15 million gallons per day (mgd) to prevent groundwater discharge from flooding some roadways (Sanderson, 1993). Heating or cooling using some of this water may be feasible. Irrigation wells, which are typically unused during the heating season, could be a source of groundwater for heating on many farms.

An estimated 600,000 GSHP systems have been installed in the United States (Liu, 2010). Some of these are for schools and other large public and commercial buildings (Bloomquist, 1999). However, if all 600,000 units were installed in single-family houses, they would only account for ~0.5% of the over 127 million houses in the U.S. Liu (2010) estimated that if 20% of American

single-family homes were retrofitted with GSHPs, it would reduce primary energy use by 9.0%, CO_2 emissions by 9.1%, and summer peak electrical demand by 11.2%.

GSHP system configurations are classified as closed-loop or open-loop. In closed-loop systems, heat transfer fluid circulates through a tube and a heat pump. The fluid does not contact the soil or groundwater. The tube can be immersed in a dedicated borehole (vertical system), buried horizontally in the ground, or submerged in a pond or lake (Bloomquist 2003; Omer 2008; Self et al. 2013). Closed-loop systems are the most commonly installed GSHP systems. Roughly 45% of GSHP systems in the U.S. are vertical closed-loop, 35% are horizontal closed-loop, and 20% open-loop (Lund et al., 2005).

In an open-loop GSHP system (Figure 1), groundwater is pumped through the heat pump's heat exchanger (Omer, 2008). Despite the name, there is no closed path of water flow in a properly designed open-loop system. However, the terminology is very common. In a one-well system, the outflow from the heat pump flows to a drain. In a two-well system, outflow from the heat pump is returned into a second well. The wells must be located such that the return water is not captured by the source well in normal operation (short-circuiting) (Banks, 2008). For a large-scale system, there may be significant heating or cooling around the return wells (Freedman et al., 2012).

This project focused on two areas in Illinois with abundant groundwater. The first is Mason County, a mostly rural area with thousands of irrigation wells. The other is the American Bottoms area, a largely urbanized area in the Mississippi River floodplain on the Illinois side in the vicinity of East St. Louis (Figure 2). First, the hydrogeological setting of each area is outlined for groundwater availability. Next, calculations of the groundwater pumping rate needed for heating and cooling single-family houses in the study areas are presented. The calculations are based on groundwater temperatures, weather data for the study areas, models of heat pump performance, and heating and cooling demands of single-family homes. A one-well system is assumed, although the calculations are equally valid for a properly sited two-well system. Finally, groundwater quality is characterized in each area with respect to solutes that may cause heat pump fouling or corrosion.

The thermal calculations presented in this report apply equally well to one-well and properly designed two-well open loop systems. However, injection wells are prone to clogging (Bouwer, 2002) and well rehabilitation would certainly affect the economic feasibility of GSHP. Therefore, for the sake of simplicity, the rest of this report addresses only one-well open-loop systems.

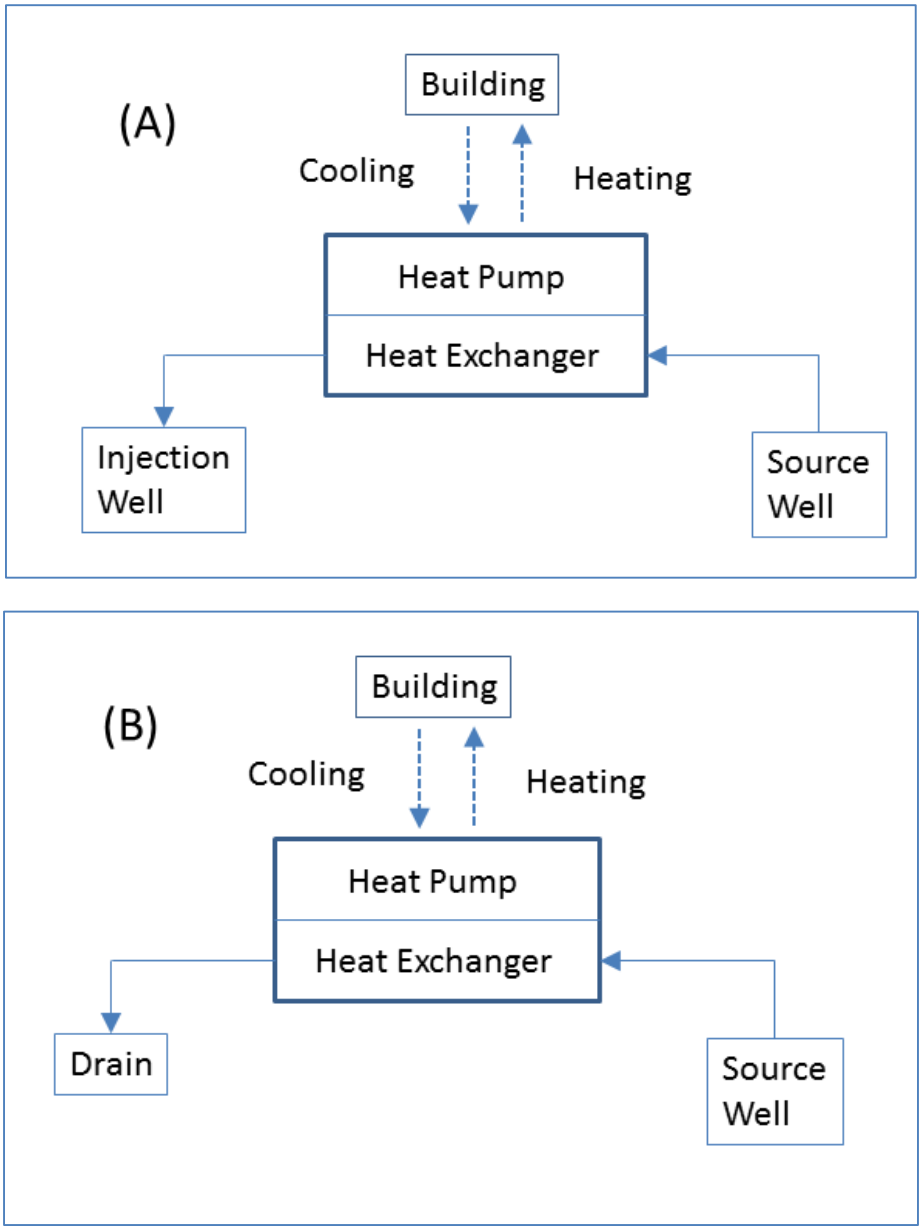

Figure 1. Schematics of open-loop systems. A. Well doublet. B. Single-well system. Solid arrows indicate water flow. Dashed arrows indicate heat flow.

Figure 2. Locations of study areas.

GROUNDWATER AVAILABILITY

American Bottoms

The American Bottoms consists of the broad Mississippi River floodplain located in southwestern Illinois (Figure 3). This industrialized urban area is part of the larger Metro-East area in Madison and St. Clair Counties. The American Bottoms area extends between 2 and 9 miles from the Mississippi River to the bluff that marks the eastern edge of the floodplain with the narrowest width at the north and south ends of the project area. The area is about 30 miles north to south. Although relatively flat, the topography of the American Bottoms is characterized by swales, ridges, and oxbow lakes that were produced by the meandering of the Mississippi River over time. A terrace occupies a position a little above the adjacent floodplain and occurs in a rather narrow band adjacent to the bluff in the northeastern part of the American Bottoms.

Bedrock and the overlying glacial deposits and loess (Grimley and Phillips, 2006; Grimley and Phillips, 2011) comprise the bluff along the eastern edge of the American Bottoms. The bedrock in the bluff is the wall of the bedrock valley that underlies the American Bottoms and is filled with sediment. Although steep on its eastern edge, the bottom of the bedrock valley gently slopes to a relatively narrow channel incised into the bedrock surface near the center of the valley (Figure 4). The thickness of the sediments filling the bedrock valley ranges from less than 20 feet near the valley wall to more than 160 feet in the northern part of the project area (Figure 5). The maximum reported thickness is 171 feet in the northern part of the project area. The thickness of the valley fill averages about 120 feet. The thicker part of the valley fill follows the trend of the channel that is incised into the bedrock surface. The valley-fill sediments underlying the American Bottoms become coarser with depth. The coarsest sediments, which directly overlie bedrock, consist of glacial meltwater deposits that are composed predominantly of medium to coarse sand with abundant gravel (Bergstrom and Walker, 1956). Large pebbles and cobbles are reported in drillers' logs with the presence of boulders noted in some drillers' logs, most commonly in the lower 15 feet of the valley fill (Grimley et al., 2007). Recent alluvial deposits comprising the sediments at or near land surface consist of mostly silt and clay with some fine silty sand (Bergstrom and Walker, 1956).

The sand and gravel of the valley fill, where saturated, comprises the aquifer underlying the American Bottoms (Bergstrom and Walker, 1956). Groundwater in these deposits occurs under leaky confined to unconfined conditions. The leaky confined conditions exist where the sand and gravel aquifer is overlain by fine-grained alluvial deposits and the potentiometric surface of the aquifer is above the top of the aquifer. Unconfined conditions exist where the fine-grained sediments are absent, and the potentiometric surface is the water table. Groundwater development has caused unconfined conditions to occur where the potentiometric surface has been lowered to a level below the base of the fine-grained alluvium. Saturated thicknesses (Figure 6) are less than 40 feet adjacent to the eastern edge of the valley where the valley fill is thin, and increase to more than 80 feet over much of the American Bottoms. Transmissivity values (Figure 7) range from 50,000 gallons per day per foot (gpd/ft) near the eastern edge of the valley and near the southern part of the Chain of Rocks Canal to more than 300,000 gpd/ft near the southern end of the project area (Schicht, 1965).

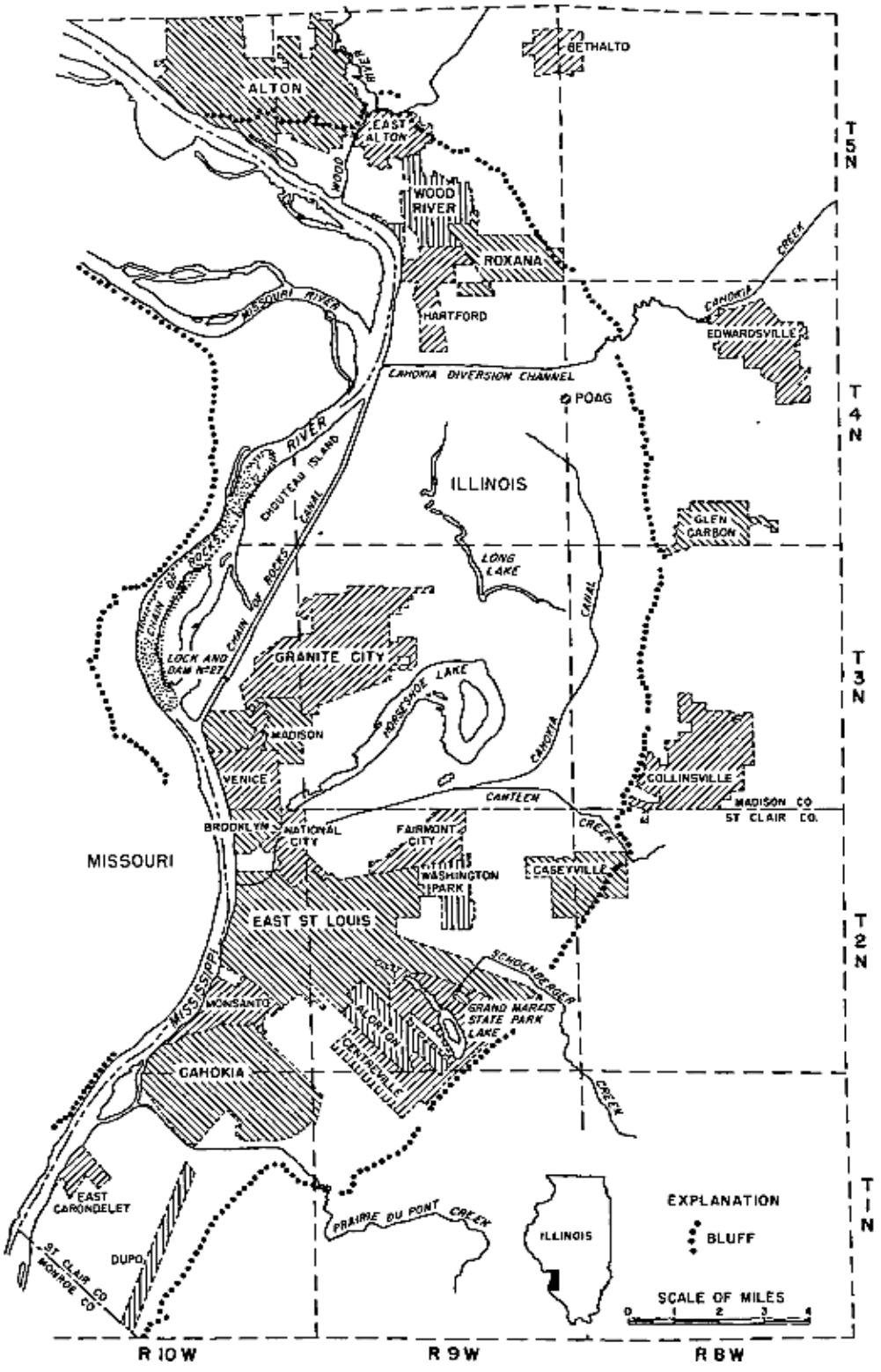

Figure 3. The American Bottoms study area (from Schicht and Jones, 1962).

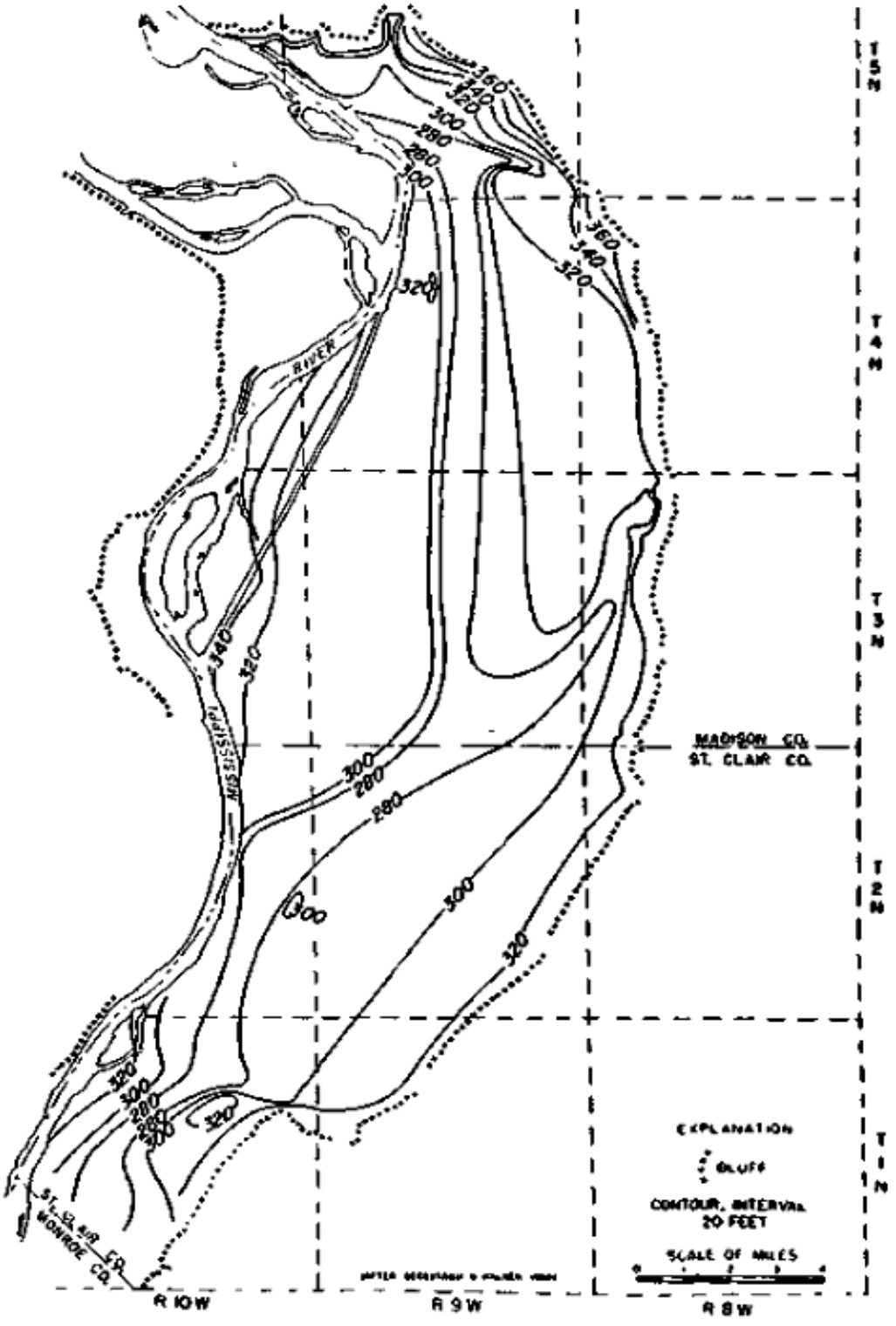

Figure 4. Topography of the bedrock surface, American Bottoms area (from Schicht, 1965).

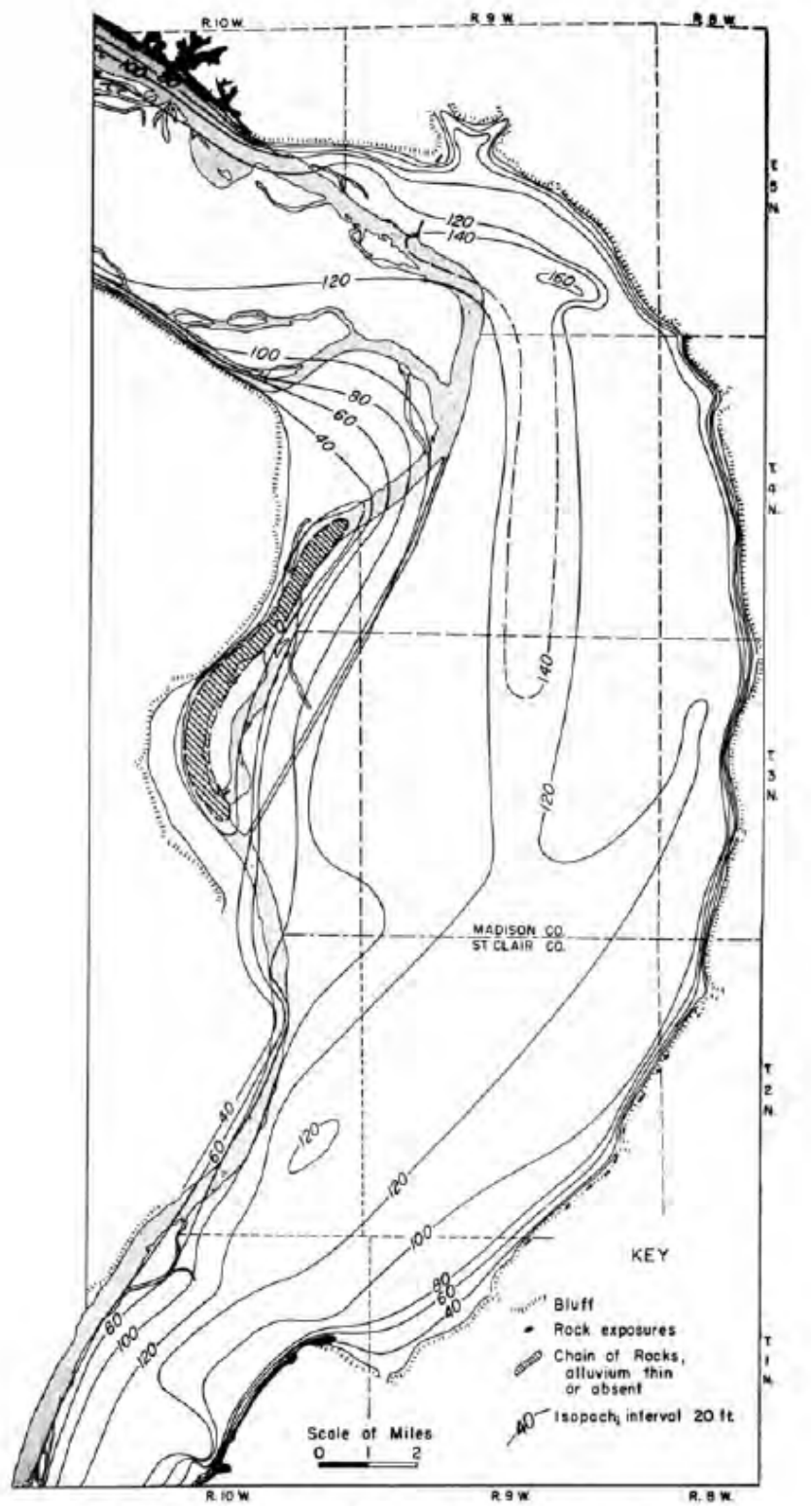

Figure 5. Thickness of sediments underlying the American Bottoms area (from Bergstrom and Walker, 1956).

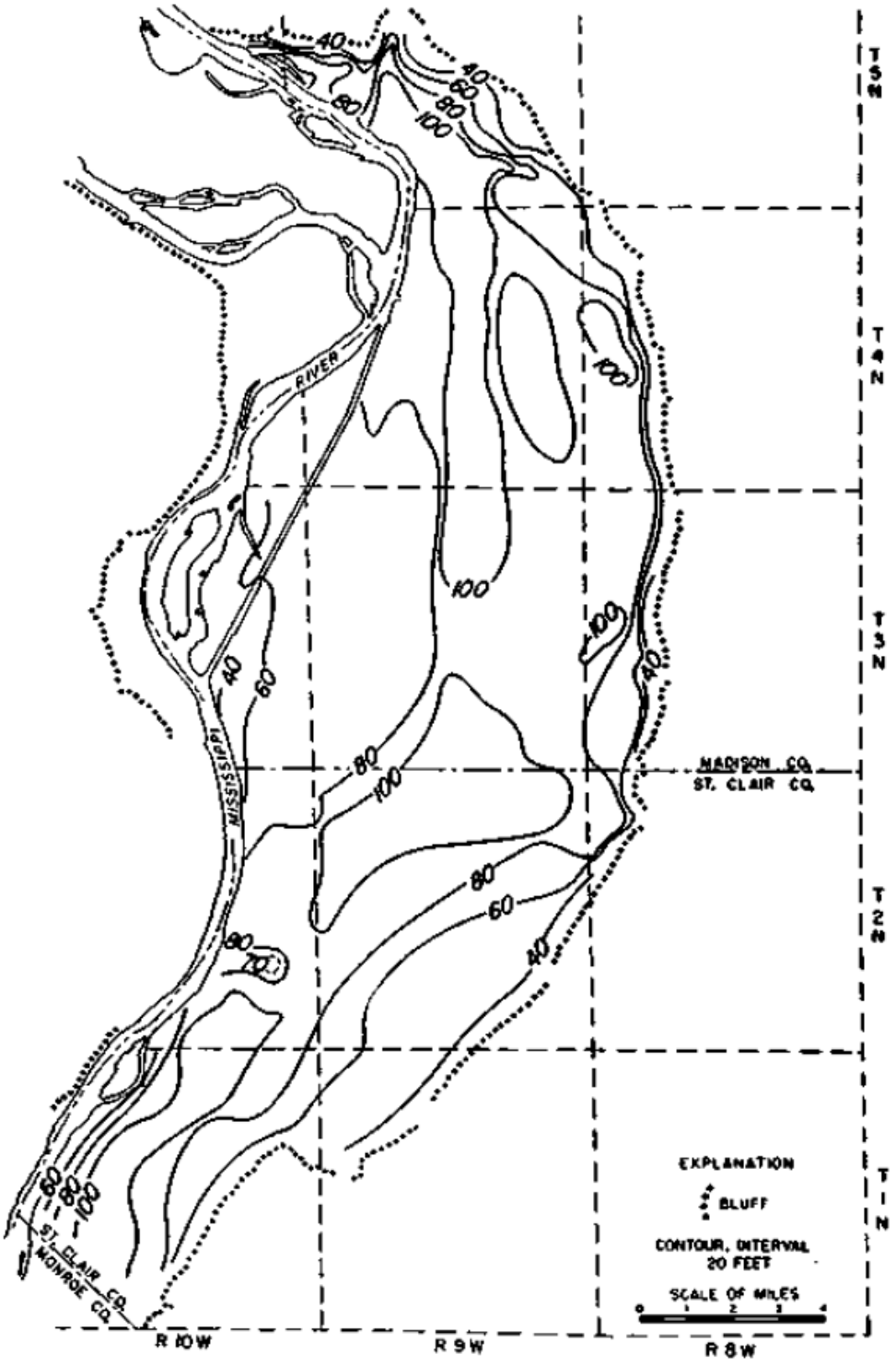

Figure 6. Saturated thickness of sediments underlying the American Bottoms area (from Schicht, 1965).

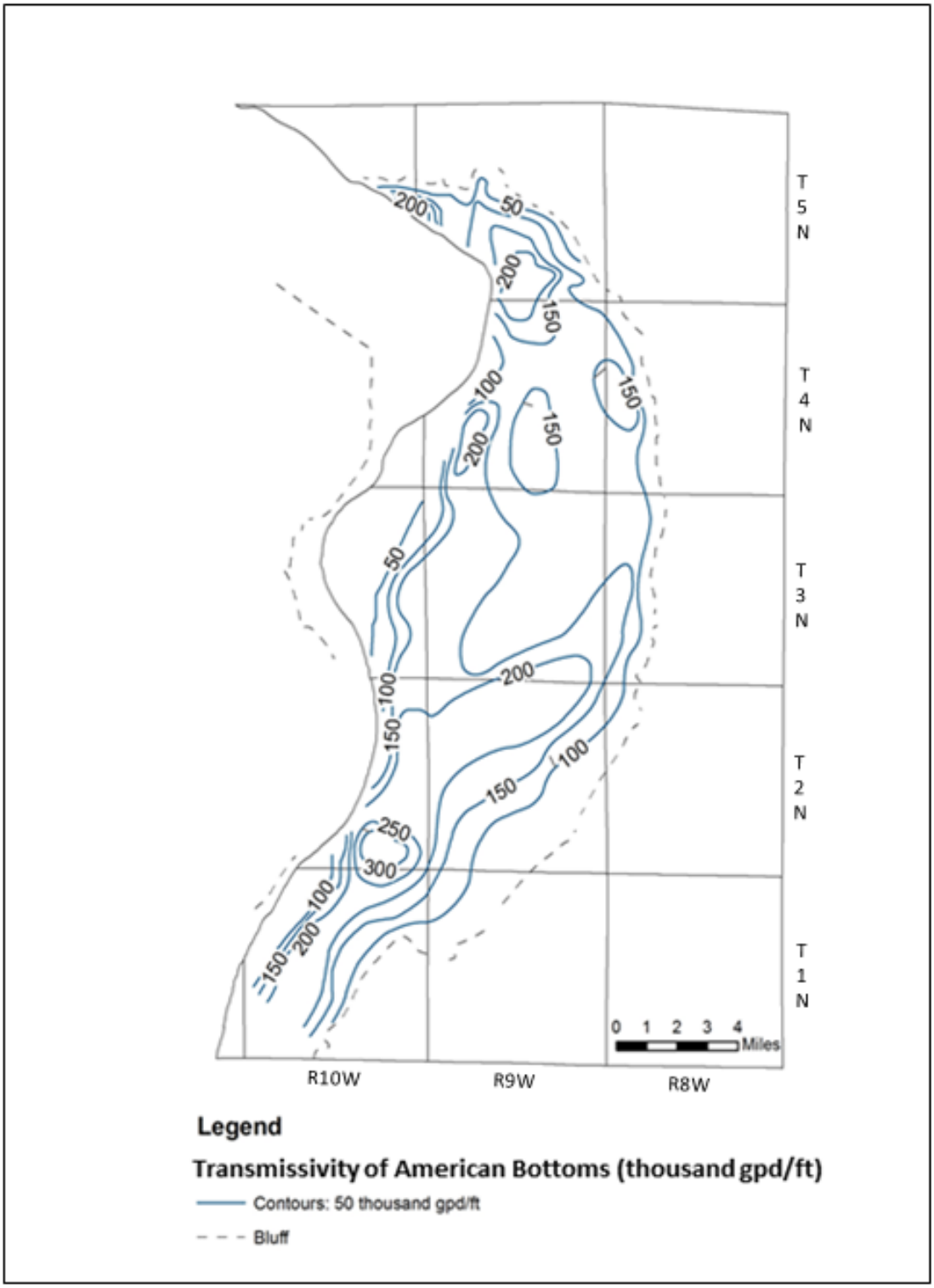

Figure 7. Transmissivity of American Bottoms aquifer (re-drawn from Schicht, 1965).

The aquifer within the American Bottoms is an important groundwater resource that has been used for over 100 years. Schicht and Buck (1995) note that groundwater pumping began in the late 1890s at about 2.0 million gallons per day (mgd) and peaked at 111.0 mgd in 1956. Most of the groundwater supplied industrial and municipal uses. Groundwater use had declined to 58.7 mgd by 1990 (Schicht and Buck, 1995). Schicht (1965) estimated the yield of the aquifer to be 188 mgd, based on the results obtained from a groundwater-flow model of the area. The decline in groundwater use resulted in recovery of the potentiometric surface of the aquifer to the extent that flooding of roadways became a problem that the Illinois Department of Transportation (IDOT) addressed with groundwater dewatering systems. The volume of groundwater pumped in 1990 for dewatering was estimated at 11.2 mgd (Schicht and Buck, 1995).

The quantity of groundwater available from a well is critical to successful implementation of groundwater source heat pumps. Schicht (1965) includes the results obtained from six aquifer tests and 32 specific-capacity tests conducted on production wells. The specific capacity of a well is calculated by dividing the pumping rate of the well by the drawdown associated with that pumping rate. For example, if the pumping rate is 500 gallons per minute (gpm) and the drawdown is 20 feet, the specific capacity is 500 gpm ÷ 20 feet = 25 gpm per foot of drawdown.

These results characterize the water-yielding properties of the aquifer underlying the American Bottoms. The pumping rates for the six aquifer tests ranged from 308 to 1,100 gpm, saturated thicknesses ranged from 60 to 100 feet, and transmissivities ranged from 95,600 to 212,000 gallons per day per foot (gpd/ft) (Table 1). The pumping rates for the 32 specific-capacity tests ranged from 104 to 1,905 gpm, drawdown ranged from 3 to 19 feet, transmissivity ranged from 19,000 to 370,000 gpd/ft, and specific capacity ranged from 14.9 to 266 gallons per minute per foot (gpm/ft) (Table 2). Schicht (1965), in his table 16, includes the results of specific-capacity tests that were performed by the U.S. Army Corps of Engineers on 65 relief wells from 1952 through 1960. The wells were tested at 500 gpm for two hours with drawdown measured in the well. The results of the tests showed that transmissivity ranged from 14,000 to 305,000 gpd/ft and specific capacity ranged from 15 to 238 gpm/ft.

Because the aquifer underlying the American Bottoms is characterized by relatively high transmissivity and specific-capacity values, it can support well yields ranging from 500 to 1,100 gpm. The volume of groundwater pumped daily for dewatering conclusively demonstrates the productivity of the aquifer.

Table 1. Results of aquifer tests in the American Bottoms(from Schicht, 1965).

Location	Pumping Rate (gpm)	Saturated Thickness (ft)	Transmissivity (gpd/ft)
T2N-R10W-section 25	630	73	212,000
-section 27	1100	75	210,000
T4N-R8W-section 20	308	84	131,000
T5N-R9W-section 19	760	90	95,600
-section 28	491	60	134,000
-section 33	510	100	210,000

Table 2. Results of specific-capacity tests – production wells in the American Bottoms (from Schicht, 1965).

Location	Pumping Rate (gpm)	Drawdown (ft)	Transmissivity (gpd/ft)	Specific Capacity (gpm/ft)
T2N-R8W-section 06	470	6.55	90,000	72.0
-section 06	450	6.00	77,000	75.0
T2N-R9W -section 01	349	10.00	60,000	34.9
T2N-R10W-section 01	1248	8.18	200,000	152.5
-section 01	1230	6.55	250,000	188.0
-section 12	475	3.00	190,000	158.0
T3N-R8W-section 05	104	7.00	19,000	14.9
-section 29	420	6.35	120,000	66.0
-section 29	325	3.10	110,000	105.0
-section 30	468	5.38	180,000	87.0
-section 31	1150	17.7	105,000	68.0
-section 31	627	4.80	165,000	130.0
-section 31	1001	11.00	130,000	91.0
T3N-R9W -section 05	820	5.10	180,000	161.0
-section 06	1120	7.88	140,000	140.0
-section 14	768	15.50	70,000	49.5
-section 17	1150	5.78	230,000	199.0
T4N-R9W -section 13	1650	19.00	98,000	87.0
-section 29	1000	5.48	210,000	182.0
T5N-R9W -section 16	560	9.00	62,000	62.2
-section 19	1905	7.17	370,000	266.0
-section 21	300	11.70	42,000	25.6
-section 22	320	5.20	80,000	62.0
-section 22	305	4.25	100,000	72.0
-section 22	460	7.00	83,000	65.0
-section 26	730	11.00	105,000	66.4
-section 26	405	6.00	115,000	73.6
-section 26	925	6.00	200,000	135.0
-section 26	758	6.50	150,000	117.0
-section 27	530	6.00	120,000	88.0
-section 34	1125	17.00	94,000	61.0

Mason County

Mason County is located in central Illinois (Figure 8). The county, which is situated just east of the Illinois River, is predominantly rural with irrigated crops a major feature of the county. The rural character of the county was the primary reason for selecting it for evaluating the potential for geothermal resources in an agricultural region.

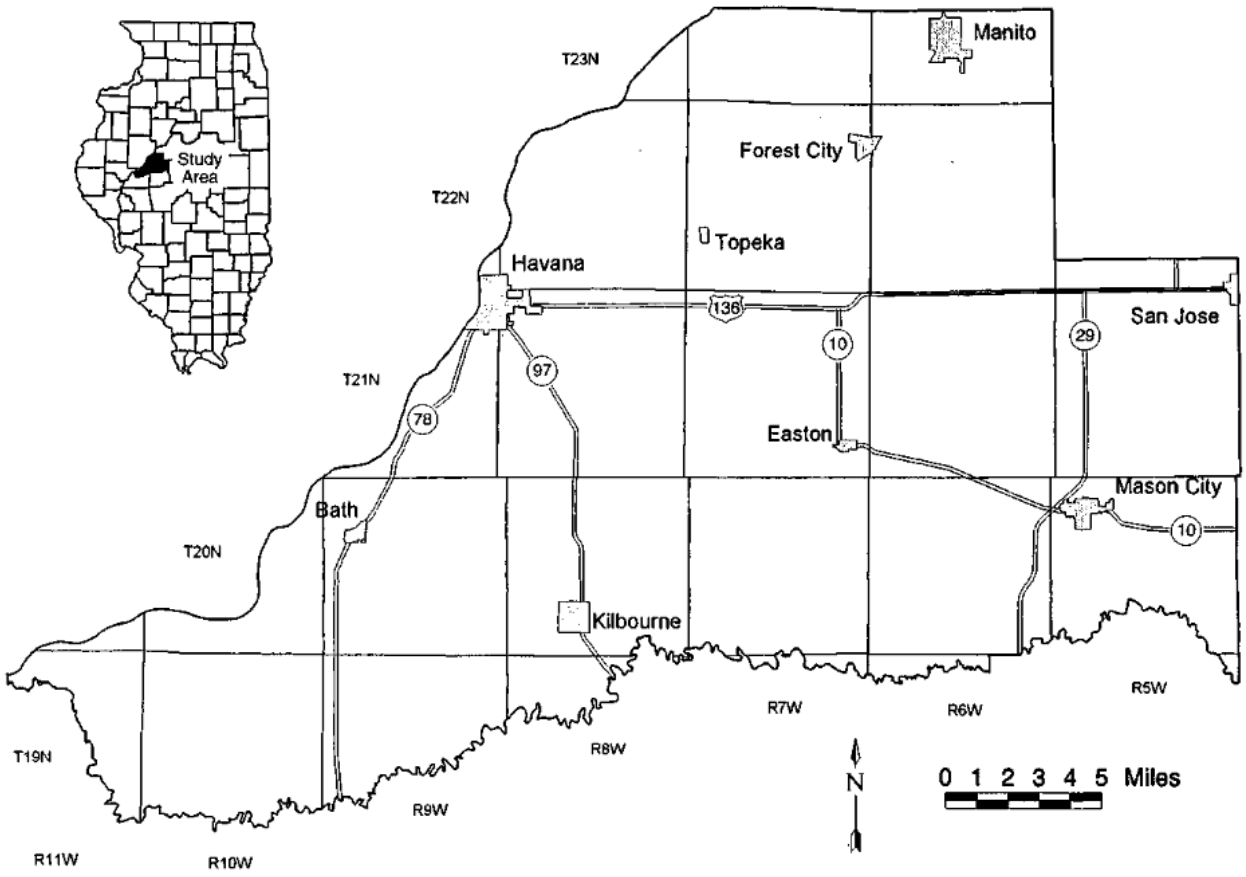

Figure 8. Location of Mason County, Illinois (from Anliker and Woller, 1998).

The land surface of Mason County, except the southeastern part, is a sand plain with rolling topography and in an area known as the Havana Lowlands (Walker et al., 1965). Quaternary deposits consisting primarily of sand and gravel underlie the Havana Lowland and overlie the bedrock (Figure 9). In the southeastern part of the county, the land surface rises as an upland that was formed by glaciation during the Illinois Episode. The deposits creating the upland consist mostly of glacial till with sand and gravel. Much of the upland is covered with a thin layer of loess. The Quaternary deposits in Mason County rest on bedrock. The top of the bedrock forms a surface the main features of which are the valleys that enter Mason County from Tazewell, Logan, and Menard Counties (Figure 10). These bedrock valleys carried preglacial drainage through Mason County. During continental glaciation, meltwater flowing from the ice sheets deposited sand and gravel in these bedrock valleys. Because of this deposition, the sand and gravel that underlies the Havana Lowlands extends under the upland in southeastern Mason County. The thickness of the Quaternary deposits, which is determined by the topography of the land surface and the bedrock surface, ranges from 100 to 200 feet over most of Mason County (Figure 11). The deposits are 200 to 300 feet thick in the middle of Mason County because of the presence of high sand hills (Walker et al., 1965). The 200 to 400 feet of Quaternary deposits across southeastern Mason County reflects the upland in that part of the county. The thickness of the Quaternary deposits along the western margin of Mason County is due to the rise of the bedrock surface near the walls of the bedrock valley and the decline in land surface in the Illinois River valley.

The sand and gravel that underlies the Havana Lowlands and the adjacent upland, where saturated, comprises the principal groundwater resource of Mason County, the Mahomet Aquifer. This aquifer is under unconfined conditions within the Havana Lowland. This means that the water table is the top of the aquifer, and the thickness of the aquifer varies with the fluctuation of the water table. The Mahomet Aquifer is under confined conditions in southeastern Mason County where the fine-grained sediments of the upland provide the confining layers. This means that the potentiometric surface of this part of the aquifer is above the top of the aquifer, and the sand and gravel comprising the aquifer is fully saturated. The thickness of the Mahomet Aquifer in Mason County ranges from about 60 feet near the Illinois River to about 200 feet near San Jose and is greater than 100 feet over much of the county (Figure 12). Walker et al. (1965) reported values for hydraulic conductivity (permeability) derived from aquifer tests and well production tests and subdivided the aquifer into Area 1 and Area 2 based on these values (Figure 13). Walker et al. (1965) noted that the values within Area 1 are typically greater than those within Area 2 and reflect the overall coarser texture of the sand and gravel found in Area 1. The 14 reported hydraulic conductivity values (Figure 13) in Mason County are clustered around the center of the county. The potential yield of water wells throughout the county cannot be estimated from these sparse data. Obtaining and analyzing additional data to augment the number of hydraulic conductivity values were beyond the scope of this project, but is a study that would be very valuable.

High-capacity wells are relatively widespread across the Havana Lowlands, and some are located in the upland of southeastern Mason County (Anliker and Woller, 1998). Based on the thickness of the aquifer (Figure 12), the potential yield to wells may range from a few hundred gallons per minute where the aquifer is relatively thin along the Illinois River to about a thousand gallons per minute where the aquifer is thicker. Actual well yields are influenced by hydrogeological factors

such as the hydraulic properties and heterogeneities of the aquifer, the location of wells with respect to aquifer boundaries, and well interference effects among wells. Walker et al. (1965) also provide the pumping rates for the aquifer tests and well production tests from which the hydraulic conductivity values for Mason County were derived. These values range from 60 gpm at Easton, which is located in Area 2 near the center of the county, to 1,735 gpm for a well located south of Forest City in Area 1 (Figure 14).

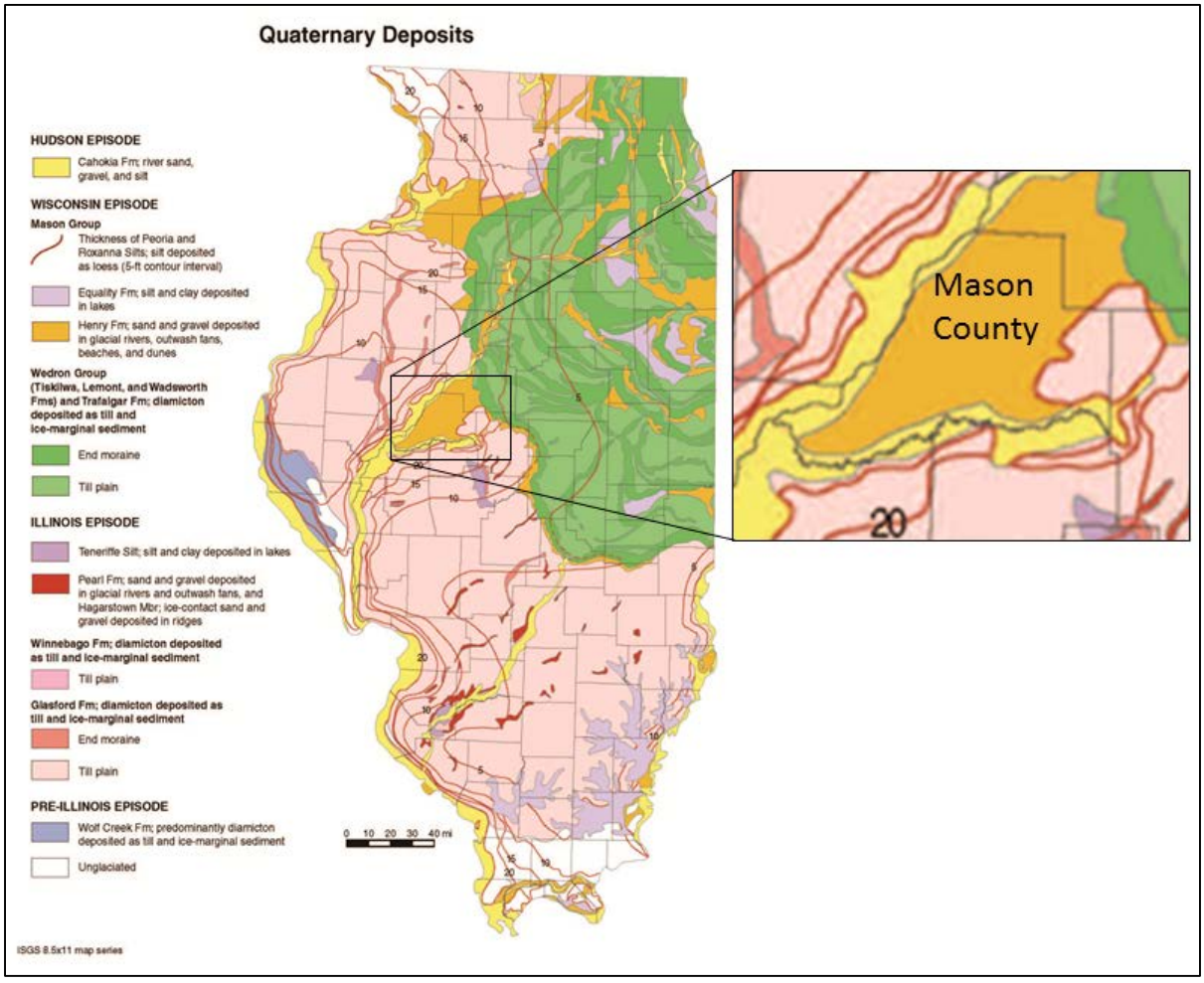

Figure 9. Mason County Quaternary deposits (from Hansel and Johnson, 1996).

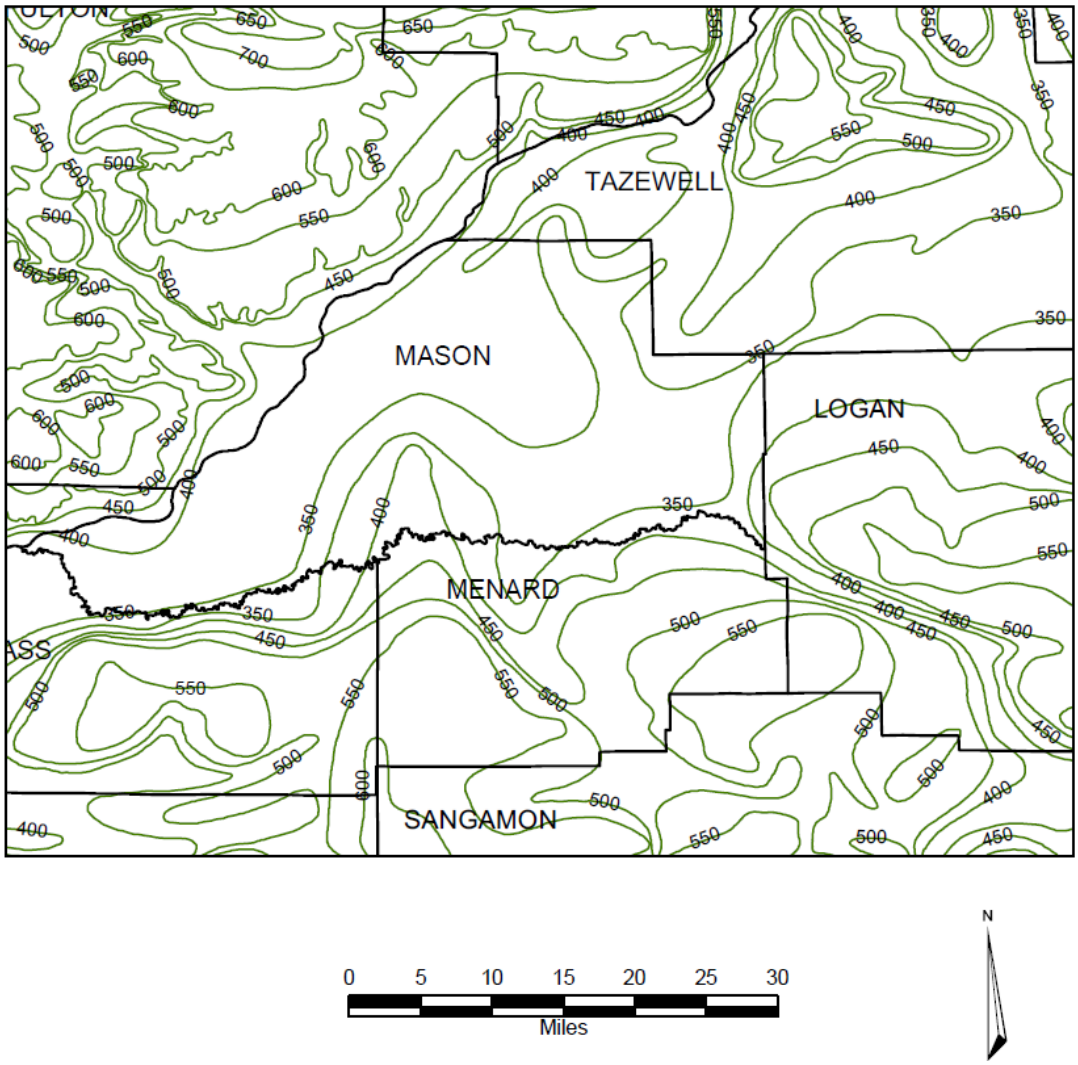

Figure 10. Topography of the bedrock surface in central Illinois (from Herzog et al., 1994).

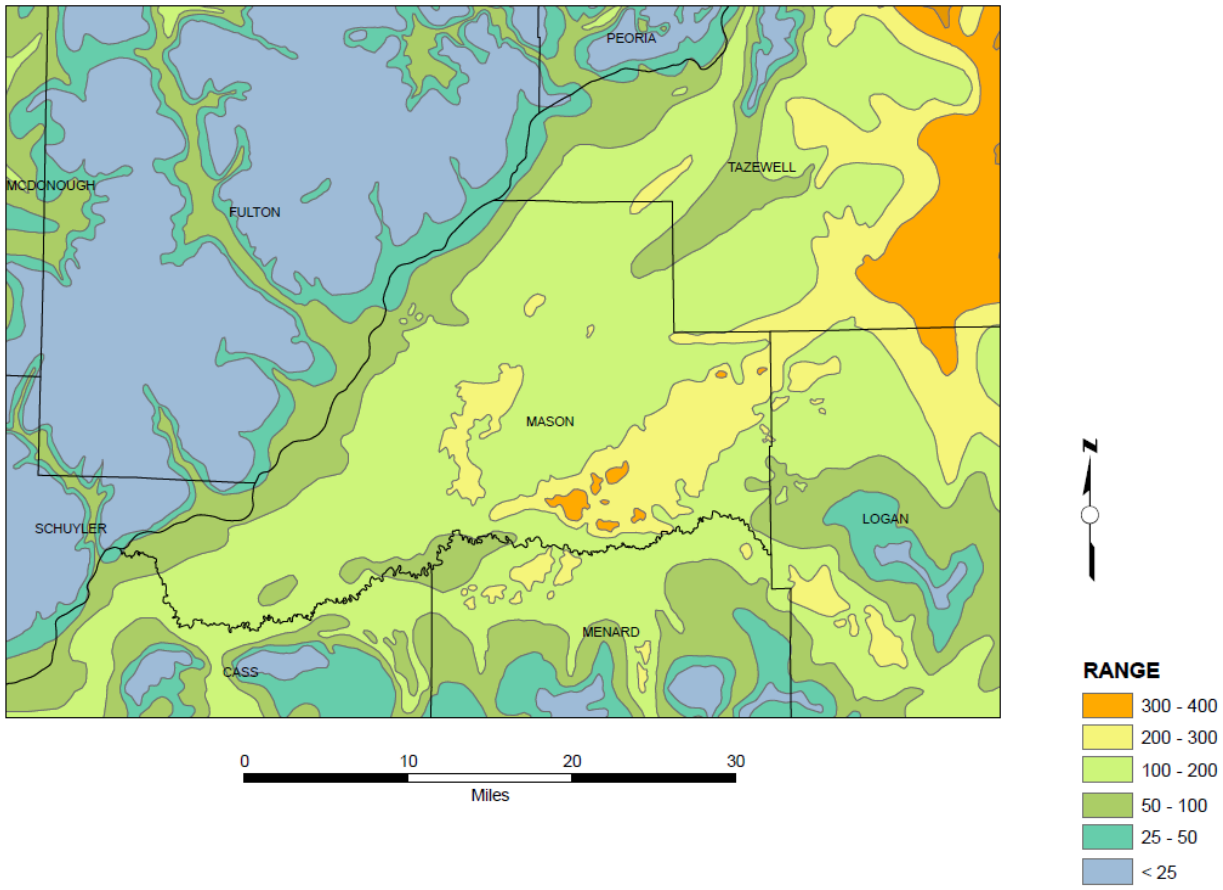

Figure 11. Thickness (feet) of sediments overlying bedrock in Mason County (from Piskin and Bergstrom, 1975).

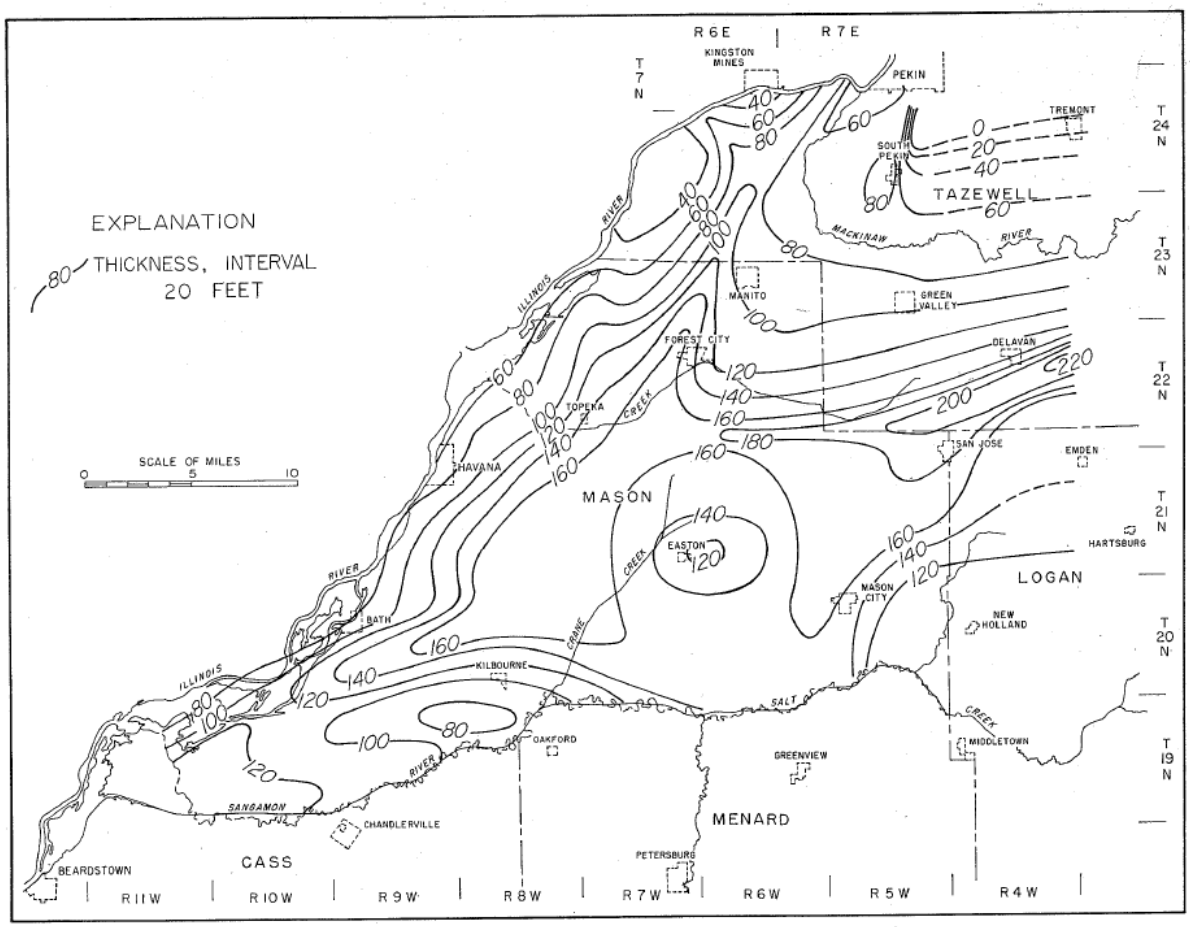

Figure 12. Saturated thickness of Mason County unconsolidated deposits in 1960 (from Walker et al., 1965).

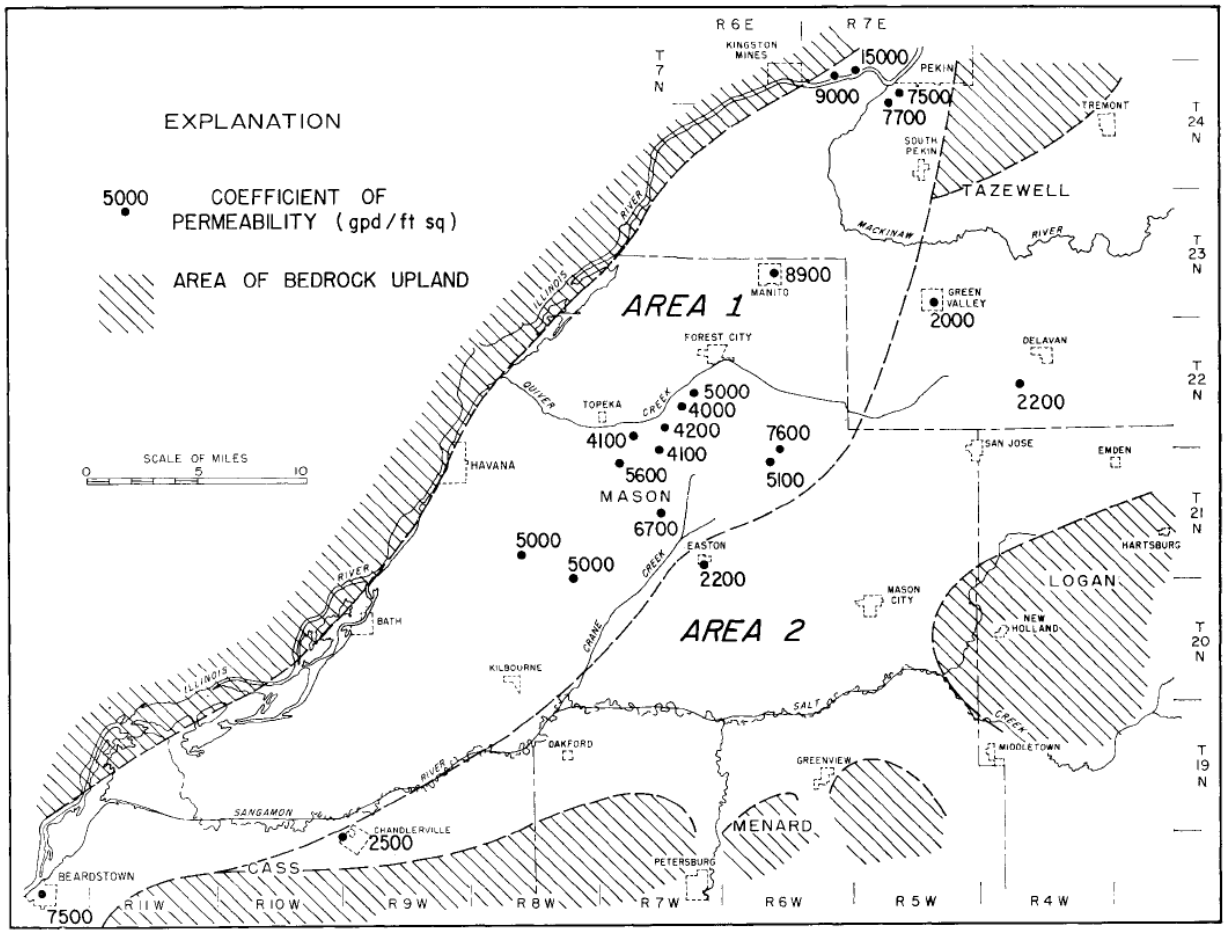

Figure 13. Areas of relatively high (Area 1) and low (Area 2) permeabilities of unconsolidated deposits (from Walker et al., 1965).

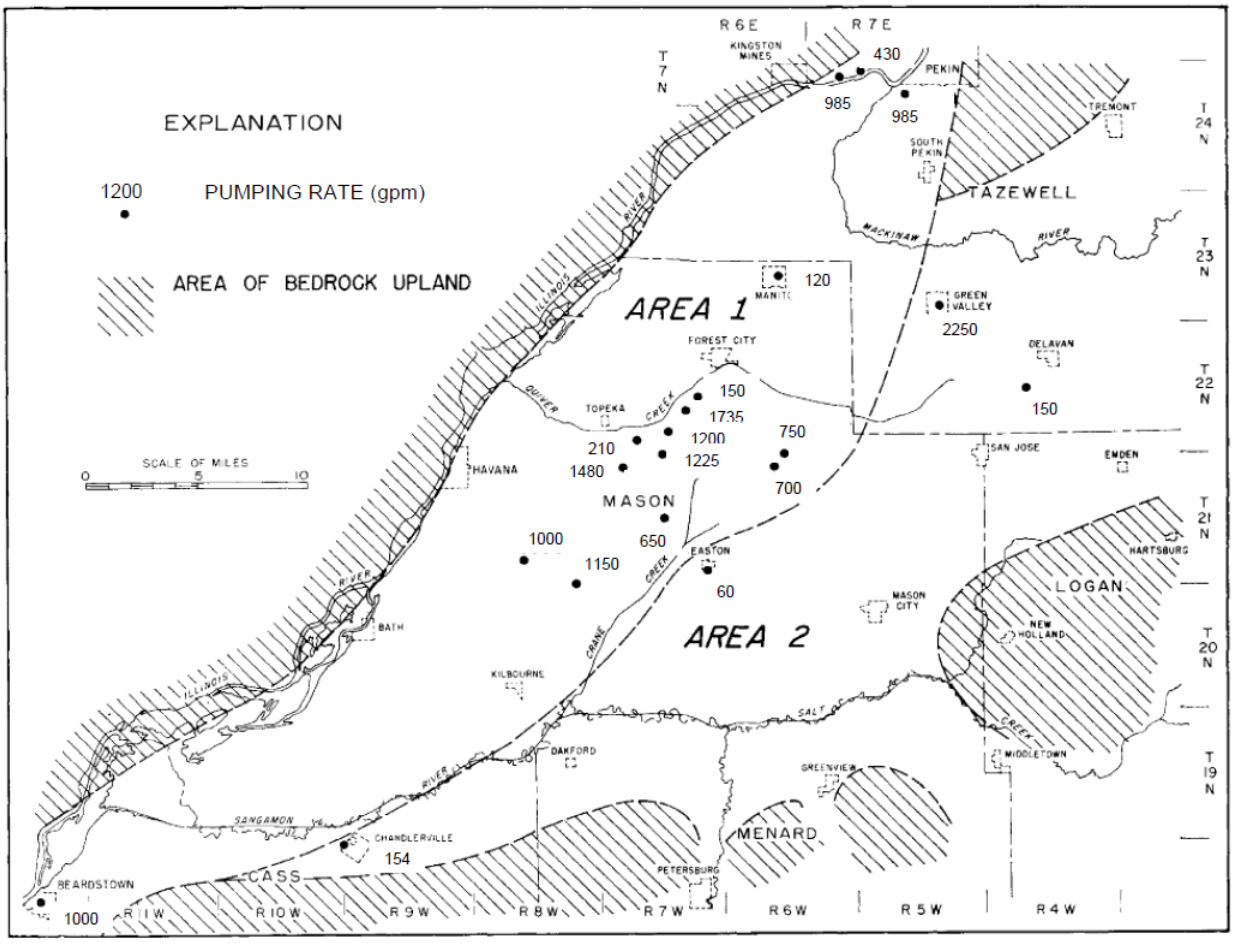

Figure 14. Pumping rates of some Mason County wells (from Walker et al., 1965).

ESTIMATE OF HEATING AND COOLING POTENTIALS BASED ON ASSESSMENT OF GROUNDWATER SOURCE HEAT PUMP PERFORMANCE

Groundwater Source Heat Pump Model

Figure 15 shows a schematic diagram of the groundwater source heat pump (GSHP) in both heating and cooling modes (Sauer and Howell, 1983; Kavanagh and Rafferty, 1997; Natural Resources Canada, 2002; Omer, 2008; Egg and Howand, 2011). In heating mode, groundwater is a heat source for a heat pump, which provides space heating or hot water. In cooling mode, groundwater is a heat sink for a heat pump, which provides space cooling or chilled water. Heat exchange often occurs indirectly through an additional heat exchanger in order to protect the more sensitive heat exchangers inside the heat pump. “Thermally used” groundwater that has passed through the heat exchanger is discharged either to a stream, pond, drainage ditch, or other such feature.

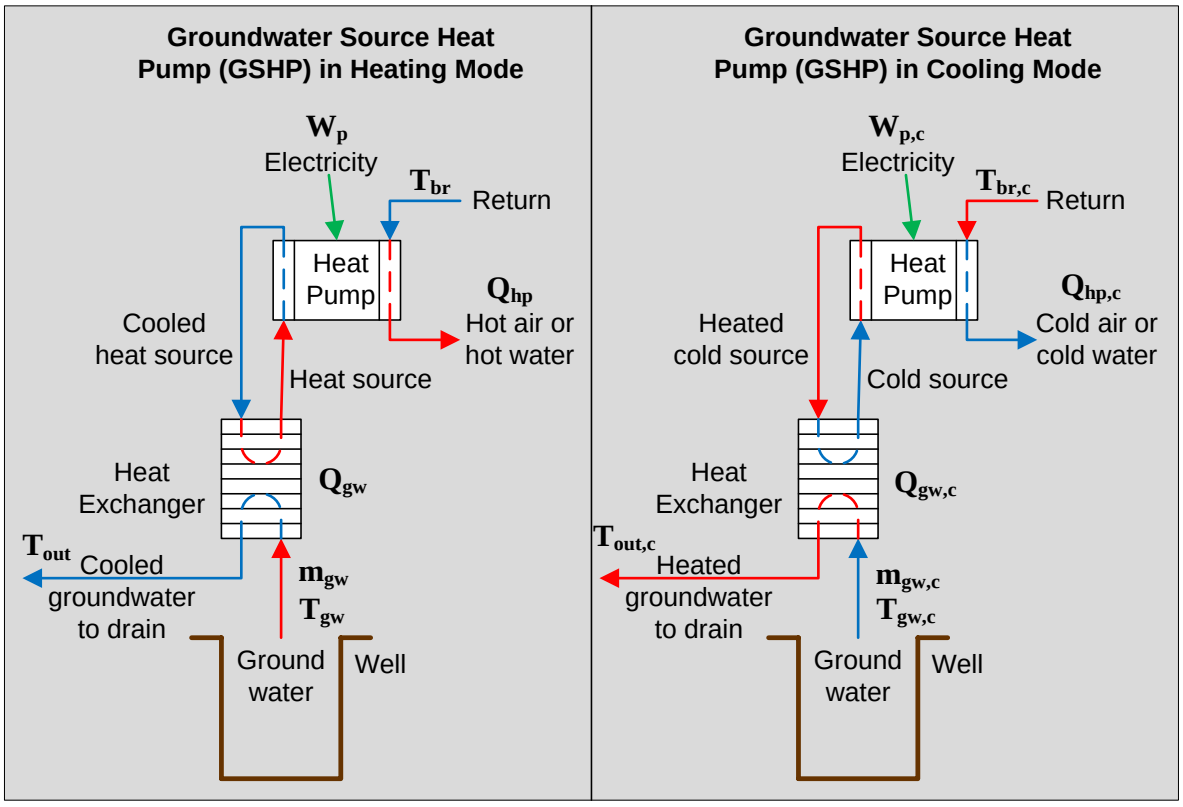

Figure 15. Schematic diagram of a ground source heat pump in heating and cooling mode.

Energy Balance of the GSHP System for Heating Mode

The heat exchanged between a GSHP and groundwater is given by Equation 1,

$$Q_{gw} = m_{gw} C_p \Delta T \tag{1}$$

where Q_{gw} is the groundwater heating potential in kilowatts (kW), m_{gw} is the mass flow rate of groundwater into the heat exchanger in kilograms per second (kg/s), C_p is the specific heat of water, 4.18 kilojoules per kilogram per degree celsius (kJ/kg·°C), and ΔT is the temperature difference in °C between the supply water and return water of the (groundwater) heat exchanger, as shown in Figure 15. In heating mode, ΔT is given by Equation 2,

$$\Delta T = T_{gw} - T_{out} \tag{2}$$

where T_{gw} is the groundwater temperature, i.e., supply water temperature to the heat exchanger, and T_{out} is the outlet groundwater temperature from the heat exchanger. In heating mode, it is cooled groundwater to discharge.

To determine the heat pump heating capacity, the coefficient of performance (COP) of a heat pump (Equation 3) is usually used.

$$COP = \frac{Q_{HP}}{W_p} \tag{3}$$

In Equation 3, Q_{HP} is the real heating capacity supplied by the heat pump to the buildings or users (kW) and W_p is the power (electricity) necessary to operate the heat pump (usually used by the compressor of the heat pump) (kW). COP is dimensionless. Q_{HP} is determined from Equation 4.

$$Q_{HP} = Q_{gw} + W_p \tag{4}$$

Combining Equations 3 and 4 gives Equation 5, the relationship between Q_{HP} and Q_{gw}.

$$Q_{HP} = \left(\frac{COP}{COP - 1} \right) Q_{gw} \tag{5}$$

The real heating capacity (heating potential) of a heat pump (Q_{HP}) can be estimated once the groundwater heating potential Q_{gw} and COP of the heat pump are known.

Energy Balance of the GSHP System for Cooling Mode

The heat exchanged between GSHP and groundwater in cooling mode, $Q_{gw,c}$, the groundwater cooling potential, is given by Equation 6

$$Q_{gw,c} = m_{gw,c} C_p \Delta T \tag{6}$$

where $m_{gw,c}$ is the mass flow rate of groundwater into the heat exchanger in cooling mode as shown in Figure 15, in kg/s, and ΔT is the temperature difference between the return water of the groundwater heat exchanger and the supply water from the well. In cooling mode, ΔT_c is expressed as

$$\Delta T_c = T_{out,c} - T_{gw,c} \tag{7}$$

where $T_{out,c}$ is the outlet groundwater temperature at the heat exchanger in cooling mode or the temperature of the heated groundwater to discharge and $T_{gw,c}$ is the groundwater temperature supplied to the heat exchanger in cooling mode.

To determine the heat pump cooling capacity, the coefficient of performance of a heat pump in cooling mode (COP_c) is usually used. COP_c is defined as follows,

$$COP_c = \frac{Q_{HP,c}}{W_{p,c}} \tag{8}$$

where $Q_{HP,c}$ is the real cooling capacity supplied by the heat pump to the buildings or users (kW) and $W_{p,c}$ is the power (electricity) necessary to operate the heat pump (kW). $Q_{HP,c}$ is determined as

$$Q_{HP,c} = Q_{gw,c} - W_{p,c} \tag{9}$$

Combining Equations 8 and 9, the relationship between $Q_{HP,c}$ and Q_{gw} is obtained:

$$Q_{HP,c} = \left(\frac{COP_c}{COP_c + 1} \right) Q_{gw,c} \tag{10}$$

Thus, the real cooling capacity (cooling potential) of a heat pump ($Q_{HP,c}$) can be estimated once the groundwater cooling potential $Q_{gw,c}$ and COP_c are known. Note that in cooling mode $Q_{HP,c} < Q_{gw,c}$, whereas in heating mode $Q_{HP} > Q_{gw}$.

Factors Affecting the Determination of Groundwater Heating and Cooling Potentials

In Eq. (1), C_p is a constant, so Q_{gw} is merely a function of m_{gw} and ΔT. The working temperature difference, ΔT, varies from case to case. The main factors that influence the value of ΔT are: 1. the supply water temperature; 2. the cost-effective return water temperature, which is usually determined based on engineering economics; 3. environmental regulations, such as the considerations of the issue of sensitivity of aquatic life to water temperature changes if the used groundwater is discharged to surface water bodies such as ponds, lakes, and rivers; and 4. groundwater quality, which requires us to consider the sensitivity of well scaling or corrosion to water temperature changes. The groundwater heating potential (Q_{gw}) can be estimated once m_{gw} and ΔT are determined. The groundwater cooling potential ($Q_{gw,c}$) can be determined in a similar way from Equations (6) and (7).

Groundwater Heat Pump Performance: COP and COP_c Values

To estimate the heat pump heating and cooling capacities (i.e., the real heating and cooling potentials to the building), it is necessary to know the COP and COP_c values as defined in Equations 3, 5, 8, and 10. Different commercial heat pumps have different COP or COP_c values (Sanner et al. 2003; Inalli and Esen 2004; Ozgener and Hepbasli 2005; Tarnawski et al. 2009). In this study, the ranges of COP and COP_c values are identified first based on the Buyer's Guide for the Commercial Earth Energy Systems by Natural Resources Canada (2002). For GSHP system applications, $3.0 < COP < 4.0$ for heating and $3.5 < COP_c < 6.7$ for cooling.

Cooling performance is sometimes expressed as the energy efficiency ratio (EER) (Sauer and Howell, 1983; Kavanaugh and Rafferty, 1997; Egg and Howand, 2011) and has dimensions of [Btu/hr-W], whereas COP_c is dimensionless. The relationship between EER and COP_c is $EER = COP_c \times 3.412$. The range of EER values for groundwater heat pumps is $11.0 < EER < 23.0$.

The effects of COP and COP_c values were considered in the calculations in the present work. A typical COP or COP_c value of a commercial heat pump was chosen to compare groundwater pumping rates for heating and cooling one-and two-story houses and to compare the models of heating and cooling loads. Sensitivity studies (based on the ranges of COP and COP_c values) were carried out to consider the influences of different COP and COP_c values on the heat pump heating and cooling potentials.

Weather Data and Groundwater Temperatures

Weather data are required to estimate the heating and cooling requirements of residential buildings (Zogou and Stamatelos, 1998). In this study, we used data from the Midwestern Regional Climate Center (MRCC) at the Illinois State Water Survey (ISWS) (http://mrcc.isws.illinois.edu/).

Weather data for Mason County (Table 3) was from the station at Mason City, IL. Weather data for the American Bottoms (Table 4) was from the Cahokia station which is the closest one to the study area. These data were used for estimating the heating and cooling requirements of typical residential houses in the two study areas.

Groundwater temperatures were taken from the ISWS groundwater quality database. Figure 16 is a box and whisker plot that shows the 10th, 25th, 50th (median), 75th, and 90th percentiles and values below the 10th and above the 90th percentiles as individual points. The values of the temperature statistics are given in Appendix B, Table B1. For both study areas, most of the data lie in a fairly narrow range; the 25th and 75th percentiles differ by only 1°C. As expected, the median temperature for the American Bottoms area (14.5°C) is higher than that for Mason County (14.0°C). Shallow groundwater temperature is related to the mean air temperature (NGWA, 2012).

Temperatures in the 25th to 75th percentiles for Mason County are similar to those measured on-site in nearby McLean and Tazewell Counties using a flow-through cell, a procedure expected to give reasonably accurate temperature measurements (Holm et al., 2004). They are within 1°C of average shallow groundwater temperatures mapped by the U.S. Environmental Protection Agency (USEPA, 2012).

Clearly, groundwater with a temperature above 20°C or below 13°C would be a valuable resource for geothermal heating or cooling. However, the temperatures below the 10th percentile or above the 90th percentile are probably inaccurate. The high outliers may have been measured in direct sunlight on hot days or at room temperature for samples brought to the laboratory. Similarly, the low outliers may have been measured in samples allowed to sit outside on cold days.

Table 3. Weather data used to estimate heating and cooling potentials in Mason County.

	JAN	FEB	MAR	APR	MAY	JUN	JUL	AUG	SEP	OCT	NOV	DEC	ANN
Max °F	33.1	39.2	52.0	65.1	75.6	84.3	87.4	85.5	79.5	67.3	51.0	37.6	63.1
Min °F	15.7	20.6	30.5	40.5	51.3	60.4	64.1	62.2	54.5	43.5	32.4	21.3	41.1
Mean °F	24.4	31.1	41.3	52.8	63.5	72.4	75.8	73.8	67.0	55.4	41.7	29.5	52.3
HDD*	1,259	983	736	375	150	11	0	10	59	312	698	1,102	5,695
CDD*	0	0	0	8	101	232	333	281	118	15	0	0	1,088

*HDD heating degree days; CDD cooling degree days; both base 65.

Table 4. Weather data to estimate heating and cooling potential of American Bottoms.

	JAN	FEB	MAR	APR	MAY	JUN	JUL	AUG	SEP	OCT	NOV	DEC	ANN
Max °F	38.1	44.5	55.4	66.7	75.7	84.2	88.7	86.8	79.7	69.1	54.6	42.6	65.5
Min °F	20.0	24.2	35.1	45.5	55.1	64.0	68.4	66.4	58.2	46.6	35.5	25.8	45.4
Mean °F	29.1	34.4	45.3	56.1	65.4	74.1	78.6	76.6	69.0	57.9	45.1	34.2	55.5
HDD	1,114	859	613	281	105	6	0	2	43	248	599	956	4,826
CDD	0	0	0	14	116	278	421	362	161	26	0	0	1,378

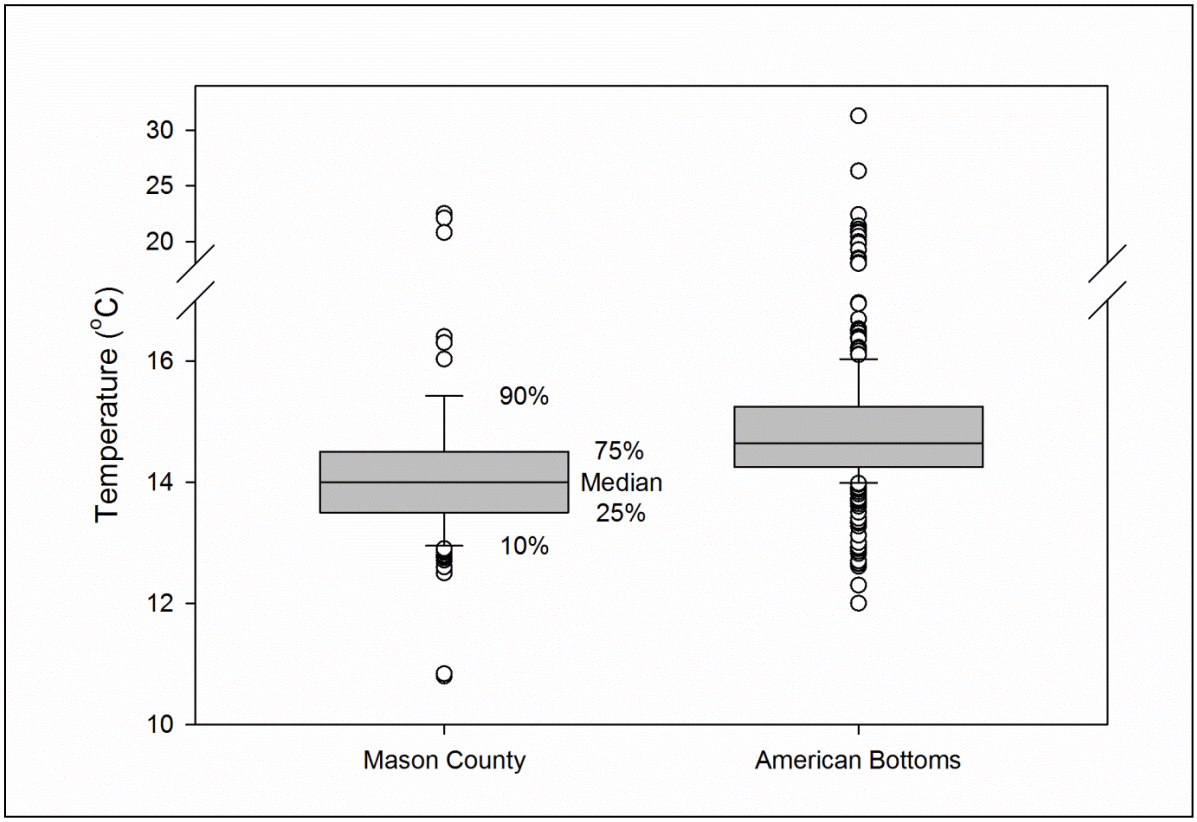

Figure 16. Box and whisker plot of groundwater temperatures in Mason County and the American Bottoms area (Madison and St. Clair Counties).

Inlet and Outlet Temperatures of the Heat Pump System

The median groundwater temperature in the two study areas is approximately 15°C. The 10^{th} and 90^{th} percentiles span the relatively narrow range of 13°C - 16°C. The inlet temperature in both heating (T_{gw}) and cooling ($T_{gw,c}$) modes was taken to be 15°C. In heating mode, DT was taken to be 5°C, so the outlet temperature of the heat exchanger (T_{out}, the temperature of the cooled groundwater to drain) was 10°C.

In cooling mode, the outlet temperature of the heat exchanger (the temperature of the heated groundwater to drain) is the sum of the building return temperature ($T_{br,c}$) and the heat exchanger approach (Anonymous 2002). The value of $T_{br,c}$ was taken as 24°C. The heat exchanger approach is 2°C for plate heat exchangers. Therefore, $T_{out,c}$ was 26°C .

Because the specific heat of water changes only 0.3% from 10°C to 26°C (Weast, 1972), (the range of temperatures for both heating and cooling calculations) the specific heat of water is essentially constant and the effects of temperature variations on thermal calculations are negligible.

Heating and Cooling Requirements of Typical Single-Family Houses

The heating and cooling requirements of typical residential houses at the two study areas were estimated using two models. One model is from a Lawrence Berkeley Laboratory (LBL) Report (Huang et al., 1986). Since the cooling correlation generated in that report was specific to southern California and Arizona, only the general form of the heating model in that report is used to estimate the heating requirements and is described below.

Huang et al. (1986) found that the monthly heating requirements of single-family houses in diverse areas of the U. S. are correlated with the number of heating degree days (equation 11),

$$HL = \left(k_{house} \times 24\right)\left(A \times HDD\right) \times 10^{-3} \tag{11}$$

where *HL* is the monthly heating load of the building (kW·hr), k_{house} is the overall heat transfer coefficient (W/°C), *A* is a dimensionless coefficient with values 0.87 for detached houses and 0.85 for townhouses, and HDD is the monthly heating degree days value (day·°C). Two prototype houses were considered. For a one-story (1540 ft^2) house, k_{house} = 223.2 W/°C (423.1 Btu/hr·°F), while for a two-story (2240 ft^2) house, k_{house} = 288.6 W/°C (547.0 Btu/hr·°F). Note that because HL is in kW·hr and Qhp in kW, the following relationship exists

$$Q_{HP} = \frac{HL}{t_{month}} \tag{12}$$

In Equation 12, t_{month} denotes the total number of hours in a month (30.5 days times 24 hours per day). Combining Equations 1, 5, and 12, the average mass flow rate $\bar{m}_{gw}$ can be calculated by

$$\bar{m}_{gw} = \frac{HL}{t_{month} C_p \Delta T \left(\frac{COP}{COP - 1}\right)} \tag{13}$$

Here, $\bar{m}_{gw}$ is the monthly average mass flow rate of groundwater (in kg/s) necessary to supply the monthly heating requirements, HL, in kW·hr.

The calculated $\bar{m}_{gw}$ values for each month at the two study areas are shown in Table A1 in Appendix A. The mass flow rate in kg/s is calculated first. It is then converted to gallons per minute (gpm) and in gpm/square foot, respectively. A COP value of 3.0 and a ΔT value of 5°C were chosen for the calculation.

The other model used for estimating the heating and cooling requirements was based on the spreadsheets available at www.moorepage.net (Moore, 2012). These spreadsheets calculate heat transfer based on parameters such as exterior surface area, R-value (resistance to heat transfer), and outside temperature. Surface areas were set to correspond to the one- and two-story houses in the Huang et al. (1986) model. Typical R-values suggested by Moore (2012) were used.

For the same two prototype houses and weather data used in the LBL model and taking COP = 3.0, the calculation of heating requirements (HL) is quite straightforward using this calculator. The value of the HL obtained from the calculator has a unit in Btu/hr, which is then converted into kW by dividing by a factor of 3.41. The corresponding values in gpm and in gpm/square foot for each month at the two study areas (Mason County and the American Bottoms) are given in Table A2 of Appendix A. The average well production rates for heating (in gpm) at Mason County and American Bottoms are shown in Figure 17 and Figure 18. As expected, the maximum flow rates are in the winter months and there is no heating requirement in the summer months. The average January flow rates for one-story and two-story houses were 2.86 and 2.22 gpm (25% difference).

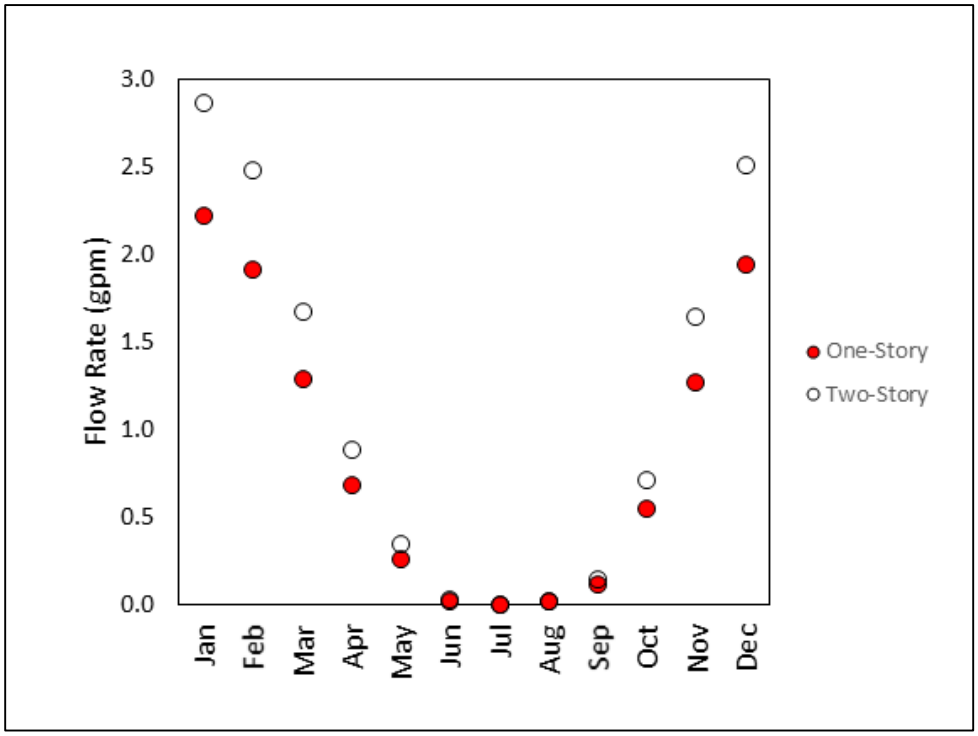

Figure 17. The average well production rate for heating in Mason County.

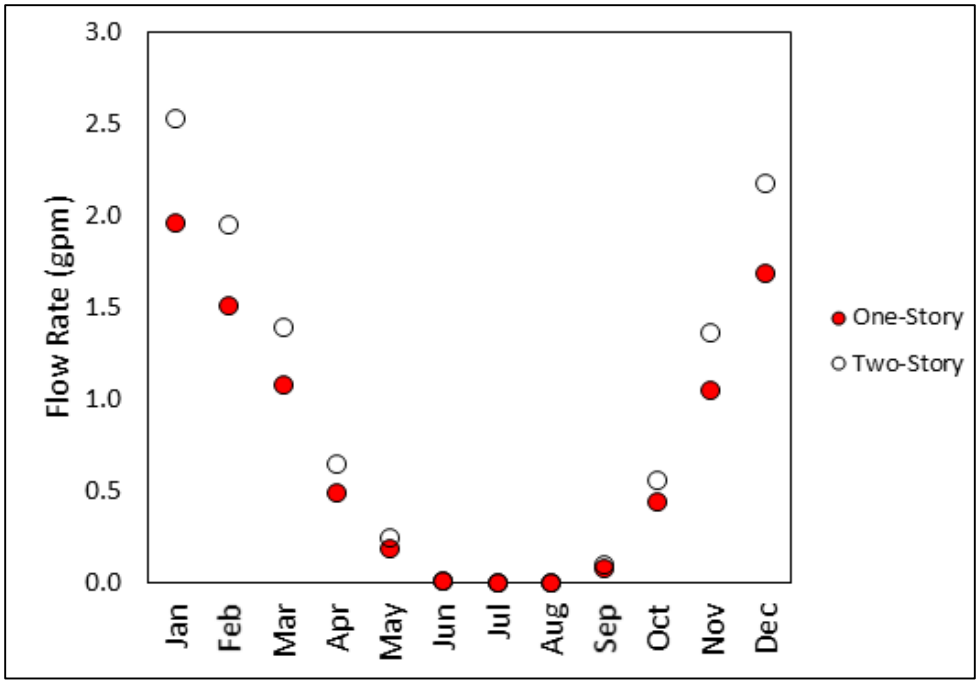

Figure 18. The average well production rate for heating in American Bottoms.

In the cooling mode, a similar calculation procedure is applied as for the heating mode. The following relationship, similar to Eq. (12), also exists:

$$Q_{HP,c} = \frac{HL_c}{t_{month}} \tag{14}$$

where HL_c is the cooling requirement obtained from the calculator.

Combining Equations 6, 10, and 14 gives an Equation for the monthly average mass flow rate of the groundwater ($\overline{m}_{gw,c}$ in kg/s) necessary to supply the monthly cooling requirement (Equation 15).

$$\overline{m}_{gw,c} = \frac{HL_c}{t_{month} C_p \Delta T_c \left(\frac{COP_c}{COP_c + 1} \right)} \tag{15}$$

The calculated mass flow rate in gpm and in gpm/square foot for each month in the two study areas is given in Table A3 in Appendix A. In this calculation, the value of COP_c is taken as 5.0. The average well production rates for cooling in gpm at Mason County and American Bottoms are shown in Figure 19 and Figure 20. As expected, the maximum flow rates for cooling are in the May to September time period. There is no cooling requirement from October through April. The July cooling flow requirements for one-story and two-story houses in Mason County were 3.11 and 2.87 gpm (8% difference).

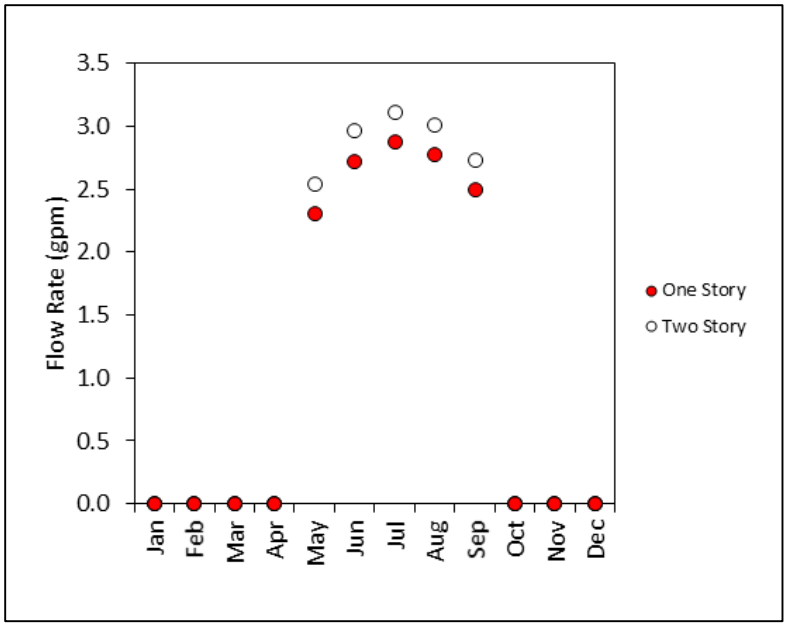

Figure 19. The average well production rate for cooling in Mason County.

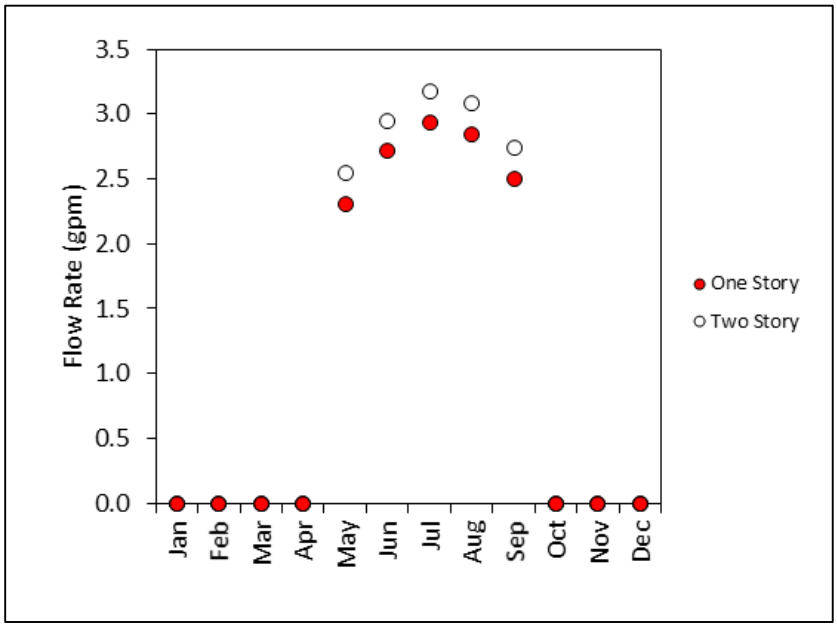

Figure 20. The average well production rate for cooling in American Bottoms.

Comparison of the Heating Requirements Estimated by the LBL and Moorepage Models

The estimated heating requirements obtained by the LBL Model and the Moorepage Model were compared to see whether they are close enough so that they can be considered to be first-order correct. The comparison of the heating requirements in Mason County and American Bottoms are shown in Figure 21 and Figure 22. The two models therefore agreed fairly well. For both study areas, the relative standard deviation (standard deviation divided by average value) of flow rates in a given month was better than 10%. This agreement gives confidence in the heating load estimates.

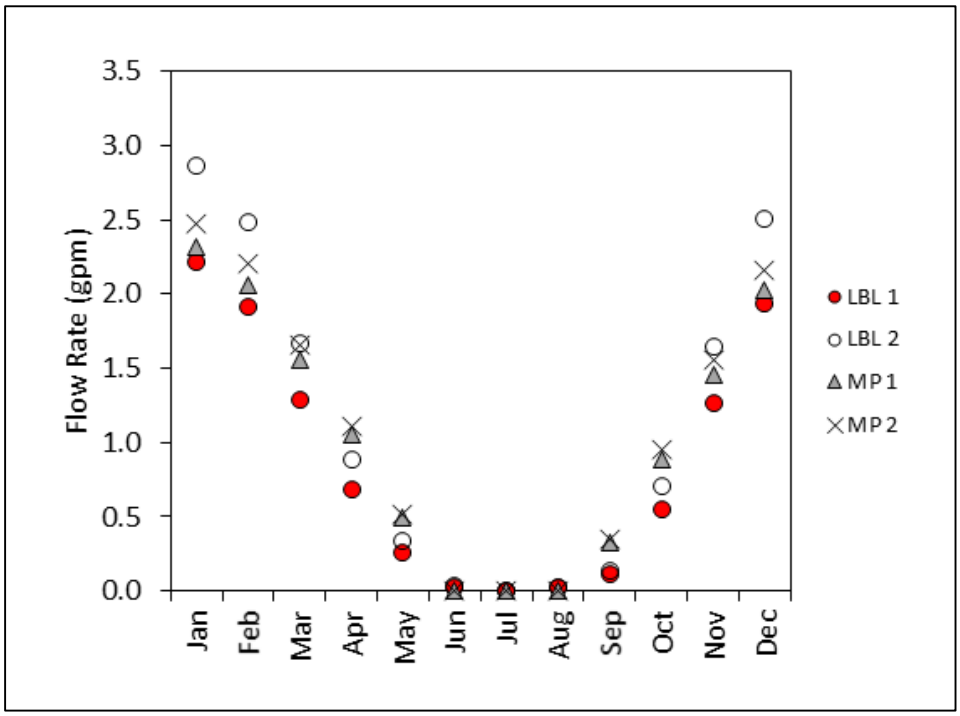

Figure 21. Comparison of the pumping rate to fulfill estimated heating requirements in Mason County. LBL 2 Lawrence Berkeley two-story. MP 1 Moorpage one-story. MP 2 Moorepage two-story.

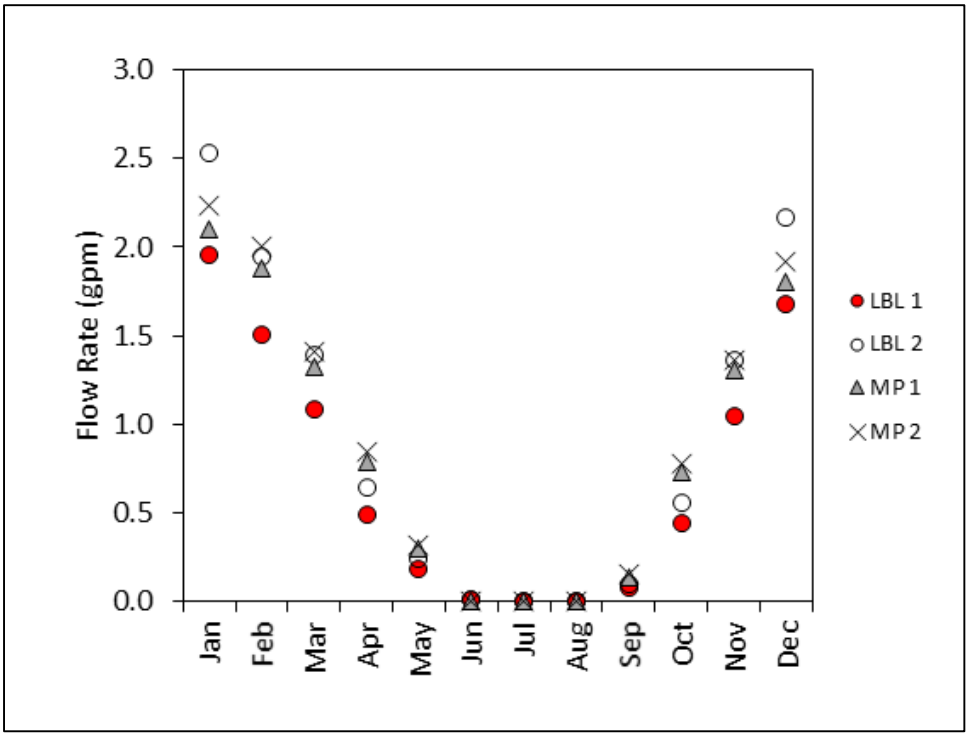

Figure 22. Comparison of the pumping rate to fulfill estimated heating requirements in American Bottoms. LBL 1 Lawrence Berkeley one-story. LBL 2 Lawrence Berkeley two-story. MP 1 Moorpage one-story. MP 2 Moorepage two-story.

Sensitivity Analysis of the Influence of COP and COP_c on Well Production Rates

To understand the influence of different values of COP or COP_c on the monthly average well production rates, a sensitivity study for both heating and cooling modes at the two study areas was carried out by varying the values of COP and COP_c within the typical ranges of commercial heat pump systems (Natural Resources Canada, 2002). Figure 23 and Figure 24 show the calculated results for a two-story house for the heating and cooling modes.

In the heating mode (Figure 23), for a given heating load of the two-story house, a heat pump system with a higher COP requires a higher well production rate. This relationship is shown in Eq. 5, which is easy to understand because a heat pump with a higher COP has a greater ability to withdraw heat from the groundwater per unit of input power (electricity). The highest monthly average well production rate occurs in January with COP = 4.0. It is 2.78 gpm in Mason County and 2.51 gpm in the American Bottoms.

In cooling mode (Figure 24), the lower the value of COP_c, the higher the well production rate for a given cooling load (Equation 10). As the cooling mode is the reverse cycle of the heating mode, a heat pump with a lower COP_c value has a lower ability to withdraw heat from the home per unit of input power (electricity). In other words, to supply a given cooling load to a home, a heat pump with a lower COP_c needs more power to operate than one with a higher COP_c and,

hence, the reason why more heat needs to be discharged to the groundwater. The highest monthly average well production rate occurs in July with COP_c = 3.0. For Mason County, the corresponding well production rate is 3.45 gpm, which is slightly lower than the rate of 3.52 gpm for the American Bottoms.

The pumping rates shown in Figures 18 – 25 are monthly averages. Building heating and cooling loads surely vary with the weather, time of day (or night), and other factors. A geothermal well and pump should probably be capable of at least twice the estimated monthly average pumping rate to satisfy peak heating and cooling loads.

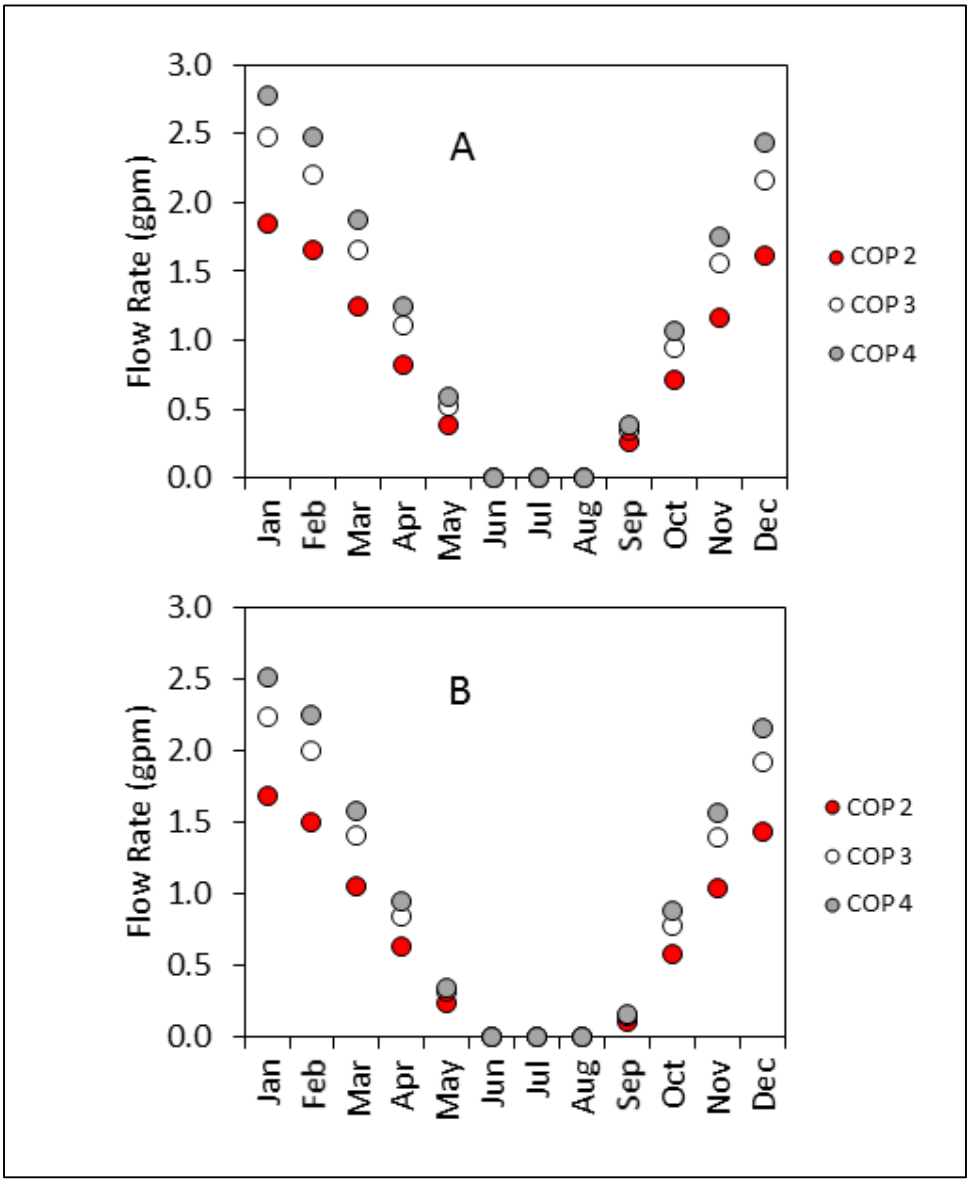

Figure 23. Sensitivity study showing the influence of different values of COP on the monthly average well production rates of heating mode. A. Mason County, B. American Bottoms.

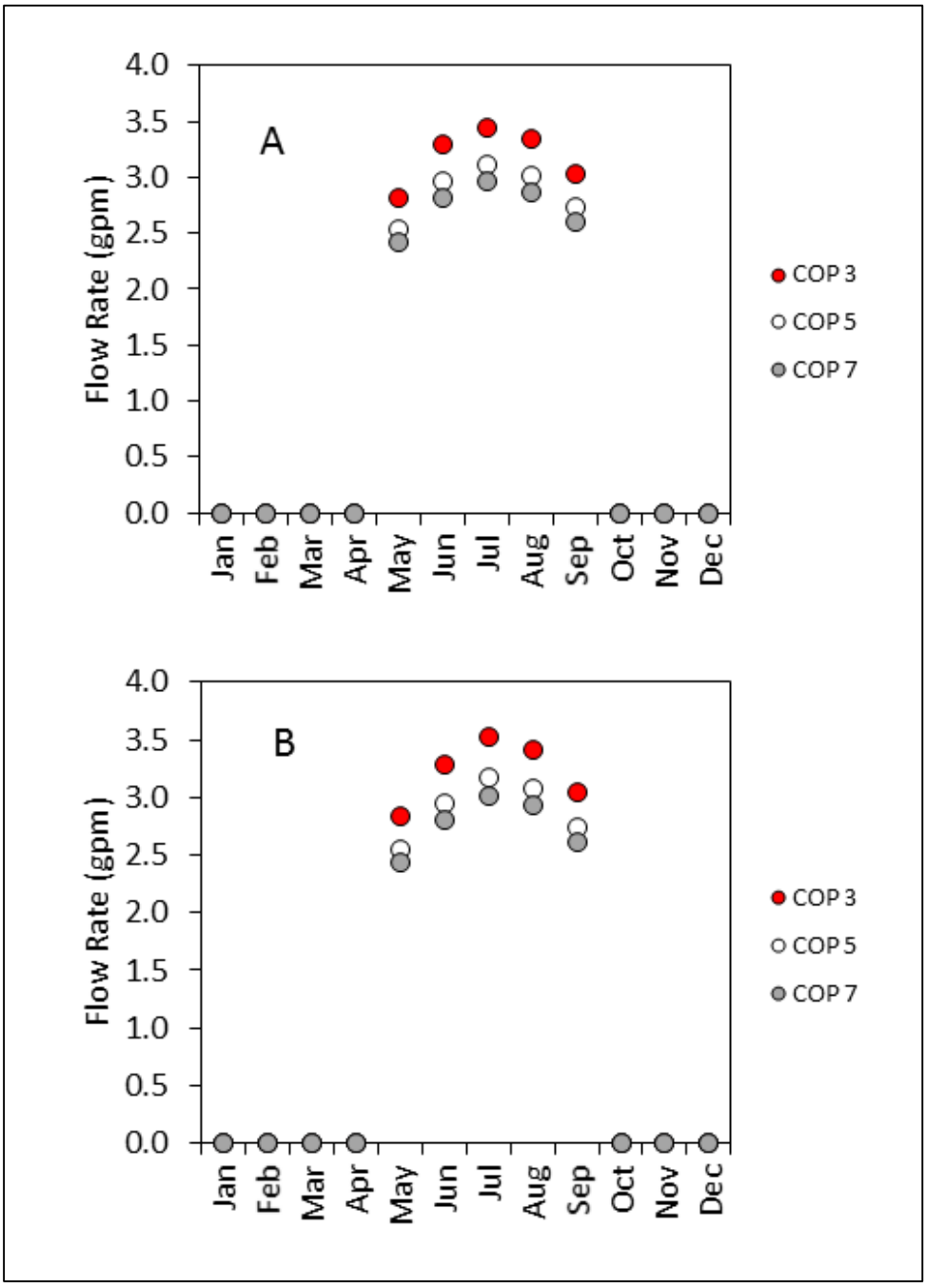

Figure 24. Sensitivity study showing the influence of different values of COP_c on the monthly average well production rates of cooling mode. A. Mason County. B. American Bottoms.

Estimate of Gross Heating and Cooling Potentials of the Study Areas

For both study areas, the well production rate of the cooling mode in July is greater than that of the heating mode in January. The values are 3.45 gpm for Mason County and 3.52 gpm for the American Bottoms. These maximum values were used to estimate the groundwater heating and cooling potentials for each area. Groundwater availability was estimated as follows:

(1) American Bottoms: The entire floodplain area of Madison and St. Clair Counties was considered. The pumping rates from Schicht (1965) were used for the calculation.

(2) Mason County: For this calculation the irrigation pumping estimate from Roadcap et al. (2011) was used as the pumping rate.

Given the documented pumping rates for each area, the total number of typical two-story single-family houses using GSHP was determined based on the highest monthly average well production rate per house (obtained in the last section). Then the monthly and yearly heating and cooling loads (potentials) in each studied area supplied by the groundwater were estimated.

Table 5 shows the subtotal pumping rate of each studied area and the estimated numbers of the typical two-story single-family houses that the GSHP can supply.

Table 5. Subtotal pumping rate of each study area and estimated numbers of the typical two-story houses that the ground source heat pump (GSHP) can supply.

	Single House Pumping Rate (gpm)	Total Area Pumping Rate (gpm)	Number of Houses that can be Heated and Cooled by GSHP	Equivalent Areas that can be Heated and Cooled by GSHP[1]
American Bottoms	3.52	24,411	6,935	1.6×10^7
Mason County	3.45	66,667	19,321	4.4×10^7

Notes: [1]two-story house, 2,240 ft^2

The Imperial Valley Water Authority includes all of Mason County and four adjacent townships in Tazewell County. Roadcap et al. (2011) estimated the irrigation pumping rate for this area as 128 mgd or 88,889 gpm. Mason County makes up ~75% of the water authority area. Therefore, we used 66,667 gpm as the potential pumping rate for Mason County. This pumping rate can supply groundwater to 19,324 two-story single-family houses to use GSHPs, equivalent to 4.3×10^7 ft^2 residential areas.

Table 6 shows the estimated groundwater heating potentials with GSHP applications in the studied areas. The monthly groundwater heating loads for COP = 2, 3, and 4 were calculated for each area. It can be seen that the highest heating load at each area corresponds to the COP = 4. In Mason County, the groundwater heating potential is 9.14×10^{11} Btu/year, equivalent to the total pumpage of 1.22×10^{10} gallons/year. In American Bottoms, the groundwater heating potential and the equivalent groundwater pumpage are 2.79×10^{11} Btu/year and 3.72×10^9 gallons/year, respectively.

Table 7 shows the estimated groundwater cooling potentials with GSHP applications in the study areas. The highest cooling load for each area corresponds to a COP value of 3. In Mason County, the groundwater cooling potential is 1.80×10^{12} Btu/year, which is equivalent to 1.33×10^{10} gallons/year. In the American Bottoms, the estimated groundwater cooling potential is 6.51×10^{11} Btu/year, which needs a groundwater supply of 4.82×10^9 gallons/year.

In summary, the sum of the heating and cooling potentials in Mason County is 3.61×10^{12} Btu/year or 3.81×10^{12} kJ/year. In American Bottoms, the total heating and cooling potentials is 9.30×10^{11} Btu/year or 9.81×10^{11} kJ/year. The sum of the heating and cooling potentials of the two study areas is 4.54×10^{12} Btu/year or 4.79×10^{12} kJ/year. The energy of 4.79×10^{12} kJ/year is equivalent to 1.33×10^9 kWh/year. To have a general idea of the value of 1.33×10^9 kWh/year, we compared it with the power generation of the UIUC Abbott Power Plant, which has a total installed capacity (steam turbine-generators) of 47.0 MW. If all the turbines were to run continuously for one year at their full loads, Abbott Power Plant could generate 4×10^8 kWh/year of electricity, which is only about one-third of the total heating and cooling potentials of the two study areas. In reality, the annual power generation of the Abbott Power Plant is much less than this value. For example, the electricity generated in 2005 was only 20,429 MW, which means the sum total of the heating and cooling potentials of the two studied areas is about 57 times the electricity generated at the Abbott Power Plant in 2005. This further indicates that the groundwater in the study areas has great heating and cooling potentials and can be a great resource for heat pump applications.

Table 6. Groundwater heating potentials for groundwater source heat pump applications for the two study areas.

Mason County 19,324 two-story houses													
	Jan	Feb	Mar	Apr	May	Jun	Jul	Aug	Sep	Oct	Nov	Dec	Total
Heating Load													
Per house (10^3 Btu/hr)	17.0	15.0	11.0	7.5	3.5	0	0	0	2.3	6.4	11.0	15.0	
Total (10^{10} Btu/mo)	23.0	21.0	16.0	10.0	4.9	0	0	0	3.3	8.9	15.0	20.0	122.0
Total groundwater heating load (10^{10} Btu/mo)													
COP = 2	12.0	10.0	7.8	5.2	2.5	0	0	0	1.6	4.5	7.3	10.0	61.0
COP = 3	15.0	14.0	10.0	7.0	3.3	0	0	0	2.2	5.9	9.7	14.0	81.3
COP = 4	17.0	15.0	12.0	7.8	3.7	0	0	0	2.5	6.7	11.0	15.0	91.4
Total well production rates (10^9 gal/mo)													
COP = 2	1.5	1.4	1.0	0.70	0.33	0	0	0	0.22	0.59	0.97	1.4	8.13
COP = 3	2.1	1.8	1.4	0.93	0.44	0	0	0	0.29	0.79	1.3	1.8	10.8
COP = 4	2.3	2.1	1.6	1.0	0.49	0	0	0	0.33	0.89	1.5	2.0	12.2
American Bottoms 6,935 two-story houses													
Heating Load													
Per house (10^3 Btu/hr)	15.0	13.5	9.5	5.7	2.1	0	0	0	1.0	5.3	9.4	12.9	
Total (10^{10} Btu/mo)	75.0	68.0	47.0	28.0	11.0	0	0	0	4.9	26.0	47.0	65.0	372.0
Total groundwater heating load (10^{10} Btu/mo)													
COP = 2	38.0	34.0	24.0	14.0	5.3	0	0	0	2.5	13.0	23.0	32.0	186.0
COP = 3	50.0	45.0	32.0	19.0	7.1	0	0	0	3.3	18.0	31.0	43.0	248.0
COP = 4	56.0	51.0	36.0	21.0	8.0	0	0	0	3.7	20.0	35.0	48.0	279.0
Total well production rates (10^8 gal/mo)													
COP = 2	5.0	4.5	3.2	1.9	0.7	0	0	0	0.3	1.8	3.1	4.3	24.8
COP = 3	6.7	6.0	4.2	2.5	0.9	0	0	0	0.4	2.3	1.2	5.7	33.0
COP = 4	7.5	6.8	4.7	2.8	1.1	0	0	0	0.5	2.6	4.7	6.5	37.2

Table 7. Groundwater cooling potentials for groundwater source heat pump applications for the two study areas.

Mason County 19,324 two-story houses													
	Jan	Feb	Mar	Apr	May	Jun	Jul	Aug	Sep	Oct	Nov	Dec	Per Year
Cooling Load													
Per house (10^4 Btu/hr)	0	0	0	0	1.7	2.0	2.1	2.0	1.8	0	0	0	
Total (10^{11} Btu/mo)	0	0	0	0	2.4	2.8	2.9	2.8	2.6	0	0	0	13.5
Total groundwater cooling load (10^{11} Btu/mo)													
$COP_c = 3$	0	0	0	0	3.2	3.7	3.9	3.8	3.4	0	0	0	18.0
$COP_c = 5$	0	0	0	0	2.9	3.3	3.5	3.4	3.1	0	0	0	16.2
$COP_c = 7$	0	0	0	0	2.7	3.2	3.3	3.2	2.9	0	0	0	15.4
Total well production rates (10^9 gal/mo)													
$COP_c = 3$	0	0	0	0	2.4	2.7	2.9	2.8	2.5	0	0	0	13.3
$COP_c = 5$	0	0	0	0	2.1	2.5	2.6	2.5	2.3	0	0	0	12.0
$COP_c = 7$	0	0	0	0	2.0	2.4	2.5	2.4	2.2	0	0	0	11.4
American Bottoms 6,935 two-story houses													
Cooling Load													
Per house (10^4 Btu/hr)	0	0	0	0	1.7	2.0	2.1	2.1	1.8	0	0	0	
Total (10^{11} Btu/mo)	0	0	0	0	0.9	1.0	1.1	1.0	0.9	0	0	0	4.9
Total groundwater cooling load (10^{11} Btu/mo)													
$COP_c = 3$	0	0	0	0	1.1	1.3	1.4	1.4	1.2	0	0	0	6.4
$COP_c = 5$	0	0	0	0	1.0	1.2	1.3	1.2	1.1	0	0	0	5.8
$COP_c = 7$	0	0	0	0	1.0	1.1	1.2	1.2	1.1	0	0	0	5.6
Total well production rates (10^8 gal/mo)													
$COP_c = 3$	0	0	0	0	8.5	9.8	11.0	10.0	9.1	0	0	0	48.4
$COP_c = 5$	0	0	0	0	7.6	8.8	9.5	9.2	8.2	0	0	0	43.3
$COP_c = 7$	0	0	0	0	7.3	8.4	9.0	8.8	7.8	0	0	0	41.3

GROUNDWATER QUALITY AND ITS POTENTIAL EFFECTS ON HEAT PUMP OPERATION

Groundwater quality may affect heat pump operation by coating heat exchanger surfaces (fouling), clogging well screens, and corroding metal pipes and fittings. Fouling gradually reduces heat transfer efficiency and increases the pressure drop in piping. Clogging of well screens, which is often caused by iron bacteria, may reduce pumping efficiency. Corrosion may result in increased maintenance costs and shortened lifetimes of system components. All of these processes may require costly maintenance. This chapter reviews groundwater quality as it may impact heat pump operation in Mason County and the American Bottoms area.

Methodology

The data were obtained from the ISWS groundwater quality database. The database was compiled from the ISWS Public Service Laboratory (PSL), ISWS groundwater research projects, and the Illinois Environmental Protection Agency (IEPA) ambient groundwater quality network. The IEPA data were for public water supply wells. The PSL data were for private and public wells. The ISWS project data were from private wells and wells drilled specifically for some projects.

Database queries for Mason County and those parts of Madison and St. Clair Counties in the American Bottoms area yielded 2,871 records, but the number of usable records was only a small fraction of the total. The ISWS PSL data go back to the early part of the twentieth century. Although data for the study areas are available from as early as 1902, only data from 1970 or later were used. Some wells had multiple records. Only the latest record was considered for these wells. Records that lacked more than one or two constituents of interest (given below) were not used. Although there is a field indicating whether the well water was treated or untreated, the information is not always reliable. Records with unusually low calcium and magnesium values were assumed to be for softened water and the records were not used. Table 8 shows the number of records chosen.

Table 8. Number of records from the ISWS water quality database.

	Mason County	St. Clair County*	Madison County*
Total records	510	754	1,607
Usable records	101	99	180

*Only records from the floodplain areas of these counties were considered.

Descriptive statistics, including mean, standard deviation, and quartiles, were calculated for each analyte. For analytes with some values listed as 0 or less than a detection limit (left-censored data), statistics were estimated using the Kaplan-Meier method (Helsel, 2011).

Chemical equilibrium modeling was performed using Visual Minteq (Gustafsson, 2012). This program uses the same thermodynamic database and computational methods as MinteqA2 (Allison et al., 1991; Allison et al., 1996), which was developed for the U.S. Environmental Protection Agency. Two kinds of modeling were performed, descriptive and predictive. For both kinds of modeling, the input includes the temperature, pH, and total dissolved concentrations of calcium, magnesium, sodium, iron, carbonate, chloride, and sulfate (the components). These solutes are expected to affect scale deposition. A system of coupled linear mass balance and nonlinear mass action equations is solved to give the free (uncombined) concentrations of the components (Morel and Morgan, 1972).

Descriptive equilibrium modeling was performed with the pH fixed at the measured value, at the median temperature of the area of interest (14.0°C for Mason County or 14.6°C for American Bottoms), and without precipitation of any minerals. This type of modeling gives the speciation of the component ions (the distribution among the various chemical forms) and saturation indices (defined below) for the minerals that could be formed from the components.

The saturation index can be explained using an example. The dissolution and precipitation of calcite, a form of calcium carbonate, are described by Equation 16, where *s* and *aq* indicate solid and aqueous phases and the double arrow indicates equilibrium.

$$CaCO_3(s) \rightleftharpoons Ca^{2+}(aq) + CO_3^{2-}(aq) \tag{16}$$

The concentrations of Ca^{2+} and CO_3^{2-} at equilibrium are related by Equation 17, where K_{so}' is the conditional solubility product, which is valid for a particular temperature and ionic strength, and square brackets indicate molar concentrations.

$$K_{so}' = [Ca^{2+}][CO_3^{2-}] \tag{17}$$

The saturation index of a water sample is given by Equation 18 (Nordstrom and Munoz, 1986; Stumm and Morgan, 1996).

$$SI = Log_{10}\frac{[Ca^{2+}][CO_3^{2-}]}{K_{so}'} \tag{18}$$

A system (water plus calcite) that is at equilibrium with respect to calcite is said to be saturated and has an SI value of 0 (or “nearly” 0). A range of $-0.3 < SI < 0.3$ allows for uncertainties in pH, concentration of Ca, alkalinity (from which $[CO_3^{2-}]$ is calculated), and the value of the solubility product. Appendix C shows how the different variables affect the uncertainty of SI. If the SI value is greater than 0.3, the water is said to be oversaturated and has a tendency to precipitate $CaCO_3$. Conversely, an SI value less than -0.3 indicates the water is undersaturated

and has a tendency to dissolve $CaCO_3$. The saturation indices of calcite and siderite ($FeCO_3$) are of particular interest because these two substances may foul heat exchangers.

In predictive or mass-transfer modeling, the pH is allowed to vary (there is a mass balance on H^+ as well as the other components) and minerals that are oversaturated are allowed to precipitate. The total dissolved H^+ concentration is calculated in descriptive modeling. Equilibrium modeling gives the maximum amounts of $CaCO_3$ and $FeCO_3$ that could form for the given conditions.

The solubility products of both calcite and siderite decrease as the temperature increases and increase as temperature decreases (Singer and Stumm, 1970; Plummer and Busenberg, 1982; Greenberg and Tomson, 1992). As a result, space cooling (transferring heat to groundwater) causes these minerals to become less soluble and there is an increased tendency for fouling. Conversely, heating (transferring heat from groundwater), causes these minerals to be more soluble. Scale deposition is only expected to be an issue for cooling with a groundwater heat pump and not with heating. The temperatures used for mass transfer modeling were 24.0°C for Mason County and 24.6°C for American Bottoms, the median of the temperature of the area of interest plus 10°C (the ΔT value for cooling).

Chemical equilibrium calculations were performed for all data sets with entries for pH, calcium, magnesium, sodium, iron, alkalinity, chloride, and sulfate and charge balance errors of 5% or less. Although there are at least three known polymorphs of calcium carbonate (calcite, aragonite, and vaterite), calcite is the form that precipitates at temperatures below 30°C (Cho et al., 1997). Dolomite (calcium-magnesium carbonate) does not precipitate from oversaturated solutions at 25°C (Drever, 1982). For these reasons, saturation indices of aragonite, vaterite, and dolomite are not reported for descriptive modeling, and precipitation of these minerals was not allowed in mass transfer modeling.

Results and Discussion

Groundwater Chemistry

Table 9 summarizes the concentrations of solutes likely to affect fouling and corrosion in Mason County groundwater. The data are described by the statistics mean, standard deviation, minimum, maximum, and quartiles (including the median). For some solutes there were missing data or undetectable concentrations. Statistics for other solutes are given in Appendix B.

Table 9. Mason County groundwater quality, solutes that may form scale deposits or affect scale deposition.

	pH	Ca	Mg	Na	Fe	Alkalinity	Cl^-	SO_4^{2-}	Si
Units		mg/L	mg/L	mg/L	µg/L	mg/L as $CaCO_3$	mg/L	mg/L	mg/L
Records with no data	35	27	27	36	0	0	2	39	83
Nondetects	0	0	0	1	25	0	4	0	0
Mean	7.78	65.0	24.9	6.1	779.7	192.0	13.3	58.0	14.6
Standard Deviation	0.35	18.7	9.6	5.9	1,520.6	66.3	54.5	97.3	4.0
Maximum	8.20	122.0	55.2	46.0	7,600.0	489.0	540.0	792.0	22.4
75th Percentile	8.00	73.8	30.0	7.0	796.0	220.0	11.5	55.3	17.8
Median	7.85	64.5	22.7	4.6	100.0	179.0	5.3	40.9	14.0
25th Percentile	7.71	49.9	17.4	3.3	20.0	146.0	2.8	27.4	11.8
Minimum	6.60	35.6	11.7	0.0	*	82.7	0.0	9.6	8.0

Notes: total records 101; * indicates minimum value was below detection.

The charge balance is an indicator of data quality. Aqueous solutions are electrically neutral, i.e., the sum of cation charges equals the sum of anion charges (Stumm and Morgan, 1996). The apparent charge imbalance, a data artifact, can be expressed by the charge balance error, which is based on the so-called major ions calcium, magnesium, sodium, bicarbonate, sulfate, and chloride (Equations 19-21).

$$TotCation = 2[Ca^{2+}] + 2[Mg^{2+}] + [Na^{+}] + [K^{+}] \tag{19}$$

$$TotAnion = [HCO_3^{-}] + 2[CO_3^{2-}] + [Cl^{-}] + 2[SO_4^{2-}] \tag{20}$$

$$CBE = \frac{2\left|TotCation - TotAnion\right|}{TotCation + TotAnion} \times 100\% \tag{21}$$

Of the 56 Mason County records that had entries for all of the major cations and anions, 24 (42%) had charge balance errors of 5% or less.

Figure 25 summarizes the major ion composition of Mason County groundwater in a Piper diagram. In this type of graph, the relative concentrations of the metal cations calcium, magnesium, sodium, and potassium are plotted as fractions of the total cationic charge on the left-hand trilinear diagram and the anions chloride, sulfate, and bicarbonate/carbonate are plotted as fractions of the total anionic charge on the left-hand diagram. The diamond plot is a projection of the two trilinear plots. The ion concentrations are in units of equivalents per liter (molar concentration multiplied by ionic charge) (Hem, 1985). Only data sets with charge balance errors of 5% or less were plotted. The dominant cation in Mason County groundwater was calcium (50 to 65% of cation charge in most samples). Magnesium and sodium plus potassium accounted for 30 to 45% and 5 to 15% of cation charge, respectively. The dominant anion was bicarbonate, which made up 75 to 95% of anion charge. Chloride and sulfate accounted for 0 to 15% and 0 to 20% of the anion charge.

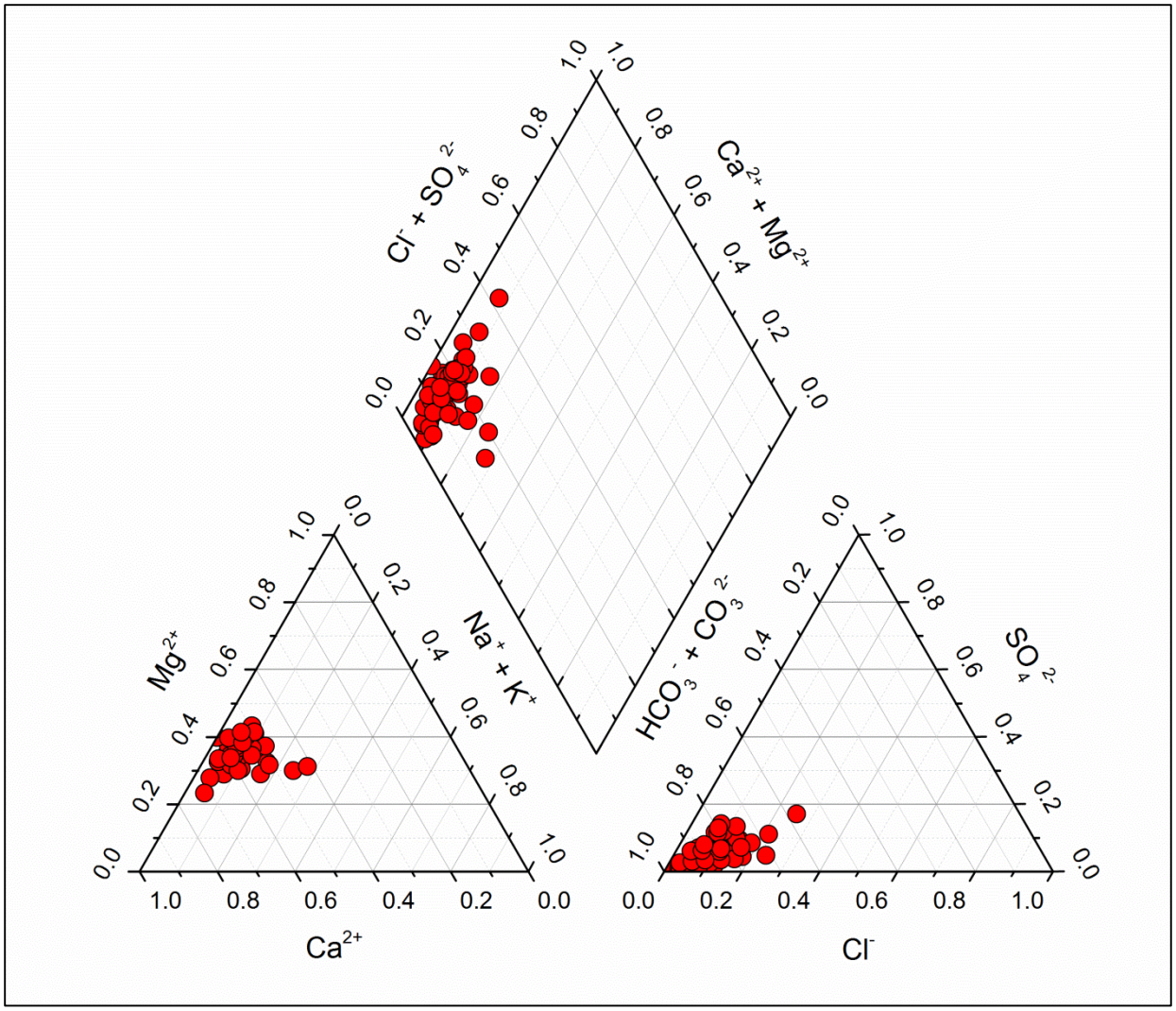

Figure 25. Piper diagram showing the relative concentrations of cations and anions in Mason County groundwater.

Table 10 summarizes the concentrations of solutes likely to affect fouling and corrosion in groundwater in the American Bottoms area. The data are described by the statistics mean, standard deviation, minimum, quartiles, and maximum. For some solutes, there were missing data or undetectable concentrations. Statistics for other solutes are given in Appendix B.

As for Mason County, only data sets for which the charge balance error was 5% or less were used for the Piper plot for American Bottoms (Figure 26). The dominant cation and anion in American Bottoms groundwater were also calcium (35 to 55%) and bicarbonate (40 to 80%). Magnesium and sodium plus potassium accounted for 30 to 50% and 5 to 30% of cation charge, respectively. Chloride and sulfate accounted for 0 to 50% and 0 to 30% of the anion charge, respectively. The charge balance of the American Bottoms data was somewhat better than that of

Mason County. Of the 83 American Bottoms records that had entries for all of the major cations and anions, 62 (75%) had charge balance errors of 5% or less.

The concentrations of the major ions in Mason County and American Bottoms groundwater are presented in Figure 27 and Figure 28. The concentration units were mg/L for Ca, Mg, Na, Fe, and chloride; mg/L as $CaCO_3$ for alkalinity; and mg/L as SO_4 for sulfate. For both areas, the range of concentrations of calcium and magnesium and the alkalinity values were relatively narrow (less than a factor of two). The ranges of iron and chloride, on the other hand, covered 1.5 to 3.0 orders of magnitude. Statistics on all solutes are given in Appendix B.

Table 10. American Bottoms groundwater quality, solutes that may form scale deposits or affect scale deposition.

	pH	Ca	Mg	Na	Fe	Alkalinity	Cl^-	SO_4^{2-}	Si
Units		mg/L	mg/L	mg/L	µg/L	mg/L as $CaCO_3$	mg/L	mg/L	mg/L
Records with no data	49	31	31	31	3	1	3	25	55
Nondetects	0	0	0	0	10	0	0	3	0
Mean	7.23	109.1	34.5	40.0	5,156.8	302.9	43.2	133.7	26.3
Standard Deviation	0.49	42.6	15.9	52.5	5,306.7	87.3	59.7	127.7	6.6
Maximum	8.40	235.0	122.0	261.0	26,000.0	668.0	415.0	902.0	38.7
75th Percentile	7.60	130.5	43.7	41.2	7,277.5	351.5	49.4	159.0	30.2
Median	7.30	100.0	31.3	17.5	3,550.0	303.5	21.1	98.1	27.7
25th Percentile	6.84	79.9	22.5	13.0	833.8	237.0	10.0	63.7	23.1
Minimum	6.15	38.1	9.3	4.5	*	124.0	1.0	*	7.5

Notes: total records 119; * indicates minimum value below detection.

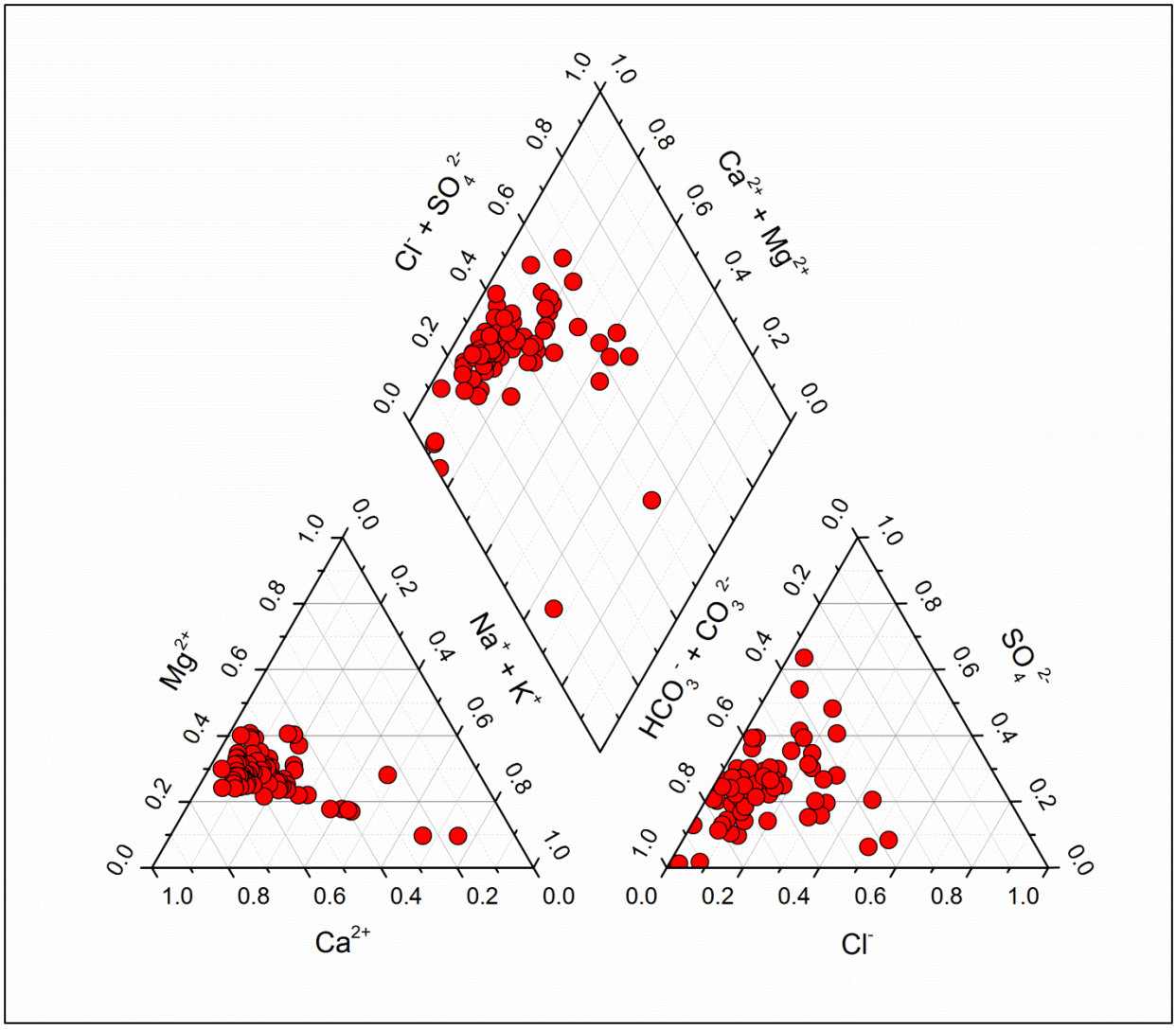

Figure 26. Piper diagram showing the relative concentrations of cations and anions in American Bottoms groundwater.

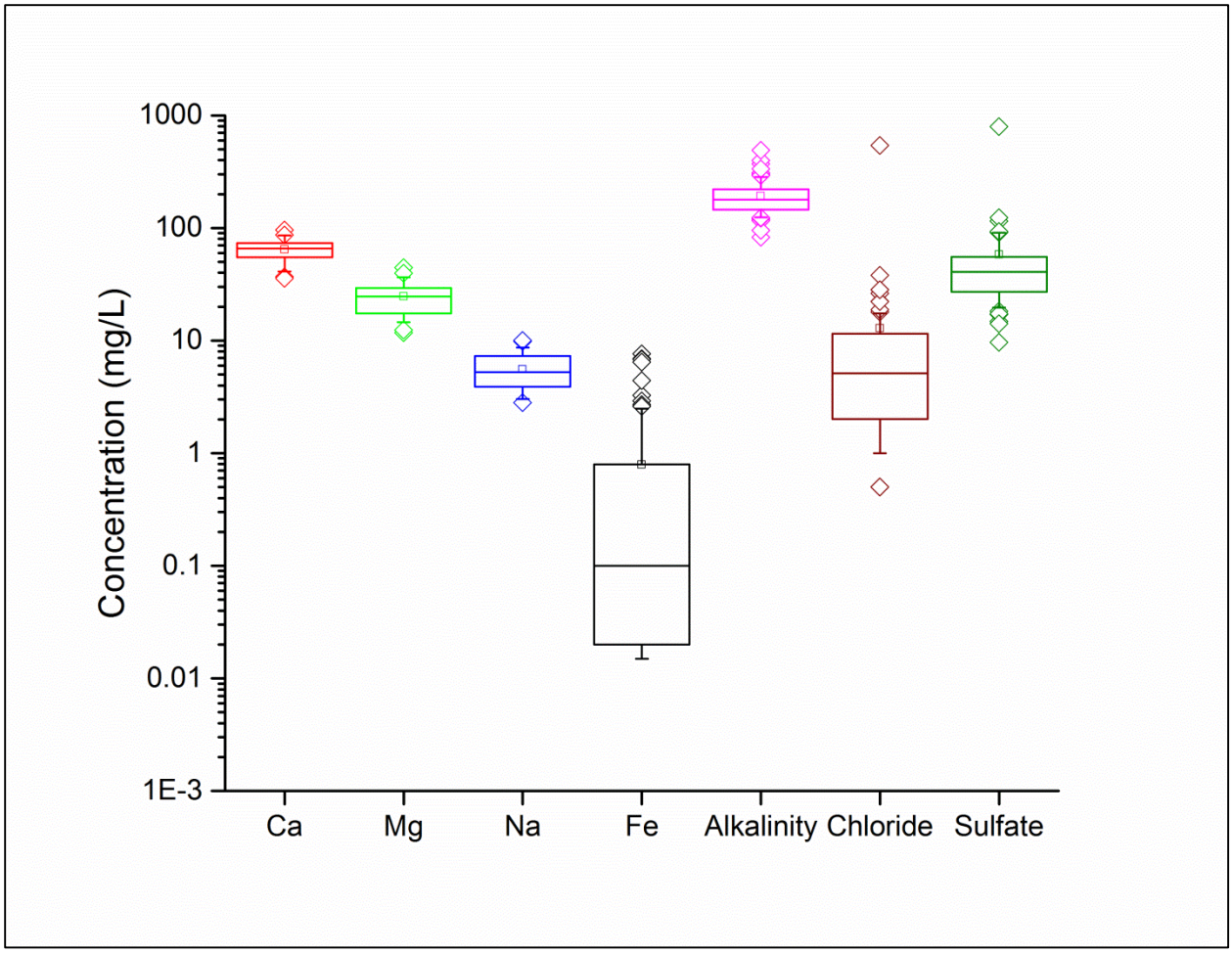

Figure 27. Box and whisker plot of concentrations of major ions and iron in Mason County groundwater.

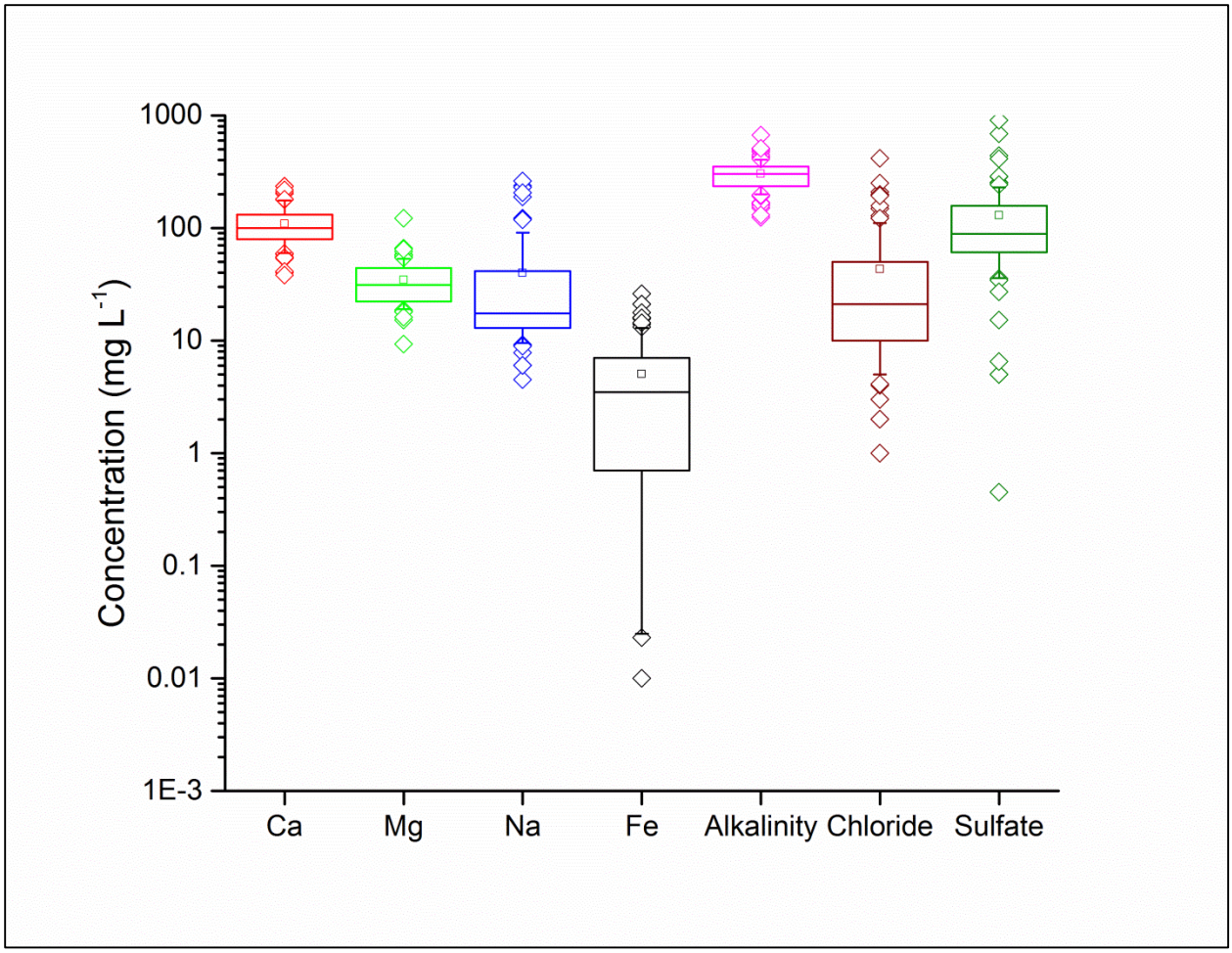

Figure 28. Box and whisker plot of concentrations of major ions and iron in American Bottoms groundwater.

Solubility Calculations

In descriptive modeling, all Mason County data sets showed calcite to be saturated (-0.3 < SI < 0.3) to oversaturated (SI > 0.3). Only about half of the American Bottoms data sets were saturated to oversaturated with respect to calcite (Figure 29), despite the higher median values of Ca and alkalinity. The median SI for Mason County was 0.4, while for the American Bottoms area, it was 0.1. The difference was most likely due to lower pH values for the American Bottoms area. Roughly half of the Mason County data sets were saturated or oversaturated with respect to siderite ($FeCO_3$), compared to three-fourths of the American Bottoms data sets. The difference was most likely due to higher iron concentrations in the American Bottoms samples.

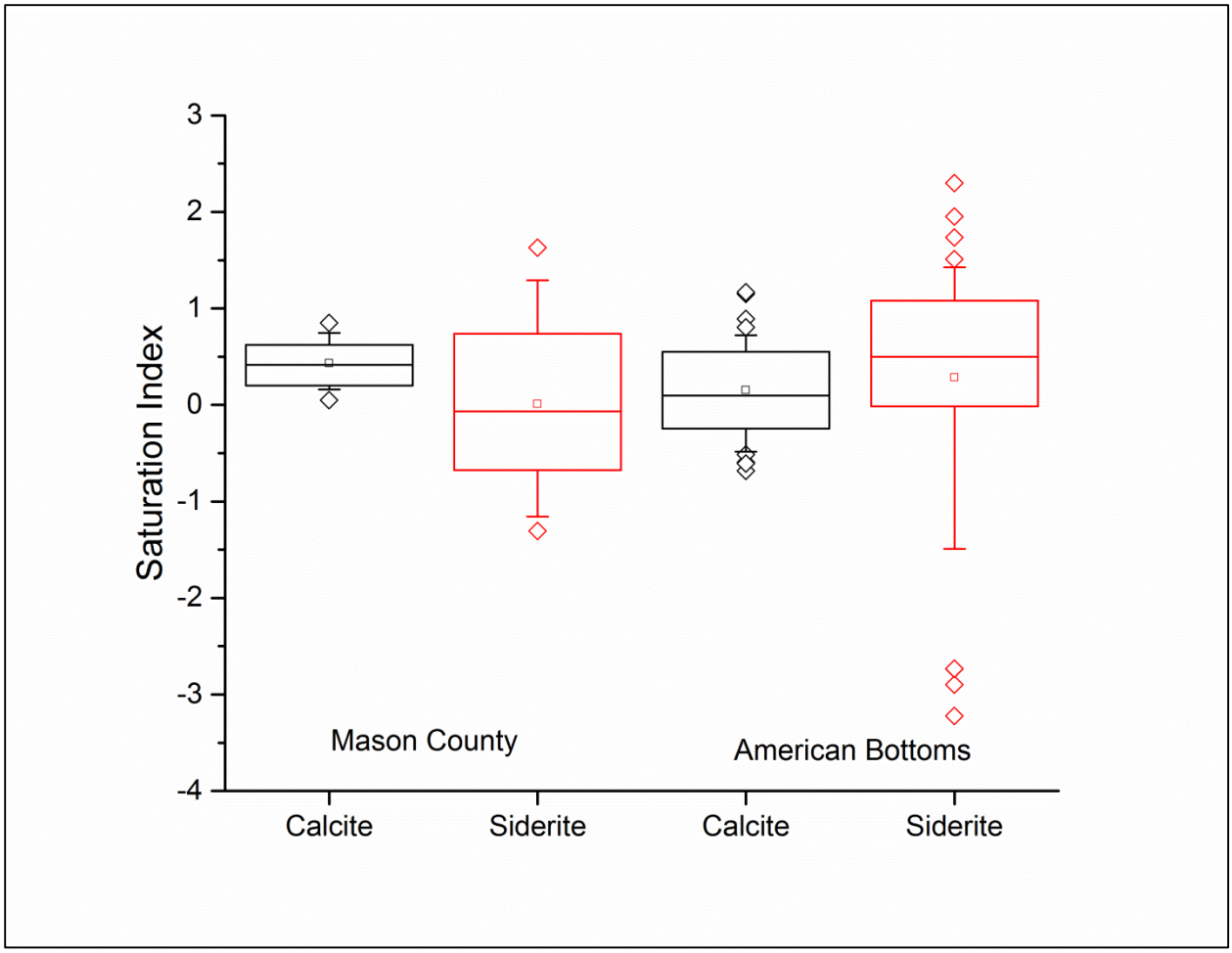

Figure 29. Box and whisker plot of calcite and siderite saturation indices for Mason County and American Bottoms groundwater.

In mass transfer modeling, calcite was predicted to precipitate for all Mason County data sets. The median amount of precipitate was 17 mg L^{-1} (Figure 30). For the American Bottoms, on the other hand, there was no calcite precipitation for at least 25% of the data sets and the median amount was 1.7 mg/L. However, there was a wider range of calcite precipitation for American Bottoms than for Mason County. In contrast with calcite, the amount of siderite calculated to precipitate was generally lower for Mason County than for American Bottoms. The 90th percentile for Mason County (4.8 mg/L) was less than the median for American Bottoms (7.2 mg/L). For the American Bottoms, the median value for siderite precipitation was greater than that of calcite (1.7 mg/L). Deposition of high-Fe scale is more likely in the American Bottoms than in Mason County. It is important to note that these are the maximum amounts of mineral deposition. Equilibrium will probably not be attained in real heat exchangers. The hydraulic residence time is too short. The relative amounts of scale are what is important.

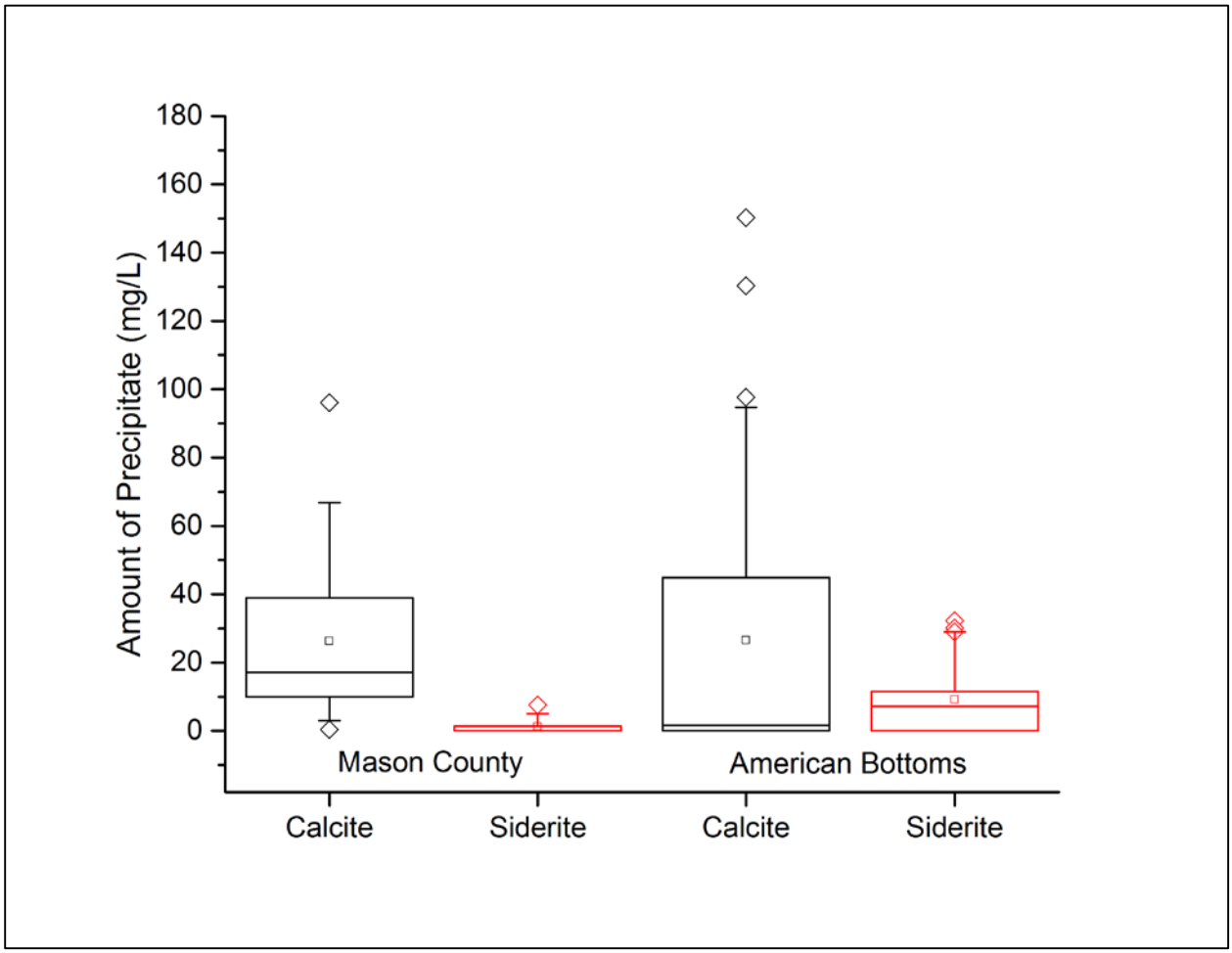

Figure 30. Box and whisker plot of calculated amounts of calcite and siderite precipitated from Mason County and American Bottoms groundwater.

The saturation index of the groundwater before heating gives a rough indication of the amount of either calcite (Figure 31) or siderite (Figure 32) predicted to precipitate after heating. Clearly, there will be no precipitation from undersaturated water. For waters with positive initial calcite or siderite SI values, the amount of precipitation increases with the initial saturation index, although there is considerable scatter. Again, for waters with positive SI values, the absolute amounts of calcite and siderite are less important than the relative amounts.

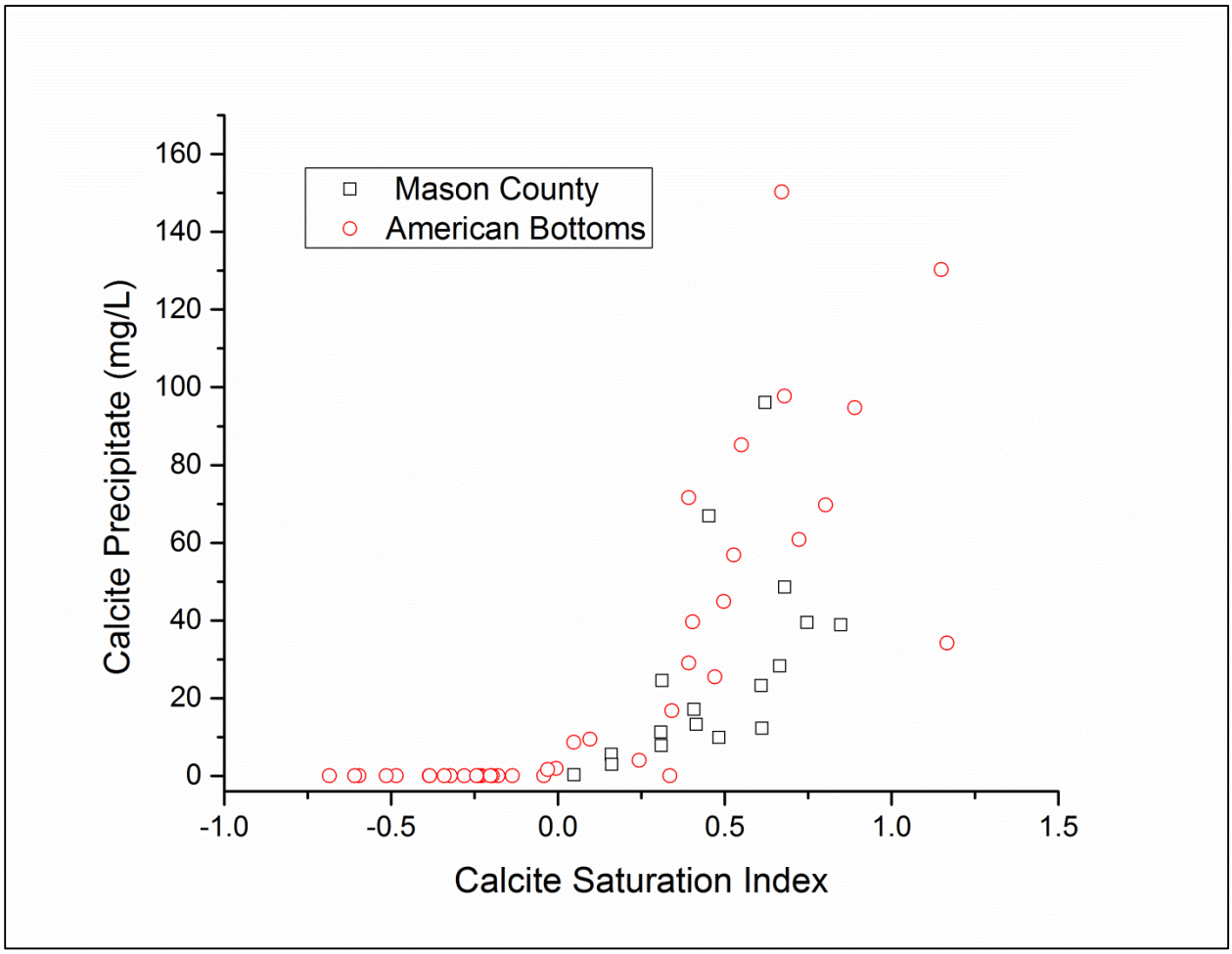

Figure 31. Calculated amount of calcite precipitated by heating Mason County and American Bottoms groundwater as a function of the initial calcite saturation index.

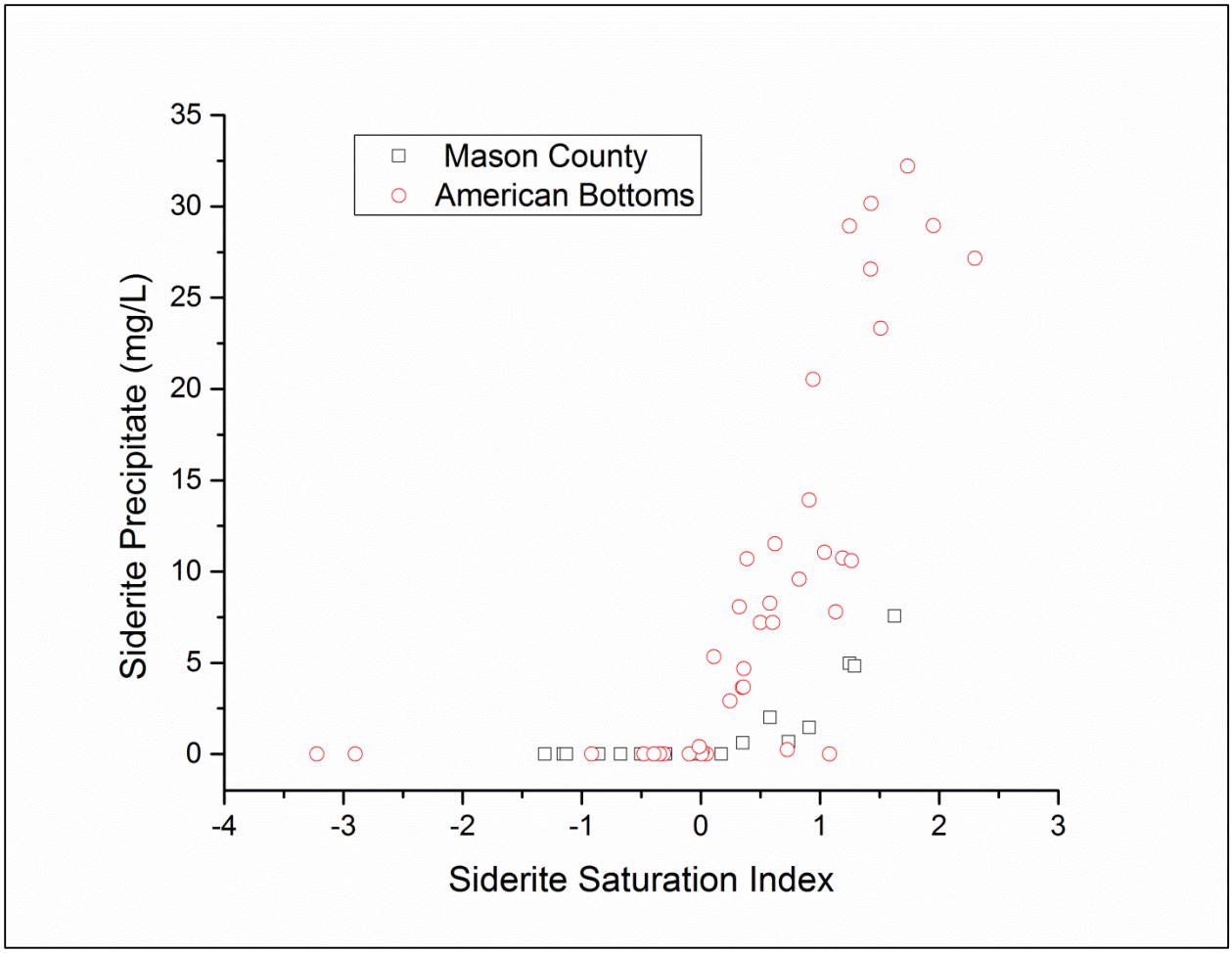

Figure 32. Calculated amount of siderite precipitated by heating Mason County and American Bottoms groundwater as a function of the initial siderite saturation index.

Rafferty (1999) used groundwater hardness to map the heat pump scaling potential in all 50 states. His map of Illinois indicates that almost the entire state, including Mason County and the American Bottoms area, has a high scaling potential. However, as shown by Figure 30 and Figure 31, hardness alone may be a poor predictor of scale deposition. Little or no calcite precipitation is expected for some groundwaters despite high hardness values. Rafferty (1999) did not consider siderite precipitation.

Fouling and Heat Transfer

Calcite has a thermal conductivity value which is only ~10% of that of stainless steel, the most common heat exchanger material (Robertson, 1988; Engineering Toolbox, 2013). As a result, a layer of calcite will reduce the efficiency of a heat exchanger with the degree of reduction proportional to the thickness of the fouling layer. Dobersek and Goricanec (2007) estimated that a 1 mm-thick calcite film would reduce heat transfer efficiency in a stainless steel plate heat

exchanger by 15%. This would clearly increase the electrical energy input and therefore reduce any economic advantage of a groundwater heat pump over conventional heating and cooling.

As an example, the average pumping rate for cooling in Mason County in July is about 3 gal/min. For a heat pump with a plate area of 1 m^2 and $CaCO_3$ precipitation rate of 18 mg/L (median value for Mason County) and assuming the system rapidly reaches equilibrium, scale would accumulate at a rate of 0.09 mm/day. At this rate it would take 11 days to accumulate 1 mm of calcite scale. Over a five month cooling season the scale deposit could be as thick as 14 mm and heat transfer would be severely inhibited.

For various reasons, the actual rate of scale accumulation is probably less than in the foregoing calculation. The rate of scale accumulation increases with both temperature and degree of oversaturation (Cho et al., 1997; Dawe and Zhang, 1997). Because of the lower temperature in a groundwater heat pump (20°C) compared to a water heater or a boiler (over 100°C at the metal-water interface), fouling is probably much slower. Calcite precipitation is inhibited (the rate is decreased) by solutes commonly found in groundwater, including magnesium, sulfate, and organic matter ("humic acid") (Zhang et al., 2001; Ketrane et al., 2010; Gauthier et al., 2012). If the fouling rate were 10% of the rate predicted from equilibrium calculations, the scale layer on the heat exchanger at the end of the cooling season would be about 1.5 mm thick, which would be tolerable. It would probably be a good idea to remove the scale at the end of every cooling season.

Iron-containing scale may inhibit heat transfer more than pure calcite. Massey (1975) gives an example of scale with "high iron content" that causes energy loss in a boiler roughly 50% greater than that of calcite. High-iron scale is more likely for American Bottoms well water than for Mason County (Figure 33).

Fouling may have other effects besides reducing heat transfer efficiency. If precipitation begins in the heat exchanger it may continue in downstream piping and increase the resistance to flow. A reduction in pipe diameter of 5% may increase the pressure drop (difference in inlet and outlet pressures) by 20 to 30% (Cho et al., 1997). Therefore, removal of deposits from drain pipes may be necessary, but probably not every year. If there is a return well, then there may be fouling in the well screen and gravel pack.

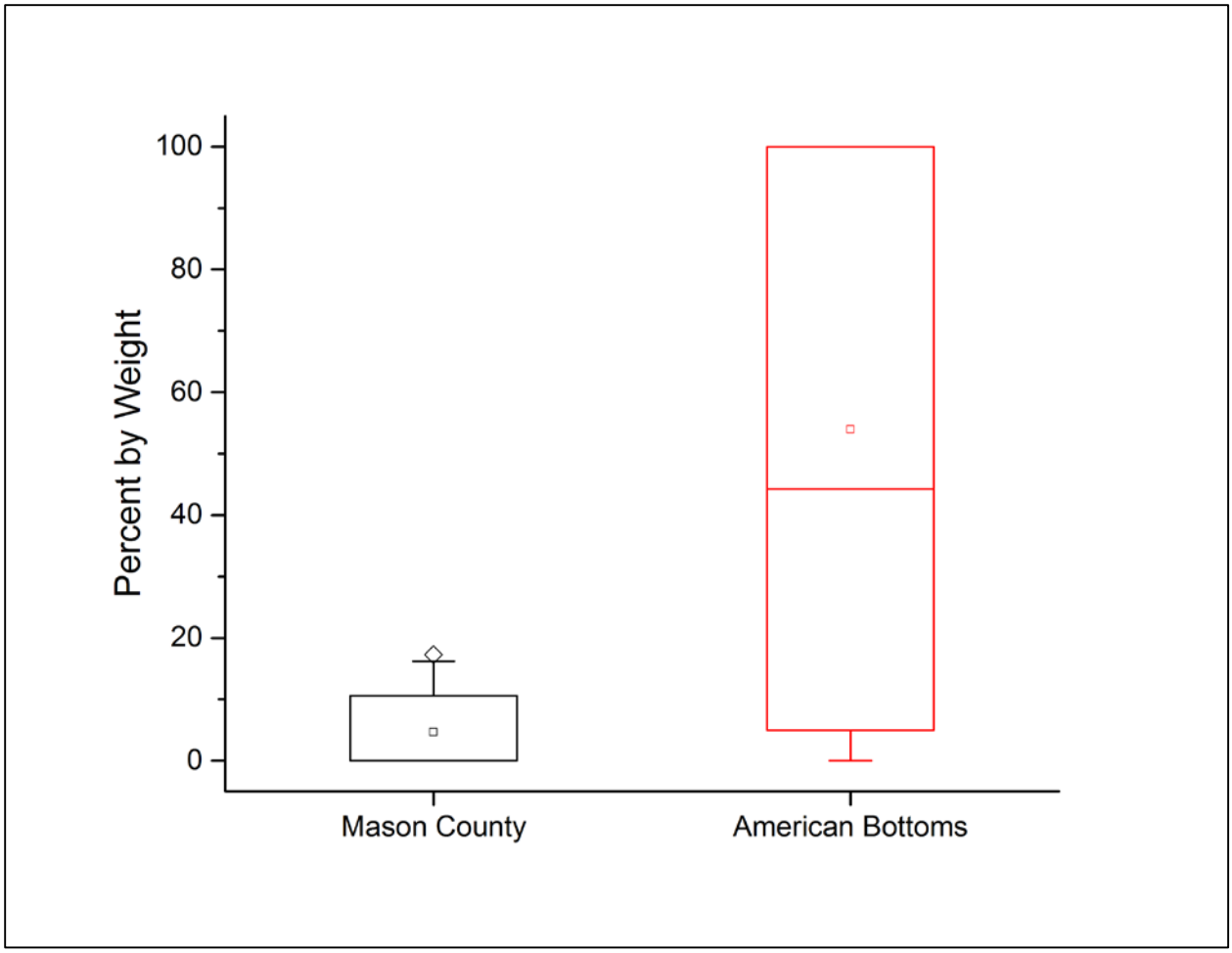

Figure 33. Box and whisker plot of percent siderite in waters predicted to precipitate either calcite or siderite.

Corrosion

Larson and Skold (1958) found that chloride and sulfate are key indicators of corrosion potential. They measured rates of corrosion of cast iron and mild steel by Lake Michigan water with added chloride and sulfate and found that a key parameter is the ratio of chloride and sulfate to bicarbonate, all in meq/L (Equation 8).

$$R_{LS} = \frac{[Cl^-] + 2[SO_4^{2-}]}{[HCO_3^-]} \quad (22)$$

In Equation 22, R_{LS} stands for the Larson-Skold ratio and square brackets indicate molar concentrations. Larson and Skold (1958) found that R_{LS} values greater than 0.8 indicated corrosive conditions and for values greater than 1.2, high corrosion rates could be expected. These values may not apply to stainless steel, the material that most heat exchangers are made of.

Figure 34 shows Larson-Skold ratios for Mason County and American Bottoms groundwater. The 90th percentile for Mason County and the 75th percentile for American Bottoms are ≤ 0.75, which may indicate limited corrosivity of these waters. On the other hand, the 90th percentile for American Bottoms is ~1.1, which indicates that some of these waters may be corrosive.

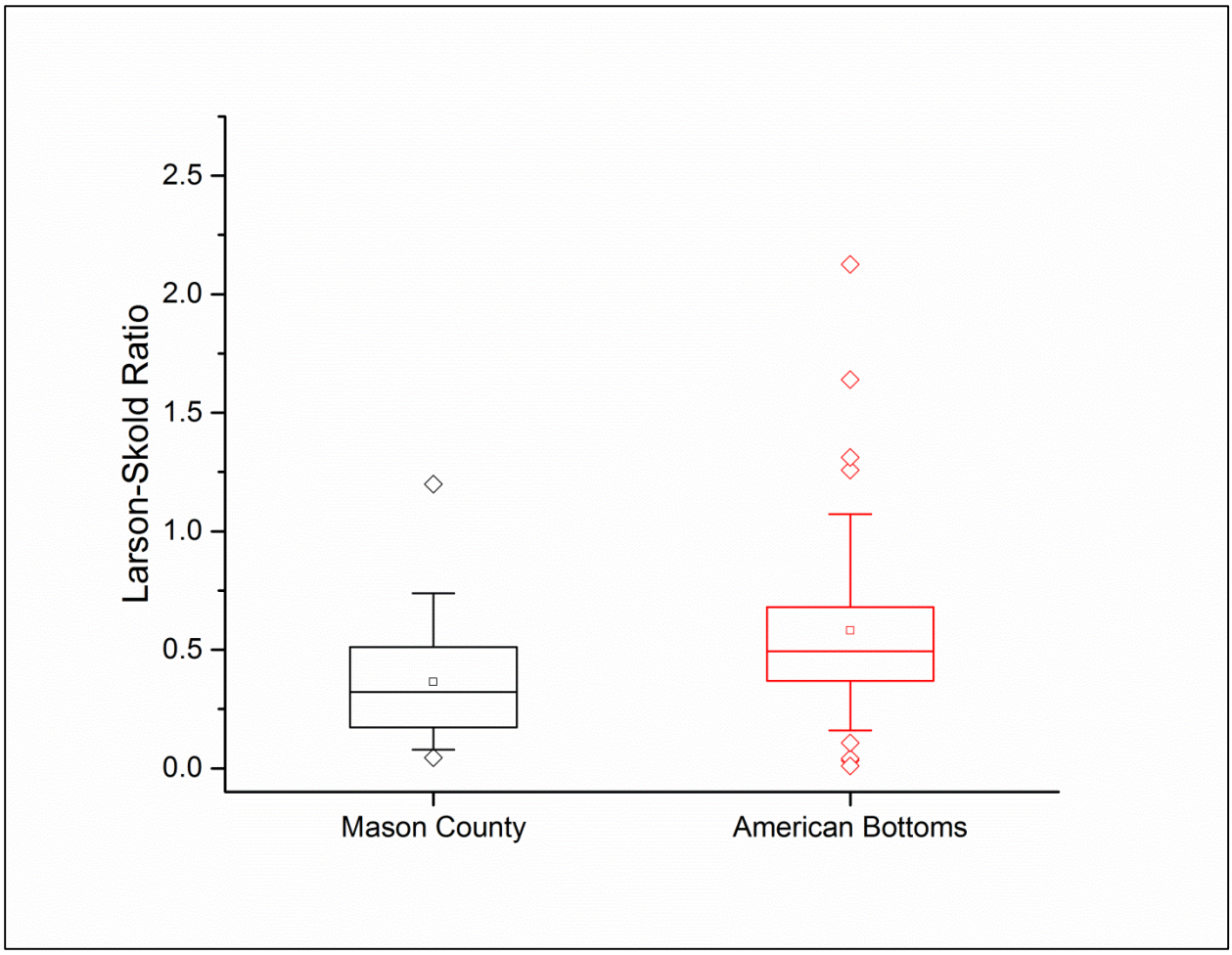

Figure 34. Box and whisker plot of Larson-Skold ratios for Mason County and American Bottoms (Madison and St. Clair Counties) groundwater.

Metals commonly have a thin surface oxide layer that tends to inhibit further oxidation (corrosion). A film of calcium carbonate on piping surfaces may provide additional corrosion protection (Singley et al., 1985; Stumm and Morgan, 1996). Therefore, the calcite saturation index (SI) of a groundwater, which indicates the tendency to precipitate calcite, may also be a useful indicator of its corrosion tendency. However, Edwards et al. (1996) found that the calcite SI was unrelated to the corrosion of copper piping. Figure 35 is a plot of the Larson-Skold ratio *vs* the calcite saturation index. Roughly half of the American Bottoms waters are undersaturated with respect to calcite (SI < 0.3) but they have chloride and sulfate concentrations that are low enough that the value of R_{SL} is in the non-corrosive range. A few waters have R_{SL} values in the "mildly corrosive" range (0.8 – 1.2) but they are all saturated to oversaturated with respect to calcite (SI $\geq$ 0.3). The two or three most "corrosive" waters are also the most oversaturated.

Many factors besides sulfate and chloride may affect corrosion rates, including temperature, pH, buffering capacity, hardness, and concentrations of dissolved oxygen, phosphate, silica, and nitrate (Singley, 1981). Silica and phosphate inhibit corrosion. Oxygen and nitrate, on the other hand, are both oxidants and promote corrosion. Groundwater in confined aquifers in Illinois generally has non-detectable levels of oxygen and nitrate (Holm and Curtiss, 1988; Holm, 1995; Holm et al., 2004; Holm et al., 2008; Holm et al., 2009). Therefore, to minimize corrosion, it is important to prevent air leakage in a groundwater heat pump system. In unconfined areas of Mason County, dissolved oxygen concentrations are near saturation at the water table but decline with depth. About 30 feet below the water table the groundwater is anoxic (Barcelona et al., 1989). Therefore, in these areas only wells that are deep enough to withdraw anoxic groundwater should be used for heat pump applications.

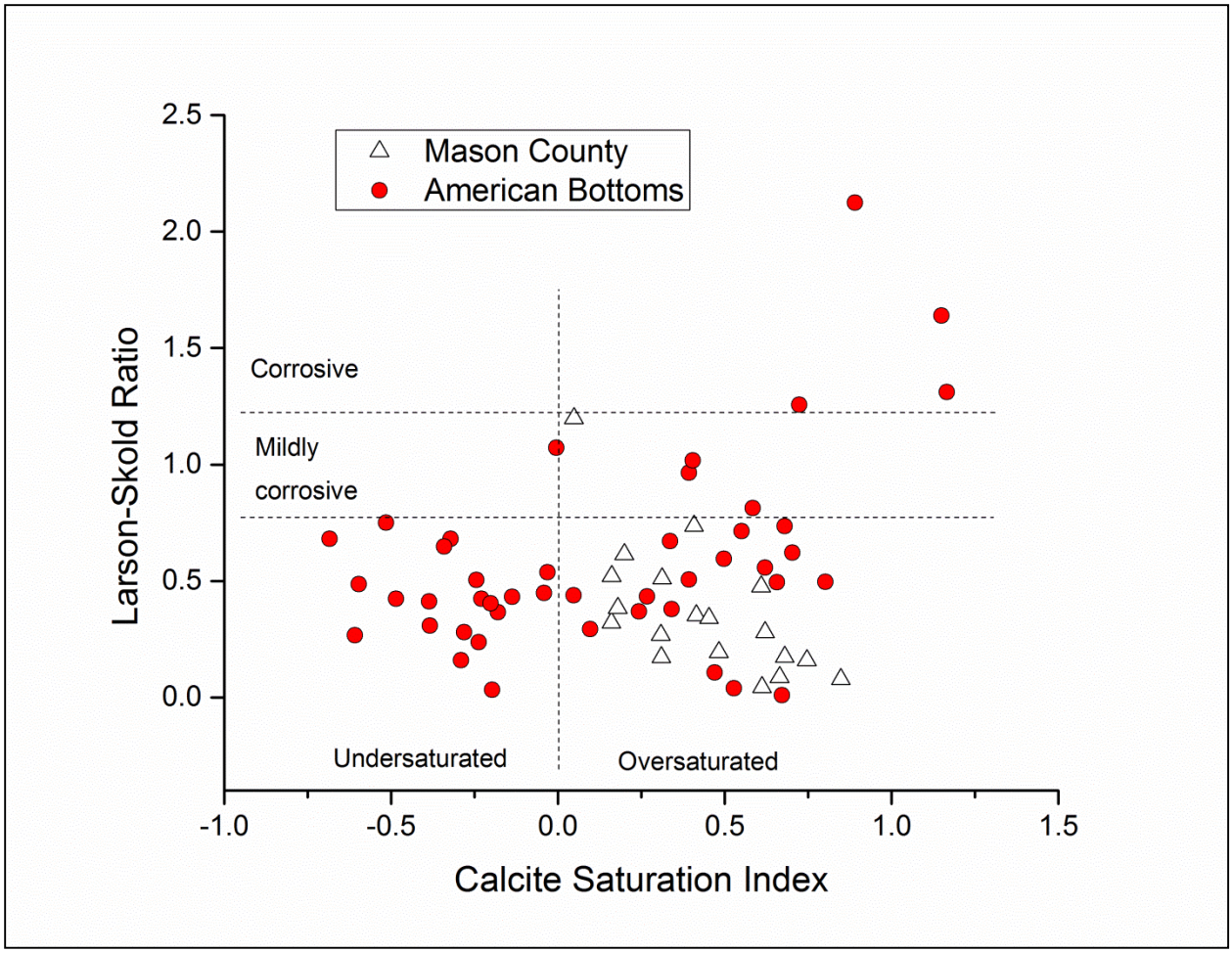

Figure 35. Plot of Larson-Skold ratio as a function of calcite saturation index.

RECOMMENDATIONS FOR FUTURE WORK

The authors recommend that energy audits of geothermal heat pumps in Illinois and neighboring states be conducted. An audit should be carried out for the heating, cooling, and maintenance of different buildings and in different areas. The aim is to obtain a data set that can be used to determine whether there are energy savings from using different geothermal heat pump systems.

The authors recommend a comparison of the costs of different heating and cooling systems, including equipment, electricity, and fuel.

The authors further recommend that research be conducted on scale deposition at the moderate temperature of a heat pump operating in cooling mode. Many papers have been written on scale deposition in boilers, with ΔT values up to 100°C, but the deposition rate would surely be different for ΔT ~10°C. The deposited material may even contain different minerals than those deposited at high temperatures. Such research could include controlled laboratory experiments as well as full-scale systems. The authors recommend seeking permission from building owners to install sample taps before and after heat pumps and access to the heat exchanger and downstream piping during routine maintenance to obtain samples of scales. Detailed records of pumping rates, electricity use, and cleaning and maintenance would be useful. Such data could be used to test the model of GSHP performance (equations 13 and 15).

REFERENCES

Allison, J. D., D. S. Brown and K. J. Novo-Gradac. 1991. Minteqa2/Prodefa2, a Geochemical Assessment Model for Environmental Systems: Version 3.0 User's Manual. United States Environmental Protection Agency, Office of Research and Development. U.S. E.P.A. EPA/600/3-91/021. Washington, DC.

Allison, J. D., S. M. Serkiz, E. M. Perdue, H. E. Allen and D. S. Brown. 1996. Correcting Errors in the Thermodynamic Database for the Equilibrium Speciation Model Minteqa2. Water Research 30(8): 1930-1933.

Anliker, M. A. and D.M. Woller. 1998. Potential Groundwater Resources for Springfield, Illinois: Illinois State Water Survey, Contract Report 627, 197 pp.

Anonymous. 2013. Illinois WARM Program Data. www.isws.illinois.edu/warm/climate.asp (Accessed June 18, 2013).

Banks, D. 2008. *An Introduction to Thermogeology: Ground Source Heating and Cooling.* Blackwell, Oxford.

Barcelona, M. J., T. R. Holm, M. R. Schock and G. K. George. 1989. Spatial and Temporal Gradients in Aquifer Oxidation-Reduction Conditions. *Water Resources Research* 25(5): 991-1003.

Bayer, P., D. Saner, S. Bolay, L. Rybach and P. Blum. 2012. Greenhouse Gas Emission Savings of Ground Source Heat Pump Systems in Europe: A Review. *Renewable & Sustainable Energy Reviews* 16(2): 1256-1267.

Bergstrom, R.E. and T.R. Walker. 1956. *Groundwater Geology of the East St. Louis Area, Illinois.* Illinois State Geological Survey Report of Investigation 191. Champaign, IL.

Berntsson, T. 2002. Heat Sources - Technology, Economy and Environment. *International Journal of Refrigeration-Revue Internationale Du Froid* 25(4): 428-438.

Bevington, P. R. 1969. *Data Reduction and Error Analysis for the Physical Sciences*. McGraw-Hill, New York.

Bloomquist, R. G. 1999. Geothermal Heat Pumps, Four Plus Decades of Experience. *GHC Bulletin*. Klamath Falls, OR, Geothermal Heat Center. 20**:** 13-18.

Bloomquist, R. G. 2003. Geothermal Space Heating. *Geothermics* 32(4-6): 513-526.

Bouwer, H. 2002. Artificial Recharge of Groundwater: Hydrogeology and Engineering. *Hydrogeology Journal* 10(1): 121-142.

Butler, J. N. 1964. *Ionic Equilibrium, a Mathematical Approach*. Addison-Wesley, Reading, MA.

Cho, Y. I., C. F. Fan and B. G. Choi. 1997. Theory of Electronic Anti-Fouling Technology to Control Precipitation Fouling in Heat Exchangers. *International Communications in Heat and Mass Transfer* 24(6): 757-770.

Dawe, R. A. and Y. Zhang. 1997. Kinetics of Calcium Carbonate Scaling Using Observations from Glass Micromodels. *Journal of Petroleum Science and Engineering* 18(3–4): 179-187.

Dobersek, D. and D. Goricanec. 2007. Influence of Water Scale on Thermal Flow Losses of Domestic Appliances. *International Journal of Mathematical Models and Methods in Applied Sciences* 2(1): 55-61.

Drever, J. I. 1982. *The Geochemistry of Natural Waters*. Prentice-Hall, Englewood Cliffs, NJ.

Edwards, M. W., M. R. Schock, and T. E. Meyer. 1996. Alkalinity, pH, and Copper Corrosion Byproduct Release. *Journal American Water Works Association*. 88: 81-94.

Egg, J. and B. C. Howand. 2011. *Geothermal HVAC: Green Heating and Cooling*. New York, McGraw-Hill.

Engineering Toolbox. 2013. *Thermal Conductivity of Some Common Materials and Gases*. http://www.engineeringtoolbox.com/thermal-conductivity-d_429.html. 2013. (Accessed January 3, 2013).

Freedman, V. L., S. R. Waichler, R. D. Mackley and J. A. Horner 2012. Assessing the Thermal Environmental Impacts of an Groundwater Heat Pump in Southeastern Washington State. *Geothermics* 42: 65-77.

Gauthier, G., Y. J. Chao, O. Horner, O. Alos-Ramos, F. Hui, J. Ledion and H. Perrot. 2012. Application of the Fast Controlled Precipitation Method to Assess the Scale-Forming Ability of Raw River Waters. *Desalination* 299: 89-95.

Greenberg, J. and M. Tomson. 1992. Precipitation and Dissolution Kinetics and Equilibria of Aqueous Ferrous Carbonate vs Temperature. *Applied Geochemistry* 7(2): 185-190.

Grimley, D. A. and A. C. Phillips. 2006. *Surficial Geology of Madison County, Illinois.* Illinois State Geological Survey, Illinois Preliminary Geologic Map IPGM Madison County-SG, 1:62,500. Champaign, IL.

Grimley, D.A. and A.C. Phillips. 2011. *Surficial Geology of St. Clair County, Illinois.* Illinois State Geological Survey, Illinois County Geologic Map ICGM St. Clair County-SG, 1:62,500. Champaign, IL.

Grimley, D.A., A.C. Phillips, and S.W. Lepley. 2007. *Surficial Geology of Monks Mound Quadrangle, Madison and St. Clair Counties, Illinois*. Illinois State Geological Survey, Illinois Preliminary Geologic Map, IPGM Monks Mound-SG.

Gustafsson, J. P. 2012. *Visual Minteq, a Free Equilibrium Speciation Model.* http://www2.lwr.kth.se/English/OurSoftware/vminteq/. 2012 (Accessed December 20, 2012).

Hansel, A.K. and W.H. Johnson. 1996. *Wedron and Mason Groups – Lithostratigraphic Reclassification of Deposits of the Wisconsin Episode, Lake Michigan Lobe Area*. Illinois State Geological Survey Bulletin 104. Champaign, IL.

Helsel, D. R. 2011. *Statistics for Censored Environmental Data Using Minitab and R*. Wiley, New York.

Hem, J. D. 1985. *Study and Interpretation of the Chemical Characteristics of Natural Water*. Water Supply Paper 2254. U. S. Geological Survey, Reston, VA.

Herzog, B.L., B.J. Stiff, C.A. Chenoweth, K.L. Warner, J.B. Sievering, and C. Avery. 1994. Buried Bedrock Surface of Illinois. Illinois State Geological Survey Map Series, Map 5, 1:500,000. Champaign, IL.

Holm, T. R. 1995. *Ground-Water Quality in the Mahomet Aquifer, Mclean, Logan, and Tazewell Counties*. Illinois State Water Survey Contract Report 579. Champaign, IL.

Holm, T. R. and C. D. Curtiss. 1988. *Arsenic Contamination in East-Central Illinois Ground Water*. Department of Energy and Natural Resources report ILENR/RE-WR-88/16. Springfield, IL.

Holm, T. R., W. R. Kelly, S. D. Wilson, G. R. Roadcap, J. L. Talbott and J. S. Scott. 2004. *Arsenic Geochemistry and Distribution in the Mahomet Aquifer, Illinois*. Waste Management and Research Center Research Report 107. Champaign, IL.

Holm, T. R., W. R. Kelly, S. D. Wilson and J. L. Talbott. 2008. Arsenic Removal at Illinois Iron Removal Plants. *Journal American Water Works Association* 100(9): 139-150.

Holm, T. R., S. D. Wilson and W. R. Kelly. 2009. *Spatial Variability of Arsenic in Groundwater*. Midwest Technology Assistance Center for Small Public Water Systems Technical Report 09-01. Champaign, IL.

Huang, Y. J., R. Ritschard, J. Bull and L. Chang. 1986. *Climate Indicators for Estimating Residential Heating & Cooling Loads*. Lawrence Berkeley Laboratory. Berkeley, CA.

Inalli, M. and H. Esen. 2004. Experimental Thermal Performance Evaluation of a Horizontal Ground-Source Heat Pump System. *Applied Thermal Engineering* 24(14-15): 2219-2232.

Kavanaugh, S. P. and K. Rafferty. 1997. *Ground-Source Heat Pumps: Design of Geothermal Systems for Commercial and Institutional Buildings*. American Society of Heating, Refrigerating and Air-Conditioning Engineering, Inc. Atlanta, GA

Ketrane, R., L. Leleyter, F. Baraud, M. Jeannin, O. Gil and B. Saidani. 2010. Characterization of Natural Scale Deposits Formed in Southern Algeria Groundwater. Effect of Its Major Ions on Calcium Carbonate Precipitation. *Desalination* 262(1–3): 21-30.

Kuo, C. P. and H. J. Liao. 2012. The Feasibility of Using Circulating Groundwater as Renewable Energy Sources for Air-Conditioning in Taipei Basin. *Renewable Energy* 39(1): 175-182.

Larson, T. E. and R. V. Skold. 1958. *Laboratory Studies Relating Mineral Quality of Water to Corrosion of Steel and Cast Iron*. Illinois State Water Survey Circular 71. Champaign, IL.

Leito, I., L. Strauss, E. Koort and V. Pihl. 2002. Estimation of Uncertainty in Routine pH Measurement. *Accreditation and Quality Assurance* **7**(6): 242-249.

Lienau, P. J., T. L. Boyd and R. L. Rogers. 1995. *Ground-Source Heat Pump Case Studies and Utility Programs*. Geo-Heat Center, Oregon Institute of Technology. Klamath Falls, OR.

Liu, X. 2010. *Assessment of National Benefits from Retrofitting Existing Single-Family Homes with Ground Source Heat Pump Systems*. Oak Ridge National Laboratory. 66 pp. Oak Ridge, TN.

Lund, J. W., R. G. Bloomquist, T. L. Boyd and J. Renner. 2005. *The United States of America Country Update*. World Geothermal Congress 2005, Ankara, Turkey.

Massey, R. G. 1975. *Energy Conservation Program Guide for Industry and Commerce, Supplement 1*. Department of Commerce, National Bureau of Standards Handbook 115, Supplement 1.

Moore. 2012. *Calculators for Estimating Heating and Cooling System Capacity Requirements, by Calculating Structure Heat Losses (Heating) and Gains (Cooling)*. http://www.moorepage.net/heatloss.html (Accessed 5 December 2012).

Morel, F. M. M. and J. J. Morgan. 1972. A Numerical Method for Computing Equilibria in Aqueous Chemical Systems. *Environmental Science & Technology* 6(1): 58-67.

Natural Resources Canada. 2002. *Commercial Earth Energy Systems: A Buyer's Guide*. Ottawa, Natural Resources Canada. 90 pp.

NGWA. 2012. *Groundwater Temperature's Measurement and Significance*. http://www.ngwa.org/Fundamentals/studying/Pages/Groundwater-temperature's-measurement-and-significance.aspx. 2012. (Accessed December 19, 2012).

Nordstrom, D. K. and J. L. Munoz. 1986. *Geochemical Thermodynamics*. Blackwell, Palo Alto, CA.

Omer, A. M. 2008. Ground-Source Heat Pumps Systems and Applications. *Renewable & Sustainable Energy Reviews* 12(2): 344-371.

Ozgener, O. and A. Hepbasli. 2005. Experimental Performance Analysis of a Solar Assisted Ground-Source Heat Pump Greenhouse Heating System. *Energy and Buildings* 37(1): 101-110.

Piskin, K. and R.E. Bergstrom. 1975. *Glacial Drift in Illinois – Thickness and Character.* Illinois State Geological Survey Circular 490. Champaign, IL.

Plummer, L. N. and E. Busenberg. 1982. The Solubilities of Calcite, Aragonite and Vaterite in CO_2-H_2O Solutions between 0 and 90 Degrees C, and an Evaluation of the Aqueous Model for the System $CaCO_3$-CO_2-H_2O. *Geochimica et Cosmochimica Acta* 46: 1011-1040.

Rafferty, K. 1999. *Scaling in Geothermal Heat Pump Systems*. Oregon Institute of Technology Contract Number DE-FG07-90ID 13040. Klamath Falls, OR.

Roadcap, G. S., H. V. Knapp, H. A. Wehrmann, and D. R. Larson. 2011. Meeting East-Central Illinois Water Needs to 2050: Potential Impacts on the Mahomet Aquifer and Surface Reservoirs. Illinois State Water Survey Contract Report 2011-08. Champaign, IL.

Robertson, E. C. 1988. *Thermal Properties of Rocks*. U. S. Geological Survey Open-File Report 88-441. Reston, VA.

Sanner, B., C. Karytsas, D. Mendrinos and L. Rybach. 2003. Current Status of Ground Source Heat Pumps and Underground Thermal Energy Storage in Europe. *Geothermics* 32(4-6): 579-588.

Sanderson, E. W. and R. D. Olson (1993). *Dewatering Well Assessment for the Highway Drainage System at Four Sites in the East St. Louis Area, Illinois (Phase 7)*. Illinois State Water Survey, Contract Report 546. Chamapign, IL.

Sauer, H. J. and R. H. Howell. 1983. *Heat Pump Systems*. New York, Wiley.

Schicht, R.J. 1965. *Ground-Water Development in East St Louis Area, Illinois*: Illinois State Water Survey, Report of Investigation 51. Champaign, IL.

Schicht, R.J. and A.G. Buck. 1995. *Ground-Water Levels and Pumpage in the Metro-East Area, Illinois, 1986-1990*: Illinois State Water Survey, Circular 180. Champaign, IL.

Schicht, R.J. and E.G. Jones. 1962. *Ground-Water Levels and Pumpage in the East St. Louis Area, Illinois, 1890-1961*: Illinois State Water Survey, Report of Investigation 44. Champaign, IL.

Self, S. J., B. V. Reddy and M. A. Rosen. 2013. Geothermal Heat Pump Systems: Status Review and Comparison with Other Heating Options. *Applied Energy* 101: 341-348.

Singer, P. C. and W. Stumm. 1970. Solubility of Ferrous Iron in Carbonate-Bearing Waters. *Journal American Water Works Association* 62(3): 198-202.

Singley, J. E. 1981. The Search for a Corrosion Index. *Journal American Water Works Association* 73(11): 579-582.

Singley, J. E., R. A. Pisigan, Jr., A. Ahmadi, P. O. Pisigan and T.-Y. Lee. 1985. *Corrosion and Calcium Carbonate Saturation Index in Water Distribution Systems*. U.S. Environmental Protection Agency EPA/600/S2-85/079. Washington, D. C.

Staffell, I., D. Brett, N. Brandon and A. Hawkes. 2012. A Review of Domestic Heat Pumps. *Energy & Environmental Science* 5(11): 9291-9306.

Stumm, W. and J. J. Morgan. 1996. *Aquatic Chemistry: Chemical Equilibria and Rates in Natural Waters, 3rd Ed.* Wiley, New York.

Tarnawski, V. R., W. H. Leong, T. Momose and Y. Hamada. 2009. Analysis of Ground Source Heat Pumps with Horizontal Ground Heat Exchangers for Northern Japan. *Renewable Energy* 34(1): 127-134.

USEPA. 2012. *Average Temperature of Shallow Ground Water*. http://www.epa.gov/athens/learn2model/part-two/onsite/ex/jne_henrys_map.html. 2012. (Accessed December 20, 2012).

Walker, W.H., R.E. Bergstrom, and W.C. Walton. 1965. *Preliminary Report on Ground-Water Resources of the Havana Region in West-Central Illinois:* Illinois State Geological Survey/Illinois State Water Survey Cooperative Groundwater Report 3. Champaign, IL.

Weast, R. C., ed. 1972. *The Handbook of Chemistry and Physics, 53rd ed*. Chemical Rubber Co., Cleveland, OH.

Zhang, Y., H. Shaw, R. Farquhar and R. Dawe. 2001. The Kinetics of Carbonate Scaling—Application for the Prediction of Downhole Carbonate Scaling. *Journal of Petroleum Science and Engineering* 29(2): 85-95.

Zogou, O. and A. Stamatelos. 1998. Effect of Climatic Conditions on the Design Optimization of Heat Pump Systems for Space Heating and Cooling. *Energy Conversion and Management* 39(7): 609-622.

APPENDIX A. THERMAL CALCULATIONS

Table A1. Estimated heating requirements of one- and two-story single family houses and corresponding well production rates using the LBL Model in the two study areas.

Mason County												
Month	**Jan**	**Feb**	**Mar**	**Apr**	**May**	**Jun**	**Jul**	**Aug**	**Sep**	**Oct**	**Nov**	**Dec**
Heating Degree Days (F day)	1259	983	736	375	150	11	0	10	59	312	698	1102
One-story												
Heating Loads of Groundwater (kWh)	2173	1697	1270	647	259	19	0	17	102	539	1205	1902
Average Well Production Rate (kg/s)	0.1398	0.1208	0.0817	0.0430	0.0167	0.0013	0.0000	0.0011	0.0068	0.0346	0.0801	0.1223
Average Well Production Rate (gpm)	2.22	1.91	1.29	0.68	0.26	0.02	0.00	0.02	0.11	0.55	1.27	1.94
Average Well Production Rate -												
per unit floor area (gpm/sq ft)	1.4E-03	1.2E-03	8.4E-04	4.4E-04	1.7E-04	1.3E-05	0.0E+00	1.1E-05	7.0E-05	3.6E-04	8.2E-04	1.3E-03
Two-story												
Heating Loads of Groundwater (kWh)	2810	2194	1643	837	335	25	0	22	132	696	1558	2459
Average Well Production Rate (kg/s)	0.1807	0.1562	0.1056	0.0556	0.0215	0.0016	0.0000	0.0014	0.0088	0.0448	0.1035	0.1582
Average Well Production Rate (gpm)	2.86	2.48	1.67	0.88	0.34	0.03	0.00	0.02	0.14	0.71	1.64	2.51
Average Well Production Rate -												
per unit floor area (gpm/sq ft)	1.3E-03	1.1E-03	7.5E-04	3.9E-04	1.5E-04	1.2E-05	0.0E+00	1.0E-05	6.2E-05	3.2E-04	7.3E-04	1.1E-03

American Bottoms												
Month	**Jan**	**Feb**	**Mar**	**Apr**	**May**	**Jun**	**Jul**	**Aug**	**Sep**	**Oct**	**Nov**	**Dec**
Heating Degree Days	1114	859	613	281	105	6	0	2	43	248	599	956
One-story												
Heating Loads of Groundwater (kWh)	1923	1483	1058	485	181	10	0	3	74	428	1034	1650
Average Well Production Rate (kg/s)	0.1237	0.0954	0.0680	0.0312	0.0117	0.0007	0.0000	0.0002	0.0048	0.0275	0.0665	0.1061
Average Well Production Rate (gpm)	1.96	1.51	1.08	0.49	0.18	0.01	0.00	0.00	0.08	0.44	1.05	1.68
Average Well Production Rate -												
per unit floor area (gpm/sq ft)	1.3E-03	9.8E-04	7.0E-04	3.2E-04	1.2E-04	6.9E-06	0.0E+00	2.3E-06	4.9E-05	2.8E-04	6.8E-04	1.1E-03
Two-story												
Heating Loads of Groundwater (kWh)	2486	1917	1368	627	234	13	0	4	96	553	1337	2134
Average Well Production Rate (kg/s)	0.1599	0.1233	0.0880	0.0403	0.0151	0.0009	0.0000	0.0003	0.0062	0.0356	0.0860	0.1372
Average Well Production Rate (gpm)	2.53	1.95	1.39	0.64	0.24	0.01	0.00	0.00	0.10	0.56	1.36	2.17
Average Well Production Rate -												
per unit floor area (gpm/sq ft)	1.1E-03	8.7E-04	6.2E-04	2.9E-04	1.1E-04	6.1E-06	0.0E+00	2.0E-06	4.4E-05	2.5E-04	6.1E-04	9.7E-04

Table A2. Estimated heating requirements of one- and two-story single family houses and corresponding well production rates using the Moorepage Model in the two study areas.

Mason County												
Month	Jan	Feb	Mar	Apr	May	Jun	Jul	Aug	Sep	Oct	Nov	Dec
Min °F	15.7	20.6	30.5	40.5	51.3	60.4	64.1	62.2	54.5	43.5	32.4	21.3
One-story												
Heat loss of heat pump (Btu/hr)	15627	13934	10513	7058	3326	0	0	0	2220	6021	9857	13692
Heat loss of groundwater (Btu/hr)	10418	9289	7009	4705	2217	0	0	0	1480	4014	6571	9128
Average Well Production Rate (gpm)	2.32	2.06	1.56	1.05	0.49	0	0	0	0.33	0.89	1.46	2.03
Average Well Production Rate -												
per unit floor area (gpm/sq ft)	1.50E-03	1.34E-03	1.01E-03	6.79E-04	3.20E-04	0	0	0	2.14E-04	5.79E-04	9.48E-04	1.32E-03
Two-story												
Heat loss of heat pump (Btu/hr)	16661	14853	11202	7513	3529	0	0	0	2349	6406	10501	14595
Heat loss of groundwater (Btu/hr)	11107	9902	7468	5009	2353	0	0	0	1566	4271	7001	9730
Average Well Production Rate (gpm)	2.47	2.20	1.66	1.11	0.52	0	0	0	0.35	0.95	1.56	2.16
Average Well Production Rate -												
per unit floor area (gpm/sq ft)	1.10E-03	9.83E-04	7.41E-04	4.97E-04	2.33E-04	0	0	0	1.55E-04	4.24E-04	6.95E-04	9.66E-04
American Bottoms												
Month	Jan	Feb	Mar	Apr	May	Jun	Jul	Aug	Sep	Oct	Nov	Dec
Min °F	20	24.2	35.1	45.5	55.1	64	68.4	66.4	58.2	46.6	35.5	25.8
One-story												
Heat loss of heat pump (Btu/hr)	14141	12690	8924	5330	2013	0	0	0	942	4950	8786	12137
Heat loss of groundwater (Btu/hr)	9427	8460	5949	3553	1342	0	0	0	628	3300	5857	8091
Average Well Production Rate (gpm)	2.10	1.88	1.32	0.79	0.30	0	0	0	0.14	0.73	1.30	1.80
Average Well Production Rate -												
per unit floor area (gpm/sq ft)	1.36E-03	1.22E-03	8.59E-04	5.13E-04	1.94E-04	0	0	0	9.06E-05	4.76E-04	8.45E-04	1.17E-03
Two-story												
Heat loss of heat pump (Btu/hr)	15075	13525	9505	5669	2127	0	0	0	984	5263	9357	12935
Heat loss of groundwater (Btu/hr)	10050	9017	6337	3779	1418	0	0	0	656	3509	6238	8623
Average Well Production Rate (gpm)	2.23	2.00	1.41	0.84	0.32	0	0	0	0.15	0.78	1.39	1.92
Average Well Production Rate -												
per unit floor area (gpm/sq ft)	9.97E-04	8.95E-04	6.29E-04	3.75E-04	1.41E-04	0	0	0	6.51E-05	3.48E-04	6.19E-04	8.56E-04

Table A3. Estimated cooling requirements of one- and two-story single family houses and corresponding well production rates using the Moorepage Model in the two study areas.

Mason County												
Month	Jan	Feb	Mar	Apr	May	Jun	Jul	Aug	Sep	Oct	Nov	Dec
Max °F	33.1	39.2	52	65.1	75.6	84.3	87.4	85.3	79.5	67.3	51	37.6
One-story												
Heat gain of heat pump - one-story (Btu/hr)	0	0	0	0	15567	18380	19382	18703	16828	0	0	0
Heat gain of groundwater - one-story (Btu/hr)	0	0	0	0	18680	22056	23258	22444	20194	0	0	0
Average Well Production Rate (gpm)	0	0	0	0	2.31	2.72	2.87	2.77	2.49	0	0	0
Average Well Production Rate -												
per unit floor area (gpm/sq ft)	0	0	0	0	1.50E-03	1.77E-03	1.86E-03	1.80E-03	1.62E-03	0	0	0
Two-story												
Heat gain of heat pump- two-story (Btu/hr)	0	0	0	0	17153	19967	20969	20290	18415	0	0	0
Heat gain of groundwater - two-story (Btu/hr)	0	0	0	0	20584	23960	25163	24348	22098	0	0	0
Average Well Production Rate (gpm)	0	0	0	0	2.54	2.96	3.11	3.01	2.73	0	0	0
Average Well Production Rate -												
per unit floor area (gpm/sq ft)	0	0	0	0	1.13E-03	1.32E-03	1.39E-03	1.34E-03	1.22E-03	0	0	0

American Bottoms												
Month	Jan	Feb	Mar	Apr	May	Jun	Jul	Aug	Sep	Oct	Nov	Dec
Max °F	38.1	44.5	55.4	66.7	75.7	84.2	88.7	86.8	79.7	69.1	54.6	42.6
One-story												
Heat gain of heat pump - one-story (Btu/hr)	0	0	0	0	15599	18348	19803	19188	16893	0	0	0
Heat gain of groundwater - one-story (Btu/hr)	0	0	0	0	18719	22018	23764	23026	20272	0	0	0
Average Well Production Rate (gpm)	0	0	0	0	2.31	2.72	2.93	2.84	2.50	0	0	0
Average Well Production Rate -												
per unit floor area (gpm/sq ft)	0	0	0	0	1.50E-03	1.77E-03	1.91E-03	1.85E-03	1.63E-03	0	0	0
Two-story												
Heat gain of heat pump - two-story (Btu/hr)	0	0	0	0	17186	19934	21389	20775	18479	0	0	0
Heat gain of groundwater - two-story (Btu/hr)	0	0	0	0	20623	23921	25667	24930	22175	0	0	0
Average Well Production Rate (gpm)	0	0	0	0	2.55	2.95	3.17	3.08	2.74	0	0	0
Average Well Production Rate -												
per unit floor area (gpm/sq ft)	0	0	0	0	1.14E-03	1.32E-03	1.41E-03	1.37E-03	1.22E-03	0	0	0

Table A4. Sensitivity analysis on the average well production rate in heating mode at the two studied areas based on the value of COP.

Mason County													
Month		Jan	Feb	Mar	Apr	May	Jun	Jul	Aug	Sep	Oct	Nov	Dec
Heat loss of heat pump - two-story (Btu/hr)		16661	14853	11202	7513	3529	0	0	0	2349	6406	10501	14595
Heat loss of groundwater - two-story (Btu/hr)													
COP	2	8331	7427	5601	3757	1765	0	0	0	1175	3203	5251	7298
	3	11107	9902	7468	5009	2353	0	0	0	1566	4271	7001	9730
	4	12496	11140	8402	5635	2647	0	0	0	1762	4805	7876	10946
Average Well Production Rate (gpm)													
COP	2	1.85	1.65	1.24	0.83	0.39	0.00	0.00	0.00	0.26	0.71	1.17	1.62
	3	2.47	2.20	1.66	1.11	0.52	0.00	0.00	0.00	0.35	0.95	1.56	2.16
	4	2.78	2.48	1.87	1.25	0.59	0.00	0.00	0.00	0.39	1.07	1.75	2.43
American Bottoms													
Month		Jan	Feb	Mar	Apr	May	Jun	Jul	Aug	Sep	Oct	Nov	Dec
Heat loss of heat pump - two-story (Btu/hr)		15075	13525	9505	5669	2127	0	0	0	984	5263	9357	12935
Heat loss of groundwater - two-story (Btu/hr)													
COP	2	7538	6763	4753	2835	1064	0	0	0	492	2632	4679	6468
	3	10050	9017	6337	3779	1418	0	0	0	656	3509	6238	8623
	4	11306	10144	7129	4252	1595	0	0	0	738	3947	7018	9701
Average Well Production Rate (gpm)													
COP	2	1.68	1.50	1.06	0.63	0.24	0.00	0.00	0.00	0.11	0.58	1.04	1.44
	3	2.23	2.00	1.41	0.84	0.32	0.00	0.00	0.00	0.15	0.78	1.39	1.92
	4	2.51	2.25	1.58	0.95	0.35	0.00	0.00	0.00	0.16	0.88	1.56	2.16

Table A5. Sensitivity analysis on the average well production rate in cooling mode at the two studied areas based on the change of COP_C.

Mason County													
Month		Jan	Feb	Mar	Apr	May	Jun	Jul	Aug	Sep	Oct	Nov	Dec
Heat gain of heat pump - two-story (Btu/hr)		0	0	0	0	17153	19967	20969	20290	18415	0	0	0
Heat gain of groundwater - two-story (Btu/hr)													
COP_C	3	0	0	0	0	22871	26623	27959	27053	24553	0	0	0
	5	0	0	0	0	20584	23960	25163	24348	22098	0	0	0
	7	0	0	0	0	19603	22819	23965	23189	21046	0	0	0
Average Well Production Rate (gpm)													
COP_C	3	0.00	0.00	0.00	0.00	2.82	3.29	3.45	3.34	3.03	0.00	0.00	0.00
	5	0.00	0.00	0.00	0.00	2.54	2.96	3.11	3.01	2.73	0.00	0.00	0.00
	7	0.00	0.00	0.00	0.00	2.42	2.82	2.96	2.86	2.60	0.00	0.00	0.00
American Bottoms													
Month		Jan	Feb	Mar	Apr	May	Jun	Jul	Aug	Sep	Oct	Nov	Dec
Heat gain of heat pump - two-story (Btu/hr)		0	0	0	0	17186	19934	21389	20775	18479	0	0	0
Heat gain of groundwater - two-story (Btu/hr)													
COP_C	3	0	0	0	0	22915	26579	28519	27700	24639	0	0	0
	5	0	0	0	0	20623	23921	25667	24930	22175	0	0	0
	7	0	0	0	0	19641	22782	24445	23743	21119	0	0	0
Average Well Production Rate (gpm)													
COP_C	3	0.00	0.00	0.00	0.00	2.83	3.28	3.52	3.42	3.04	0.00	0.00	0.00
	5	0.00	0.00	0.00	0.00	2.55	2.95	3.17	3.08	2.74	0.00	0.00	0.00
	7	0.00	0.00	0.00	0.00	2.43	2.81	3.02	2.93	2.61	0.00	0.00	0.00

APPENDIX B. WATER QUALITY STATISTICS

Table B1. Groundwater temperature descriptive statistics.

	Number of records	Mean	Standard Deviation	Minimum	25%	Median	75%	Maximum
Mason County	206	14.3	1.66	10.8	13.5	14.0	14.5	22.5
American Bottoms	653	14.0	1.57	12.0	14.3	14.6	15.2	31.3

Table B2. Water quality statistics for Mason County, IL groundwater. Total records 101.

	Alkalinity	As	B	Ba	Ca	Cl^-	Conductivity	Cu	F^-
Units	mg/L as $CaCO_3$	µg/L	mg/L	µg/L	mg/L	mg L^-_1	µS/cm	µg/L	mg/L
No data	0	56	33	51	27	2	94	54	75
Nondetects	0	16	41	0	0	4	0	32	7
Mean	192.0	3.0	38.7	46.6	65.0	13.3	499.3	9.1	0.2
Standard deviation	66.3	4.5	65.9	31.6	18.7	54.5	89.5	19.5	0.7
Maximum	489.0	23.0	300.0	138.0	122.0	540.0	614.0	35.7	3.6
75th percentile	220.0	3.0	57.3	66.5	73.8	11.5	582.0	12.0	0.2
Median	179.0	1.1	11.0	36.0	64.5	5.3	495.0	4.7	0.1
25th percentile	146.0	*	*	21.3	49.9	2.8	431.5	1.7	*
Minimum	82.7	*	*	6.0	35.6	0.0	359.0	*	*

Note: * below detection limit.

Table B2. (continued)

	Fe	K	Mg	Mn	Na	NH_3-N	NO_3-N	NPOC†	P
Units	µg/L	mg/L	mg/L	µg/L	mg/L	mg /L	mg/L	mg/L	mg/L
No data	0	56	27	37	36	68	9	94	83
Nondetects	25	27	0	20	1	14	20	0	3
Mean	779.7	3.5	24.9	178.9	6.1	0.30	4.8	2.3	0.30
Standard deviation	1520.6	8.2	9.6	253.8	5.9	1.00	7.7	2.4	0.81
Maximum	7600.0	33.5	55.2	1512.0	46.0	5.70	45.5	7.7	3.20
75th percentile	796.0	1.5	30.0	278.0	7.0	0.20	5.3	2.7	0.13
Median	100.0	1.0	22.7	102.0	4.6	0.06	1.9	1.0	0.02
25th percentile	20.0	*	17.4	*	3.3	*	0.2	0.8	*
Minimum	*	*	11.7	*	0.0	*	*	0.6	*

Notes: † non-purgable organic carbon; * below detection limit.

Table B2. (concluded)

	pH	Si	SO_4^{2-}	TDS	Zn
Units		mg/L	mg/L	mg/L	µg/L
No data	35	83	39	3	53
Nondetects	0	0	0	0	14
Mean	7.8	14.6	58.0	309.4	121.4
Standard deviation	0.3	4.0	97.3	219.3	188.4
Maximum	8.2	22.4	792.0	2277.0	927.0
75th percentile	8.0	17.8	55.3	329.8	140.0
Median	7.9	14.0	40.9	279.0	40.0
25th percentile	7.7	11.8	27.4	222.5	*
Minimum	6.6	8.0	9.6	163.0	*

Note: * below detection limit.

Table B3. Solutes with few detections, Mason County, IL groundwater.

	Ag	Al	Be	Cd	CN	Co	Cr	Li
No data	89	88	85	87	89	89	50	99
Nondetects	12	12	16	14	12	11	47	2
Maximum		103				6	10	

Notes: blank indicates no detections; all concentration units µg/L.

Table B3. (concluded)

	Hg	Mo	Ni	Pb	Sb	Se	Tl	V
No data	89	95	50	87	97	89	97	89
Nondetects	12	6	48	14	4	11	4	12
Maximum			32			1		

Table B4. Water quality statistics for groundwater in the American Bottoms area, Madison and St. Clair Counties, IL.

	Alkalinity	As	B	Ba	Ca	Cl-	Conductivity	Cr	Cu
Units	mg/L as $CaCO_3$	µg/L	mg/L	µg/L	mg/L	mg/L	µS cm^{-1}	µg/L	µg/L
No data	1	60	39	42	31	3	90	45	42
Nondetects	0	28	18	10	0	0	0	67	52
Mean	302.9	1.9	204.8	228.5	109.1	43.2	637.7	3.2	23.6
Standard deviation	87.3	2.4	284.6	164.4	42.6	59.7	282.1	6.3	46.6
Maximum	668.0	12.0	1310.0	866.0	235.0	415.0	1300.0	20.0	270.0
75th percentile	351.5	2.0	220.0	300.0	130.5	49.4	842.0	*	20.0
Median	303.5	1.4	100.0	200.0	100.0	21.1	626.0	*	10.0
25th percentile	237.0	0.8	50.0	120.0	79.9	10.0	380.0	*	*
Minimum	124.0	*	*	*	38.1	1.0	192.0	*	*

Notes: total records 119; * below detection limit.

Table B4. (continued)

	F^-	Fe	K	Mg	Mn	Na	NH_3-N	Ni	NO_3-N
Units	mg/L	µg/L	mg/L	mg/L	µg/L	mg/L	mg/L	µg/L	mg/L
No data	21	3	54	31	21	31	63	46	16
Nondetects	0	10	5	0	2	0	7	67	40
Mean	0.3	5156.8	3.9	34.5	492.6	40.0	0.51	5.8	5.9
Standard deviation	0.3	5306.7	5.7	15.9	306.2	52.5	0.74	9.2	29.7
Maximum	2.0	26000.0	45.0	122.0	1550.0	261.0	3.30	32.0	245.0
75th percentile	0.3	7277.5	4.4	43.7	601.3	41.2	0.48	11.0	1.7
Median	0.2	3550.0	3.0	31.3	485.0	17.5	0.25	*	0.7
25th percentile	0.2	833.8	1.9	22.5	300.0	13.0	0.10	*	0.3
Minimum	0.1	*	*	9.3	*	4.5	*	*	*

Note: * below detection limit.

Table B4. (concluded)

	P	pH	Se	SiO_2	SO_4^{2-}	Sr	TDS†	Zn
Units	mg/L		µg/L	mg/L	mg/L	µg/L	mg/L	µg/L
No data	69	49	68	55	25	76	3	43
Nondetects	27	0	44	0	3	0	0	45
Mean	0.5	7.23	8.9	26.3	133.7	218.2	581.9	165.1
Standard deviation	0.4	0.49	23.6	6.6	127.7	99.7	285.0	485.8
Maximum	18.2	8.40	3.8	38.7	902.0	560.0	1880.0	3000.0
75th percentile	0.2	7.60	*	30.2	159.0	248.0	674.3	120.0
Median	*	7.30	*	27.7	98.1	190.0	510.0	30.0
25th percentile	*	6.84	*	23.1	63.7	158.5	392.0	7.0
Minimum	*	6.15	*	7.5	*	60.0	243.0	*

Notes: † total dissolved solids; * below detection limit.

Table B5. Solutes with few detections, American Bottoms area, Madison and St. Clair Counties, IL groundwater.

	Ag	Al	Be	Cd	CN^-	Co	Hg
No data	69	90	80	56	75	86	72
Nondetects	50	26	37	62	41	30	46
Maximum		1880.0	4.0	10.0	0.02	12.0	0.2

Notes: blank indicates no detections; concentration units µg L^{-1} except NPOC which is mg/L.

Table B5. (concluded)

	Li	Mo	NPOC	Pb	Sb	Tl	V
No data	104	100	113	51	106	112	86
Nondetects	7	19	0	65	13	7	31
Maximum	40.0		53.1	84.0			10.0

APPENDIX C. UNCERTAINTY ESTIMATE FOR SATURATION INDICES

The calcium carbonate saturation index depends on Ca^{2+} and CO_3^{2-} concentrations, pH, ionic strength, and temperature. The concentrations of Ca^{2+} and CO_3^{2-} in equilibrium with $CaCO_3$ are related by Equation C1,

$$K'_{so} = [Ca^{2+}][CO_3^{2-}] \tag{C1}$$

where K_{so}´ is the conditional solubility product, which is valid for a given temperature and ionic strength and square brackets indicate concentrations. The saturation index is given by Equation C2.

$$SI = Log_{10}\frac{[Ca^{2+}][CO_3^{2-}]}{K'_{so}} \tag{C2}$$

The alkalinity is given by Equation C3 to a very good approximation (Stumm and Morgan, 1996).

$$Alk = [HCO_3^{-}] + 2[CO_3^{2-}] \tag{C3}$$

The concentrations of carbonate and bicarbonate ions are related by Equation C4,

$$K'_{a2} = \frac{[H^{+}][CO_3^{2-}]}{[HCO_3^{-}]} \tag{C4}$$

where K_{a2}´ is the second conditional dissociation constant of carbonic acid. Combining Equations C3 and C4 gives an expression for carbonate concentration that is accurate to better than 1% at typical groundwater pH values.

$$[CO_3^{2-}] = \frac{Alk}{\frac{[H^{+}]}{K'_{a2}} + 2} \approx \frac{K'_{a2}Alk}{[H^{+}]} \tag{C5}$$

Substituting Equation C5 into Equation C2 gives SI in terms of measured quantities,

$$SI = Log_{10}[Ca^{2+}] + Log_{10}Alk + \{Log_{10}K'_{a2} - Log_{10}K'_{so} + Log_{10}\gamma_{H^{+}}\} + pH \tag{C6}$$

where γ_{H}^{+} is the activity coefficient of H^{+}. The relative standard deviations of $Log_{10}K_{a2}$´ and $Log_{10}K_{s0}$´ are approximately 0.03% and 0.2%, respectively (Plummer and Busenberg, 1982). The value of γ_{H}^{+} can be calculated within 5% for the ionic strength of the groundwater in the study areas (Butler, 1964). Therefore, the sum inside the braces can be considered constant.

The uncertainty of a function of several variables (f(x, y, z, …)) is given by Equation C7,

$$\sigma^2(f(x,y,z,\ldots)) = \left(\frac{\partial f}{\partial x}\right)^2 \sigma^2(x) + \left(\frac{\partial f}{\partial y}\right)^2 \sigma^2(y) + \left(\frac{\partial f}{\partial z}\right)^2 \sigma^2(z) + \cdots \quad \text{(C7)}$$

where σ stands for the standard deviation. Equation C7 is a good approximation if the errors of the independent variables are normally distributed and uncorrelated (Bevington, 1969). Since Ca, alkalinity, and pH are measured separately, their errors are clearly uncorrelated. For the uncertainty estimate, it is assumed the errors in these measurements are normally distributed. The partial derivatives of SI are given by Equations C8 – C10.

$$\frac{\partial SI}{\partial [Ca^{2+}]} = \frac{0.43}{[Ca^{2+}]} \quad \text{(C8)}$$

$$\frac{\partial SI}{\partial Alk} = \frac{0.43}{Alk} \quad \text{(C9)}$$

$$\frac{\partial SI}{\partial pH} = 1 \quad \text{(C10)}$$

The value 0.43 in the denominator of equations C8 and C9 is $Log_{10}(e)$, where e is the base of natural (Napierian) logarithms. It comes from differentiation with respect to $Log_{10}[Ca^{2+}]$ and $Log_{10}Alk$. Substituting into Equation C7 gives the Equation for the uncertainty of SI.

$$\sigma^2(SI) = (0.43)^2 \left(\frac{\sigma^2([Ca^{2+}])}{[Ca^{2+}]^2} + \frac{\sigma^2(Alk)}{Alk^2} \right) + \sigma^2(pH) \quad \text{(C11)}$$

The relative standard deviation (RSD) of a quantity is the standard deviation divided by the value of the quantity. Equation C11 simplifies to the following:

$$\sigma^2(SI) = 0.185\left(RSD^2([Ca^{2+}]) + RSD^2(Alk) \right) + \sigma^2(pH) \quad \text{(C12)}$$

The relative standard deviations of Ca concentration and alkalinity from analyses of duplicate samples performed by the ISWS laboratory (Holm, 2004) are 6.5% and 0.8%, respectively. The pH is rarely measured in duplicate, but the standard deviation is expected to be better than 0.1 pH unit near the isoelectric point of a glass electrode (i.e., 6 < pH < 8) (Leito, 2002). Most groundwater pH values in Illinois are in this range. Substituting these values in Equation C12, the standard deviation of SI is 0.104. As a result, the 95% confidence interval for SI (± 2σ) is SI ±0.2.

Because of the factor of 0.185 in Equation B12, the uncertainty of SI is relatively insensitive to the uncertainties in Ca and alkalinity. As a result, the pH uncertainty accounts for most of the uncertainty in SI. Even for RSD values of 10% for both Ca and alkalinity, the width of the 95%

confidence interval of SI would still be about ± 0.2. To allow for small errors in pH electrode calibration and temperature compensation, the tolerance interval can be widened to SI ± 0.3.